www.sciencemag.org/cgi/content/full/1158684/DC1

Supporting Online Material for

High-Quality Binary Protein Interaction Map of the Yeast Interactome Network

Haiyuan Yu, Pascal Braun, Muhammed A. Yildirim, Irma Lemmens, Kavitha Venkatesan, Julie Sahalie, Tomoko Hirozane-Kishikawa, Fana Gebreab, Na Li, Nicolas Simonis, Tong Hao, Jean-François Rual, Amélie Dricot, Alexei Vazquez, Ryan R. Murray, Christophe Simon, Leah Tardivo, Stanley Tam, Nenad Svrzikapa, Changyu Fan, Anne-Sophie de Smet, Adriana Motyl, Michael E. Hudson, Juyong Park, Xiaofeng Xin, Michael E. Cusick, Troy Moore, Charlie Boone, Michael Snyder, Frederick P. Roth, Albert-László Barabási, Jan Tavernier, David E. Hill, Marc Vidal*

*To whom correspondence should be addressed. E-mail: marc_vidal@dfci.harvard.edu

Published 21 August 2008 on *Science* Express
DOI: 10.1126/science.1158684

This PDF file includes:

(SOM I) Materials and methods

Yeast two-hybrid (Y2H)

Y2H experiments were essentially as described (*1*) (fig. S3). Briefly, all Entry clones contained in the MORF collection (*2*) were transferred into AD and DB vectors using Gateway LR reactions. After bacterial transformation, miniprep plasmid DNA of all AD-Y and DB-X clones were transformed into yeast two-hybrid strains *MAT***a** Y8800 and *MAT*α Y8930, respectively. The *MAT***a** Y8800 strain was obtained from *MAT***a** Y550 strain (*3*) after mutating *CYH2* to introduce cycloheximide resistance. *MAT*α Y8930 was generated by crossing *MAT***a** Y8800 with *MAT*α Y1541 (*3*), followed by sporulation and identification of *MAT*α cycloheximide resistant yeast strain by tetrad analysis. These yeast strains have three reporter genes: *GAL2-ADE2*, *met2::GAL7-lacZ* and *LYS2::GAL1-HIS3*. The new yeast strains were used in our established Y2H pipeline, with minor modifications due to the different selection markers. All DB-X constructs were screened for growth on synthetic complete media lacking leucine and histidine (SC-Leu-His) to identify auto-activators. All auto-activators were removed from the main collection, and re-tested for auto-activation on SC-Leu-His containing 0, 1, 5, 10, and 20 mM of 3-amino-1,2,4-triazole (3-AT). All DB-X-ORFs whose auto-activation phenotype was suppressed by 5 mM 3-AT were screened at this 3-AT concentration. A total of 3,917 MORFs were then screened as DB-X baits against 5,246 MORF AD-Y preys. The AD-Y constructs were combined into minipools of 188 AD-Ys.

Proteome-wide Y2H screens were carried out as described (*1*), including additional replica-plating onto SC-Leu-His plates containing cycloheximide (CYH) to eliminate the AD plasmid and thus identify spontaneous auto-activators that can arise during the course of a screen (*4*). Lastly, six Y2H controls were included on all Y2H screening plates (*5, 6*). The plates were incubated overnight at 30°C, replica-cleaned the following day and incubated for another three days, after which Y2H positive colonies were picked and used to inoculate liquid cultures in SC-Leu-Trp-His media. After overnight growth at 30°C, a 5 µL aliquot was spotted onto each of the four Phenotyping II plates (SC-Leu-Trp-His, SC-Leu-His+CYH, SC-Leu-Trp-Ade, SC-Leu-Ade+CYH) to test for cycloheximide-sensitive expression of the *LYS2::GAL1-HIS3* and *GAL2-ADE2* reporter genes. All plates were replica-cleaned the following day and scored after three additional days. For colonies that scored positive the identity of bait and prey was determined using end-read sequencing of PCR products. The entire yeast collection was screened three times.

From the set of successfully sequenced DB-X and AD-Y pairs, all interacting protein pairs were retested to ensure the robustness of the His+ and Ade+ phenotypes and to exclude the possibility that physiologic and genetic changes that occurred during the course of the experiment gave rise to experimental artifacts. For retesting, liquid cultures of individual AD and DB constructs were inoculated from archival glycerol stocks and the yeast cells were mated the following day as described above. From the YEPD plates, yeast colonies were replica-plated onto the four assay plates identical to the ones used for Phenotyping II. Pairs which activated at least one reporter gene in a

cycloheximide-sensitive fashion were included in the final map. All pairs that exhibited cycloheximide resistance or failed to retest were excluded.

Pairwise Y2H test of published interactome datasets

To evaluate the accuracy of the different interactome datasets by Y2H, randomly picked protein pairs were tested in both directions (DB-X, AD-Y and DB-Y, AD-X) by inoculating liquid cultures in SC-Leu (DB) and SC-Trp (AD), respectively, mated in the correct pairwise combinations on YEPD plates, and then tested in the four phenotypic assays described above.

Mammalian Protein-Protein Interaction Trap (MAPPIT)

The MAPPIT experiments were carried out as described (*7*) with minor changes. Briefly, plasmids were transfected into human 293T cells using a calcium phosphate protocol. Transfected cells were cultured for 24 hours in DMEM medium supplemented with 10% fetal bovine serum, and then stimulated with ligand (Epo) or left untreated for an additional 24 hours, followed by measurement of the luciferase activity in triplicate. All protein pairs were tested twice in both directions. Protein pairs were considered for scoring ("applicable" as opposed to "not applicable") if i) cloning was considered successful for both the bait and the prey constructs; ii) expression of the bait vector was considered sufficient, *i.e.*, the receptor-bait was able to generate a fold-induction value (mean value of the Epo-stimulated cells divided by the mean value of the non-stimulated cells) higher than ten when tested in combination with a prey construct (TRIP13) which interacts

systematically with the chimeric receptor independently of the bait; and iii) the bait and the prey proteins were considered to interact specifically, *i.e.*, when the bait or prey were able to generate a fold-induction value lower than twenty when tested in combination with an irrelevant prey protein or an irrelevant bait protein, respectively. Pairs were scored positive if the fold-induction value was three-times higher or equal to the ones obtained with both the irrelevant bait and the irrelevant prey. All other scores were considered negative.

Protein Complementation Assay (PCA)

For PCA assay (*8*) yeast ORFs available in Gateway Entry vectors were transferred by Gateway LR reactions into vectors encoding the two fragments of YFP fused to the N-terminus of the ORF. Baits were fused to the F1 fragment and preys to the F2 fragment. After bacterial transformation, minipreps were done on a Qiagen BioRobot, and DNA concentrations were determined by PicoGreen assay (Invitrogen). We pooled 30 ng of each bait and prey vector plus 140 ng of a CFP control plasmid for transfection into CHO-K1 cells (ATCC) in 96-well plates, using Lipofectamine2000 (Invitrogen) reagent according to the manufacturer's instructions. Approximately 18 hrs post-transfection, cells were washed with PBS, trypsinized, suspended in 130 µl PBS and analyzed by fluorescence-activated cell sorting on a Canto II FACS (Becton Dickinson) equipped with a 96-well autosampler. In preliminary experiments, we determined that there was no spectral overlap between the YFP and CFP channels. Viable CFP positive, *i.e.*, transfected cells, were selected and analyzed for YFP signal. Protein pairs were

scored as positive when at least 30% of CFP-positive cells produced a YFP signal above threshold, and the YFP/CFP ratio was at least twice as high as the ratio of the average YFP signal over the average CFP ratio across all wells of the 96-well plate. Typically, fewer than 30% pairs tested per 96-well plate could be considered positive.

Datasets used in the analysis

Interactome (*9-16*), phosphorylome (*17*), transcriptional regulation (*18*), mutation rate (*19*) and phenotypic profiling datasets (*20*) were all downloaded from the supplementary materials of the original publications. In the phenotypic profiling data, 22 conditions were originally tested. After removal of highly correlated ones, 19 independent conditions were used in our analysis. We compiled yeast expression data for 267 conditions from the Stanford Microarray Database (SMD) (*21*). GO annotations were downloaded from the Gene Ontology website as of November 2007 (*22*). MIPS complexes were downloaded from the MIPS website as of April 2007 (*23*).

Calculation of *P*-values

Cumulative binomial distribution: To determine the significance of the difference of the fraction of a certain property between two samples (*i.e.*, datasets), we used the cumulative binomial distribution:

$$P(c \geq c_o) = \sum_{c=c_o}^{N} [\frac{N!}{N!(N-c)!}] p^c (1-p)^{N-c}$$

where N is the total number of possible gene pairs in the testing sample, c_o is the number of observed pairs with a specific property (*e.g.,* essentiality), and p is the probability of finding a gene pair with the same property randomly (picking from the entire genome) or in the control sample.

Cumulative hypergeometric distribution: To determine the significance of the overlap between two genome-scale datasets, we used the cumulative hypergeometric distribution:

$$P(i \geq O) = 1 - \sum_{i=0}^{O-1} \frac{\binom{m}{i}\binom{N-m}{n-i}}{\binom{N}{n}}$$

where m is number of pairs in one dataset, n is the number of pairs in another dataset, N is the total number of pairs in the genome (18×10^6), and O is the observed overlap between the two datasets.

t-distribution for correlation coefficients in linear regression: The probability that the correlation coefficient (R) of a linear regression is not zero (*i.e.*, the null hypothesis is R=0) follows a t-distribution:

$$t = R \times \sqrt{\frac{n-2}{1-R^2}}$$

where R is the correlation coefficient, n is the number of points in the regression. The degree of freedom for the t-distribution is n-2.

(SOM II) Positive reference set and random reference set

To generate accurate binary interaction datasets and verify their quality experimentally (as opposed to strictly computationally), a novel binary interactome

mapping framework was developed. This framework solely uses physical protein interaction strategies without relying on indirect correlations with other global biological features such as expression or phenotypic profiling. It combines multiple independent interaction assays, each with complementary advantages. Optimal experimental conditions are established for each assay using a set of well-documented protein-protein interaction pairs ("positive reference set", or PRS) and likely non-interacting negative pairs ("random reference set", RRS) (fig. S15), choosing experimental conditions that minimize detection of unexpected RRS pairs while maximizing the number of detected PRS pairs (fig. S15).

To construct PRS, we collected all yeast protein interactions (11,858 distinct ones in total) from five well-known databases: BIND, DIP, MIPS, MINT, and IntAct (*23*-*27*), from which we selected 1,172 high-quality interactions that are published in at least two papers and are recorded in at least two databases. We curated these 1,172 interactions to remove semi-high-throughput publications and interactions inferred from large complexes, resulting in 983 interactions. We compiled the Binary-GS dataset (1,318 interactions) by combining these 983 interactions with those derived from small MIPS complexes and PDB structures (SOM III). From these interactions, 116 protein pairs were picked as PRS. These 116 PRS pairs have the most reliable literature-curated information available today, supported by the highest number of publications (≥5) and curated by multiple databases (Fig. 1B). RRS was generated from a random selection out of all ~14×10^6 possible yeast protein pairs (corresponding to the available search space that can be mapped using our ORFeome collection) for which no interaction has

yet been detected by any method (Fig. 1B). 1,000 random pairs were first selected and a random subset of 116 pairs was then chosen as RRS. All 1,000 random pairs were tested in our Y2H assay and none scored positive.

PRS and RRS are representatives of true positive and negative interactions, respectively. The number of true positive interactions is expected to be much smaller than the number of negative ones (*e.g.*, for yeast the estimated number of binary interactions is ~18×10^3, and negative interactions ~14×10^6). Therefore, one important issue in constructing PRS and RRS sets is to keep the ratio between the two sets (*28*) if used as gold standard positive and negative sets. With this, one can directly estimate the precision and sensitivity of a dataset. However, implementing such large PRS and RRS is experimentally intractable. In contrast, here we are only using PRS and RRS to optimize the assay performance, which gives the window within which the data of the retest assays are optimally interpretable. PRS and RRS used this way serve as positive and negative controls. Thus far, only a handful of positive and negative controls have been used by other groups for characterizing assay performance, which we deemed insufficient for our purpose. Therefore, we used 10 to 100 times more positive and negative controls for benchmarking the interaction assays than what is generally done (*29-32*).

(SOM III) Issues in constructing gold standard datasets

Defining negative interactions is difficult

To declare that two proteins absolutely do not interact with each other, even after they are tested, is essentially impossible. Since every experimental technique has

limitations and every experiment is carried out under a certain condition, all that can be said is that these two proteins do not interact in the experiments and under any conditions that were tried.

There are two common methods for constructing a negative protein interaction set (*33*). The first is to choose negative pairs randomly from all protein pairs that are not (yet) known to interact (*33, 34*). The other is to consider protein pairs localized within different subcellular compartments unlikely to interact (*28, 35*).

To construct an unbiased negative "random reference set" (RRS) for our specificity measurements, we used the first method to randomly select 116 RRS pairs. However, this method is problematic to assess the false positive (FP) rate of published high-throughput datasets, because these datasets will have zero FP rate by definition (all the interactions in these datasets are excluded from the negative set). Therefore, we use the second method to construct a larger negative set for our computational analyses. However, subcellular localizations are not necessarily absolute and different physiological and environmental conditions can cause re-localization of proteins to distinctly different subcellular compartments leading to bona fide interactions among candidate protein pairs in the negative set.

The MIPS gold standard dataset is not appropriate for evaluating binary interactions

For assessment of yeast interactome datasets the most commonly used gold standard (GS) dataset is the MIPS complex catalog, which currently documents

187 protein complexes (*23, 36*). Typically, all possible protein pairs within each complex are considered as potential binary interactions using a matrix model (*37*) which leads to 9,193 GS interactions among 1,058 proteins.

We argue that the MIPS complex catalog is an unfair and inadequate GS dataset for evaluating physical binary interactions, *i.e.*, high-throughput yeast two-hybrid (Y2H) datasets and most low-throughput literature-curated interactions.

First and foremost, MIPS was constructed using a matrix model (*37*). Hence, most of the 9,193 protein pairs contained in the MIPS correspond to indirect and not binary interactions. For example, the 20S proteasome complex contains 28 subunits (fig. S1). Each proteasomal β subunit interacts with six neighboring proteins and each α subunit interacts with four neighboring proteins (*38*). In total 70 direct physical binary interactions form the 20S proteasome based on three-dimensional structural data (*38*). In contrast a matrix model of the complex predicting that each protein interacts with all other 27 proteins would lead to 378 interactions within proteasome in total. In this example only ~20% of matrix-based predicted binary pairs correspond to real binary interactions. Hence, just a tiny portion of the MIPS dataset corresponds to actual binary interactions potentially detectable by Y2H. This problem is the “limited sampling” issue of the MIPS. The calculated precision (SOM V) for any high-throughput Y2H dataset against the MIPS is expected to be much smaller than that of AP/MS datasets, which are converted by the same method into binary data and therefore are expected to have much larger overlaps with the MIPS.

Second, AP/MS methods preferentially detect strong interactions within stable complexes, whereas Y2H methods can identify weaker, transient or condition-specific interactions (*39*). The MIPS complex catalog is biased towards large stable complexes (*40*). Thus, many interactions detectable by Y2H are expected to be absent from the MIPS. This problem is the "biased sampling" issue of the MIPS (fig. S2). A binary GS would be expected to produce a better measurement of precision for Y2H datasets. The MIPS and AP/MS datasets are generated similarly, which introduces biased sampling and artificially higher precision for AP/MS datasets.

In summary, most MIPS interactions are indirect, and the few binary interactions contained in the MIPS are biased against weaker interactions. Both limited and biased sampling of MIPS might result in artificially high and low precision for AP/MS and Y2H datasets, respectively.

Constructing the Binary-GS set

We generated a "Binary-GS" set consisting of 1,318 high-confidence physical binary interactions assembled from three sources (*41*): i) 983 binary interactions from low-throughput experiments recorded in at least two of five widely-used databases (MIPS, BIND, IntAct, MINT and DIP) with at least two associated publications (*23*-*27*). We removed semi-high-throughput publications and interactions inferred from large complexes (SOM II). ii) 308 interactions found in small MIPS complexes of four or less subunits (*23*), and iii) 156 interactions derived from co-crystallized proteins recorded in the Protein Data Bank (PDB) (*42*).

There are 451 PDB entries providing structural information on yeast proteins and complexes. We calculated the contact surface area between any two subunit of each complex. Pairs of proteins (subunits) with sufficient contact surface areas (≥100 $Å^2$) were considered as interaction partners. There are overlaps between the interactions from the three sources.

Co-complex datasets are composed of both direct interactions and indirect associations, which cannot be distinguished from each other. This applies to the MIPS co-complex dataset as well, which is therefore inappropriate as a gold standard for evaluating direct binary interaction datasets. However, protein complexes are held together by direct protein interactions. To account for these, in constructing both Binary-GS and PRS we included all interactions within all protein complexes if structural or other evidence that demonstrated direct physical contact between two proteins was available. Moreover, we included all protein pairs from small MIPS complexes, assuming their constituents directly interact with each other (Fig. 1B). We thus represent interactions within complexes as comprehensively as possible given current knowledge. Our results do not need to be systematically corrected for under-representation of interactions within complexes.

To verify the quality of the Binary GS set, 50 pairs of interacting proteins were randomly selected and recurated from the original publications; all were confirmed to be correct binary interactions.

(SOM IV) Data quality analyses and their robustness

Quality assessment of all currently available yeast interactome datasets

We analyzed four high-throughput Y2H (*9, 10*), four high-throughput AP/MS (*11-14*), and two literature-curated datasets (*15*) (fig. S7A). We differentiated between the interactions found in Uetz *et al.* in an array setting involving 193 bait proteins tested against all yeast proteins ("Uetz-array") and those found in a proteome-scale all-by-all screen ("Uetz-screen"). Likewise, we differentiated the Ito *et al.* interactions between those found three times or more ("Ito-core") and those found one or two times ("Ito-noncore"), a distinction originally recommended by the authors. Finally, we separated literature-curated interactions between those that have been curated from a single publication ("LC-one") and those curated from two or more publications ("LC-multiple").

Using both Y2H and PCA, sampled pairs of Uetz-array, Uetz-screen, and Ito-core datasets tested positive at levels comparable to the yeast PRS (fig. S7B, C). In striking contrast, sampled pairs from Ito-noncore tested at levels comparable to RRS (P=0.23; all P-values were calculated as described in SOM I), demonstrating the extremely low quality of this particular dataset. A sample of LC-multiple tested slightly lower with Y2H ($P<10^{-16}$ between LC-multiple and Uetz-screen) (fig. S7B), while being indistinguishable with PCA (fig. S7C); hence high-quality high-throughput Y2H datasets are comparable in quality to LC-multiple. By contrast, LC-one pairs tested significantly lower ($P<10^{-3}$ between LC-one and Uetz-screen). Likewise, sampled pairs from all four high-throughput AP/MS datasets, as well as MIPS protein complexes (*23*), tested poorly using these two

binary interaction assays ($P<10^{-4}$ between Krogan and Uetz-screen; fig. S7B, C). In summary, Uetz-array, Uetz-screen, Ito-core, and LC-multiple are high-quality datasets with regard to intrinsic binary protein-protein interaction quality, while Ito-noncore and LC-one should not be used. In addition, high-throughput AP/MS, although of intrinsically good quality (see below), should be used with caution when binary interaction information is needed.

Computationally, we found that high-throughput AP/MS data are of significantly better quality than the Y2H data using MIPS, reproducing previous observations (*36, 43*) (fig. S7D). However, when measured against Binary-GS, the quality of high-throughput Y2H datasets (with the exception of Ito-noncore) is substantially better than that of high-throughput AP/MS datasets (*e.g.*, $P<10^{-11}$ between Gavin2002-spoke and Uetz-screen; fig. S7A, E). Furthermore, combined high-throughput datasets (I-AP/MS and I-Y2H), *i.e.*, where interactions have been identified in at least two independent high-throughput experiments, are of higher quality than LC-multiple ($P<10^{-10}$ between I-Y2H and LC-multiple; fig. S7E). Our computational results are robust and supported by various measurements (see below).

Robustness of our computational analyses

Our binary GS dataset is comprised of the union of three different subsets (SOM III). To account for possible biases, we re-analyzed each one of the three subsets separately. The results confirmed that high-throughput experiments are comparable in quality to literature-curated datasets and that high-throughput Y2H

and high-throughput AP/MS are comparable in precision (fig. S16A-C). While binary interactions from the five databases might contain interactions determined by low-throughput Y2H experiments and might not be appropriate to evaluate LC-one (because they have two supporting publications by definition), those interactions derived from small MIPS complexes and PDB structures do not face these limitations. Using these two subsets, the quality of LC-one is still worse than most of the high-throughput datasets (fig. S16A, B).

For further validation of our computational results, we used a Structure Interaction Network (SIN) that is derived mainly from homologous mapping based on iPfam and PDB structures (*44*). We also used the highest confidence interactions in LC-multiple, reported by at least five different publications, and repeated all calculations. The results remained unchanged (fig. S16D, E).

To further examine the robustness of our results, we randomly chose only 50% of the interactions from Binary-GS and repeated all the calculations. This step was repeated 1,000 times. The results remained exactly the same (fig. S16F). The extremely small error bars show the robustness of our analysis.

(SOM V) Measurements of dataset quality

Different measurements of data quality

There are many measurements that have been considered for comparison of different large-scale interaction datasets. The terms used in these measurements are:

1. *P*: Total number of positives in a GS positive set (Binary-GS or MIPS).

2. *N*: Total number of negatives in a GS negative set. Here, we used the widely-used GS negative set based on localization data (*35*).
3. *TP*: Number of true positives in a certain dataset according to the GS positive set.
4. *FP*: Number of false positives in a certain dataset according to the GS negative set.
5. *TN*: Number of true negatives in a certain dataset according to the GS negative set.
6. *D*: Total number of interactions in a dataset.

The measurements are:

1. **Precision** (also called positive predicted value) is the fraction of true positive interactions in a dataset among all interactions in the dataset:

$$\text{Precision} = \frac{TP}{D}$$

   One can estimate precision either computationally via gold standard sets or experimentally by an orthogonal assay (SOM VI). In the main text, we focused on the calculations of precision of each dataset because it directly measures the quality of a dataset. The precision of CCSB-YI1 and Y2H-union against the Binary-GS is comparable with other Y2H datasets and better than AP/MS datasets (fig. S17A, B).

2. **FP rate** is the fraction of false positive interactions in a dataset among all interactions:

$$\text{FP rate} = \frac{FP}{D}$$

The terms true positives (TP) and false positives (FP) are borrowed from the machine-learning field. Ideally, (1-Precision) is taken as the false positive rate. However, the situation in biological problems is fundamentally different from that of ideal classification problems. First, to determine FPs, a GS negative set is necessary which is almost impossible to define (see above) (*28*). For interaction datasets an interaction is considered to be a FP if it is in the GS negative set. In ideal cases, the classification algorithm is trained and tested on known items, including both known positives and known negatives. Therefore, the class of each item is known beforehand and every predicted positive is either a TP or a FP (fig. S18). This is rarely true for biology, especially for large-scale experiments. Normally, only a small fraction of the potential positives produced by the experiments overlaps with either GS positives or GS negatives. For the vast majority, while they may not overlap with GS positives, they most likely represent new discoveries and not necessarily FPs. Therefore, the actual value of the precision score is somewhat misleading. The seemingly small values of the precision scores mainly result from the incompleteness of the GS positive set. The overlap between the GS set and each of the six high-throughput interaction datasets are statistically highly significant, confirming the robustness of these experiments.

Here, to calculate the FP rate, we used the widely-used GS negative set based on localization data (*35*). The results (fig. S19) are similar to those in fig. S17B which shows that Ito-core and Uetz-screen have lower

FP rates than AP/MS datasets. Note that because the pairs in GS negative set are not confirmed negatives, the calculated FP rate of a dataset is less reliable than its precision. Therefore, precision is a better measurement of data quality.

3. **Sensitivity** (also called coverage) is the fraction of true positive interactions that could be recovered by the assay out of all positive interactions:

$$\text{Sensitivity} = \frac{TP}{P}$$

The sensitivity of all Y2H datasets against MIPS is low (fig. S17C), which confirms previous results (*36*). The low sensitivity arises because the MIPS were constructed with the matrix model, so many of the interactions are not direct binary interactions (SOM III).

However, against the Binary-GS the sensitivities of the Ito-core and Uetz-screen datasets are still low (fig. S17D). As discussed in the main text, the possible explanations include: low completeness (neither dataset could actually test all ORFs in the yeast genome due to technical limitations); assay-sensitivity (any assay has inherent limitations of finding certain interactions; the assay-sensitivity of our Y2H assay is about 20%); and sampling-sensitivity (the whole proteome needs to be tested multiple times before most detectable interactions can be identified). Ito-core and Uetz-screen only completed one screen of the genome. Based on our experiments, a typical high-throughput Y2H screen uncovers 30-60% of detectable interactions in a single pass.

Because of the low sensitivity of the Ito-core and Uetz-screen datasets, we decided to carry out a new proteome-scale high-throughput Y2H screen. The sensitivity of both CCSB-YI1 and Y2H-union is better than that of Ito-core and Uetz-screen, and is comparable with that of AP/MS datasets. Because the search space of CCSB-YI1 is precisely known, we could calculate exactly the sensitivity of CCSB-YI1 within the search space (*i.e.*, we only considered Binary-GS interactions that are in the search space). The sensitivity as such of CCSB-YI1 is 17%, which is in agreement with the tested assay- and sampling-sensitivity (20% x 85% = 17%).

The concept of sensitivity does not provide worthwhile insight into the quality of the datasets. We should always consider sensitivity together with precision. The precision of all Y2H dataset are significantly better than that of each individual AP/MS dataset (fig. S17B). One could imagine a perfectly bad experiment in which every protein pair in the proteome is determined to be interacting. This dataset would have perfect sensitivity no matter which GS set is used. Nonetheless, the dataset would obviously be useless.

4. **Likelihood ratio** is a measure that quantifies the discriminating power of the assay between the positive and negative interactions, which is defined as:

$$L(dataset) = \frac{P(dataset \mid pos)}{P(dataset \mid neg)} = \frac{\frac{TP}{P}}{\frac{FP}{N}}$$

L(dataset) relates prior and posterior odds according to Bayes' rule:

$$O_{post} = L(dataset) \times O_{prior}$$

As O_{prior} is fixed for a given organism, O_{post} is proportional to *L(dataset)*, *i.e.*, the higher the likelihood ratio, the more likely the interactions in the dataset are true.

Likelihood ratio is a direct and more sophisticated measurement of the quality of different datasets (*35, 45*). It considers the sensitivity of the assay as well as the specificity. The dataset comparisons based on likelihood ratios (fig. S17E, F) greatly resemble the precision comparisons (fig. S17A, B), confirming the robustness of our results.

5. **TP/FP ratio** is the ratio of true positives to false positives in a dataset. TP/FP ratio is a simplified version of the likelihood ratio and the dataset comparisons are the same as those based on likelihood ratios (fig. S17G, H).
6. **Accuracy** is the ratio of correctly identified positive and negative interactions reported in a dataset to total number of positive and negative interactions:

$$\text{Accuracy} = \frac{TP + TN}{P + N}$$

This is the most conventional definition of accuracy. However, with protein interactions there are enormously more negatives than positives ($N >> P$). Therefore, the accuracy of all datasets is ~1, which is shown in fig. S17. For comparing protein interaction datasets, the accuracy metric has little meaningful interpretation.

We have discussed several direct measurements of dataset quality. There are also indirect metrics that have been used (*46*). We argue in the main text that direct measurements of the quality of a dataset, either computationally (using carefully constructed GS sets) or experimentally (using orthogonal assays), are preferable over indirect ones. Indirect metrics evaluate the properties of the dataset, which may or may not reflect the quality of the interaction data. We discuss below several indirect metrics, pointing out their weaknesses when evident:

1. **Interaction conservation score** is defined as

$$\frac{\sum_{i,j} S_{ij}}{D}$$

where S_{ij} is the conservation score of interacting protein *i* and *j*. We mapped the interacting proteins into *C. elegans* (*47*) and *D. melanogaster* (*48-50*) through sequence homology ($E < 10^{-10}$). The conservation score for each interaction is 0 (not known to be conserved), 1 (conserved in one of the two non-yeast organisms), or 2 (conserved in both).

The Y2H datasets have better interaction conservation scores than the AP/MS datasets (fig. S20A). Overall, the dataset comparisons are highly similar to the precision calculation (fig. S17B). One possible reason for the better conservation scores, other than the default one that Y2H interactions tend to be conserved better in different organisms, is that the interactions in worm and fly were detected by Y2H methods. There are no proteome-scale AP/MS datasets for worm or fly, so any conserved complex

associations in worm and fly may not have been discovered yet. Therefore, the AP/MS datasets could have artificially lower scores because of the incompleteness of the data in worm and fly. Moreover, not all interactions are conserved in different organisms. Y2H and AP/MS experiments discover two different types of interactions, binary interactions or complex associations, respectively. It is not clear which type is more likely to be conserved across different species. The difference in conservation between these two types might have nothing to do with the quality of the data and could be purely due to the different natures of the datasets.

2. **Conservation rate coherency score** is defined as

$$\frac{\sum_{i,j} | r_i - r_j |}{N_d}$$

Here, r_i and r_j are the evolutionary rates of interacting protein *i* and *j* from Wall *et al.* (*19*), and N_d is the total number of interacting pairs in a certain dataset with evolutionary rate information for both proteins.

AP/MS datasets in general have better conservation rate coherency scores than Y2H datasets (fig. S20B). This does not necessarily mean the quality of AP/MS datasets is better. Proteins in stable complexes evolve slower than those in transient interactions (*40*), so the difference in the conservation rate coherency scores may just reflect the difference in the types of interactions detected by Y2H and AP/MS experiments.

3. **Expression correlation score** is defined as

$$\frac{\sum_{i,j} C_{ij}}{N_d}$$

where C_{ij} is the Pearson correlation coefficient between the expression profiles of interacting proteins *i* and *j*, and N_d is the total number of interacting pairs in a certain dataset with gene expression information for both proteins.

AP/MS datasets in general have better expression correlation scores than Y2H datasets (fig. S20C), in agreement with Fig. 5C. However, Y2H tends to detect transient interactions that only happen under certain conditions in the cell (*51*), so it is not expected that these interacting partners would show strong correlation (*i.e.*, high *PCC* value) of their expression profiles over different conditions. On the other hand, stable complexes tend to have stronger co-expression correlations among their constituents. Therefore, the difference in the expression correlation score is likely to reflect the different nature of interactions detected by Y2H and AP/MS, rather than reflecting the relative quality of these datasets.

4. **Log functional enrichment** is defined as

$$\log_2\left(\frac{\frac{N_s}{N_d}}{\frac{N_{sg}}{N_g}}\right)$$

where N_s is the number of functionally similar pairs in a certain dataset according to Biological Process (BP), Cellular Component (CC), or Molecular Function (MF) branches of the Gene Ontology (GO) (*22*). N_d is

the total number of interacting pairs in the dataset with functional information in the corresponding GO branch for both proteins. N_{sg} is the number of functionally similar pairs in the whole genome according to a certain GO branch. N_g is the total number of protein pairs in the genome with functional information in the corresponding GO branch for both proteins. The functional similarity between protein pairs is calculated based on the "Total Ancestry" method with a *P*-value cutoff of 10^{-3} (*52*).

Different datasets have better log functional enrichment in different GO branches (fig. S20D, E and F). Although interacting proteins can share similar functions, two interacting proteins might not have the exact same functions with each other, because a protein could be multifunctional (*53*) and may only interact with another protein to carry out a few but not all its functions. Therefore, the differences in the functional enrichment, again, might just reflect the different natures of the data, not the quality of the data.

(SOM VI) Estimation and implications of the framework parameters

Completeness of CCSB-YI1 whole-genome screen

There are ~6000 predicted genes in the *S. cerevisiae* genome [as of April 1st 2008 SGD reports 5884 genes (*54*)], which corresponds to (6000x6000)/2 = $18x10^6$ protein pairs. In this screen, we tested 5,246 ADs against 3,917 DBs that are not auto-activators. As shown in fig. S21, among these clones, 3,676 proteins were tested both as AD and as DB fusions (6,754,650 pairs in Area 1). There were 1,570 proteins tested only as AD against all 3,917 DBs (6,149,690 pairs in Area 2).

There were 241 proteins tested only as DB against all ADs (885,916 pairs in Area 3). In total, 13,790,256 unique pairs in the yeast genome were tested in our high-throughput Y2H screens. Therefore, the completeness of our screen is 13,790,256 / $18x10^6$ = 77%.

Calculation of sampling-sensitivity and its standard error

We completed eight independent screens on the search space (Fig. 2B). Though we screened in a certain order, each screen could be considered as the first screen (or second, third, etc.). Therefore, there are in total 8! (40320 – some of them are degenerate for our calculation though) different orders for these eight screens. We calculated the average number of interactions uncovered at each step and its standard error considering all of these orders. For the last data point, the standard error is zero because the total number of interactions uncovered after the eighth screen is constant.

Experimental estimation of precision and its standard error using MAPPIT and PCA

The precision of Y2H assay was measured experimentally using either MAPPIT, a binary interaction assay that takes place at the mammalian cell membrane and measures interaction by activation of STAT3 dependent reporter transcription; or PCA, in which bait and prey proteins are fused to non-fluorescent fragments of yellow fluorescent protein (YFP), which can be brought in close proximity by interacting proteins and then refold into a fluorescent protein (SOM I; fig. S22).

Under conditions giving rise to lowest RRS detection rates (no interaction detected among all RRS pairs), Y2H and MAPPIT detected 20% and 19% of the tested PRS pairs, respectively. The optimal condition for PCA gave rise to detection rates of 5% and 18% for RRS and PRS, respectively. To evaluate the quality of a protein interaction dataset a randomly chosen sample can now be tested using one or more interaction assay(s) and detection rates can be interpreted within the window defined by PRS and RRS sets (fig. S23).

The precision of Y2H assay was calculated by using MAPPIT and PCA as validation assays. Using Bayes' rule we can build relationships between true and false positive rates of Y2H and observed positive interactions by a validating assay as:

$$\Pr(A+ \mid Y+) = \Pr(A+ \mid Y+, T+) \times \Pr(T+ \mid Y+) + \Pr(A+ \mid Y+, T-) \times \Pr(T- \mid Y+)$$

where $A+$ correspond to observing a positive interaction using the validating assay, $Y+$ corresponds to observing a positive interaction using Y2H, and $T+\,(T-)$ corresponds to an interaction being a real positive (negative) interaction. The precision of the Y2H is the term $\Pr(T+ \mid Y+)$ [which is also equal to $1-\Pr(T- \mid Y+)$]. The $\Pr(A+ \mid Y+)$ term was estimated by randomly selecting 188 Y2H interactions and re-measuring them with MAPPIT and PCA. The $\Pr(A+ \mid Y+, T+)$ term can be estimated from interacting protein pairs present in PRS, but the associated statistics are unreliable, as there are only 8 interactions within PRS that are detected by Y2H and could be tested by either assay. Moreover, it is not plausible to empirically estimate the $\Pr(A+ \mid Y+, T-)$ term because all the known sources of possible false positives (*e.g.*, auto-activators, *de*

novo auto-activators) are eliminated by the new stringent Y2H protocol. However, the fundamental differences between the assays could imply conditional independence between assays. For instance, in the Y2H assay interactions are detected in the nucleus of yeast cells whereas interactions are detected at the mammalian plasma membrane or at endogenous localization sites in mammalian cells with MAPPIT and PCA, respectively. Furthermore, we can look at the subset of PRS that was originally reported by Y2H (PRS-Y2H) and see whether in this subset there is a bias for MAPPIT and PCA to detect an interaction. Out of 116 PRS interactions, 73 have Y2H support in the literature. The ability of PCA and MAPPIT to detect PRS-Y2H interactions is statistically indistinguishable from the full PRS (fig. S4), which supports the conditional independence of these two assays with Y2H.

If we accept conditional independence between the validating assay (*e.g.*, MAPPIT or PCA) and Y2H, we can write:

$$\Pr(A+\,|\,Y+) = \Pr(A+\,|\,T+)\times\Pr(T+\,|\,Y+) + \Pr(A+\,|\,T-)\times\Pr(T-\,|\,Y+)$$

Solving for the precision of the Y2H assay yields:

$$\Pr(T+\,|\,Y+) = \frac{\Pr(A+\,|\,Y+) - \Pr(A+\,|\,T-)}{\Pr(A+\,|\,T+) - \Pr(A+\,|\,T-)}$$

$\Pr(A+\,|\,T+)$ and $\Pr(A+\,|\,T-)$ were measured in the PRS and RRS experiments. So, for our Y2H assay we can write precision as:

$$\text{Precision} = \frac{F_{CCSB\text{-}YI1} - F_{RRS}}{F_{PRS} - F_{RRS}}$$

where $F_{CCSB\text{-}YI1}$ is the fraction positive by an assay (MAPPIT or PCA) for a sample of CCSB-YI1 which is the best estimator for $\Pr(T+\,|\,Y+)$, F_{PRS} is the fraction

positive by the assay for PRS, the estimator for $\Pr(A+|T+)$, and F_{RRS} is the fraction positive by the assay for RRS, the estimator for $\Pr(A+|T-)$.

The standard errors of $F_{CCSB\text{-}YI1}$, F_{PRS}, and F_{RRS} are calculated using the standard error for binomial distributions:

$$\text{StdErr} = \sqrt{\frac{F(1-F)}{N}}$$

where F is the fraction positive by the assay (*i.e.*, $F_{CCSB\text{-}YI1}$, F_{PRS}, or F_{RRS}) and N is the total number of pairs tested.

To estimate the standard error for the precision, we used the standard delta method:

$$\sigma_X^2 = \left(\frac{\partial f}{\partial A}\sigma_A\right)^2 + \left(\frac{\partial f}{\partial B}\sigma_B\right)^2 + \left(\frac{\partial f}{\partial C}\sigma_C\right)^2 + \cdots$$

where $X = f(A, B, C, \ldots)$. A, B, C, … are independent random variables.

Here, the standard error of the precision is calculated as:

$$\sigma_{\text{precision}} = \sqrt{\left(\frac{1}{F_{PRS} - F_{RRS}}\right)^2 \times \sigma_{CCSB\text{-}YI1}^2 + \left(\frac{F_{CCSB\text{-}YI1} - F_{RRS}}{F_{PRS} - F_{RRS}}\right)^2 \times \sigma_{PRS}^2 + \left(\frac{F_{CCSB\text{-}YI1} - F_{PRS}}{F_{PRS} - F_{RRS}}\right)^2 \times \sigma_{RRS}^2}$$

We have two validating assays, and we can incorporate the precision rates from these assays by calculating the average precision:

$$\text{Average Precision} = \frac{\text{Precision}_{\text{MAPPIT}} + \text{Precision}_{\text{PCA}}}{2}$$

The standard error for the average precision is calculated by the delta method as:

$$\sigma_{\text{average precision}} = \sqrt{\frac{\sigma_{MAPPIT}^2}{4} + \frac{\sigma_{PCA}^2}{4}}$$

Calculation of the size of the yeast binary interactome

With the calculation of the precision, assay-sensitivity, sampling-sensitivity, and completeness, we could estimate the size of the yeast binary interactome. Because the assay-sensitivity was estimated by testing each PRS pair both as AD-X/DB-Y and as AD-Y/DB-X, we only considered Area 1 in fig. S21, which is the space we screened in both directions. The completeness of Area 1 is 37%. There were 1,130 interactions detected in this space. Therefore, the estimated size of the yeast binary interactome is:

$$\text{Size of interactome} = \frac{N_i \times precision}{completeness \times assay\text{-}sensitivity \times sampling\text{-}sensitivity}$$

$$= \frac{1130 \times 100\%}{37\% \times 20\% \times 85\%}$$

$$\approx \text{ 18,000 pairs}$$

The standard error for the estimation is calculated using the delta method as:

$$\sigma_{\text{size}} = \sqrt{(\frac{N_i}{C \times A \times S})^2 \times \sigma_P^2 + (\frac{N_i \times P}{C \times A^2 \times S})^2 \times \sigma_A^2 + (\frac{N_i \times P}{C \times A \times S^2})^2 \times \sigma_S^2}$$

where *C* is completeness, *P* is the average precision, *A* is the assay-sensitivity, *S* is the sampling-sensitivity. The 95% confidence interval the predicted size is $1.96 \times \sigma_{\text{size}}$.

Framework parameters for Uetz-screen and Ito-core

We can calculate the completeness, assay-sensitivity and sampling-sensitivity of Uetz-screen and Ito-core. Using the information in the Table 1 of Uetz *et al.*, the completeness of this dataset can be estimated to be:

$$\frac{5341\times(5341-680)}{6000\times6000}\approx 69\%$$

We do not have quantitative information about the assay-sensitivity of this particular Y2H assay, but all of Y2H assays that we tested gave ~ 20% assay-sensitivity (Fig. 1C). As to sampling-sensitivity, we used the overlap between Uetz-screen and Uetz-array to estimate this parameter. We can assume that the array setting reached almost its full sampling-sensitivity. Uetz *et al.* report that 14 out of 48 interactions observed in the array setting are recovered in the screen setting. Hence, the sampling-sensitivity of this dataset can be estimated to be ~29%. Assuming no false-positives, we can now estimate the total number of interactions from these parameters to be:

$$\frac{691}{0.69\times0.2\times0.29}\approx 17{,}300$$

which agrees well with our estimation with CCSB-YI1.

For Ito-core there is no such detailed information, so we instead make heuristic calculations for this dataset. Ito *et al.* report that their ORF library covers ~95% of whole yeast interactome. Removing auto-activators (~10-15%) that might affect the number of baits used, we arrived at ~76% completeness (0.95×0.8 = 0.76) for this dataset. We used the generic Y2H assay-sensitivity of ~20% for this version of Y2H. Lastly, while there is no direct way to calculate the sampling-sensitivity, we can use the verified size of interactome from CCSB-YI1 and Uetz-screen to calculate its sampling-sensitivity at ~35%.

Completeness of AP/MS datasets

It is difficult to estimate the completeness for AP/MS experiments, because AP/MS does not detect pair-wise interactions, making it hard to determine which pairs have actually been tested. There are two models to convert AP/MS data into pair-wise interactions: 1) spoke model, where interactions are only considered between a bait protein and its associated prey proteins; 2) matrix model, where interactions are considered not only between a bait protein and its prey proteins but also between all of the prey proteins (*37*). Therefore, we could estimate two types of completeness for AP/MS experiments: 1) Spoke completeness, where the search space is considered as all baits being tested against all proteins encoded in the genome. Note that this is really the upper bound of the spoke completeness, because not all proteins encoded in the genome are expressed under the experimental condition. 2) Matrix completeness, where the search space is the search space for the spoke completeness plus all possible pair-wise combinations among all detected preys. Once again, this is the upper bound for the matrix completeness, because most of the detected preys are detected with different baits.

Using these two models, we calculated the completeness for the Gavin dataset:

1. **Spoke completeness**. According to Gavin *et al.* (*13*), 5,474 genes were successfully tagged and were subsequently used as baits in their experiments. Only 3,206 baits have been shown to be expressed in the cell. Therefore, the search space is (3206 x 3205)/2 + 3206 x (6000 – 3206) =

14,095,179 pairs. The spoke completeness is estimated to be 78% (fig. S5A).

2. **Matrix completeness**. Gavin *et al.* were able to successfully purify 2,760 different proteins for 1,993 baits. Therefore, they detected 767 prey-only proteins. The additional search space is (767 x 766) / 2 = 293,761 pairs. The total search space is 14,095,179 + 293,761 = 14,388,940 pairs, and the matrix completeness is estimated to be 80% (fig. S5A).

Theoretically, similar calculations can be made for Krogan *et al.* (*14*). However, the number of expressed baits is not discussed in that publication. Since they used the TAP-tagged strains constructed and tested for expression by Weissman and colleagues (*55*), we could estimate this number as 3,884 baits. Based on this estimation, the spoke completeness is 87% and the matrix completeness is 95%.

Assay- and sampling-sensitivity of AP/MS datasets

We can estimate these parameters for AP/MS datasets. We can infer the assay-sensitivity by measuring what fraction of MIPS interactions Gavin *et al.* recovered, which is ~26% (Fig. 1D). The sampling sensitivity can be estimated from the reported reproducibility of ~70%, which gives the sampling-sensitivity in each screen at ~84%. Combining these parameters, it is estimated that Gavin *et al.* identified a similar fraction of co-complex associations (~17%) as CCSB-YI1 did for binary interactions.

Binary interactions in AP/MS datasets

We can estimate the number of binary interactions within different datasets using an orthogonal assay like PCA. The window of detection, which is defined by the PRS and RRS detection levels, in PCA is limited. When the statistical significance of the difference between the confirmation rates of the datasets and RRS is calculated, only the confirmation rate of Y2H-union is significantly higher than that of RRS ($P<10^{-3}$; fig. S24A). Thus, PCA alone cannot be used to estimate the fraction of direct binary interactions in the AP/MS datasets.

The number of binary interactions can be estimated using the precision of each dataset. To account for errors, we calculated the lower bound of the precision for each dataset with the following equation:

$$\text{Precision} = \frac{(F_{Dataset} - \sigma_{Dataset}) - (F_{RRS} + \sigma_{RRS})}{(F_{PRS} + \sigma_{PRS}) - (F_{RRS} + \sigma_{RRS})}$$

where F is the fraction positive by PCA (*i.e.*, $F_{Dataset}$, F_{PRS}, or F_{RRS}) and σ is the standard error. Then, we calculated the number of binary interactions:

$$\#\text{ of binary interactions} = Precision_{Dataset} \times N_{Dataset}$$

where N is the total number of interactions in a certain dataset. We found that AP/MS datasets contain less binary interactions than Y2H-union (fig. S24B, C).

AP/MS datasets contain direct interactions which can be recapitulated by binary assays. However, due to the very principle of the methodology, in AP/MS data direct interactions cannot be distinguished from indirect ones. This information is therefore not available for many functional studies or for network analyses. Although AP/MS datasets contain many protein pairs that directly contact each other within complexes, these physical interactions are mixed with

indirect co-complex associations. In an extreme extension of this concept, an interaction assumed between all pair-wise combinations of all proteins encoded in the genome will yield an interactome map that covers 100% of true direct interactions – nonetheless this is obviously not useful information. Therefore, the concept of sensitivity alone (fig. S17D) does not provide worthwhile insight into the quality of the datasets. We should always consider sensitivity together with precision. The precision of all Y2H dataset are significantly better than that of each individual AP/MS dataset (fig. S17B). In SOM II we illustrate this point using the 20S proteasome, for which the crystal structure has been solved. The matrix model to predict interactions from the constituents of the proteasome overestimates the number of direct interactions ~5-fold. Even though AP/MS data help narrow the search space of possibly interacting pairs by knowing the membership of complexes, it does not directly provide binary information. Conversely, Y2H is currently the only available technology that enables unraveling of binary protein-protein interactions at proteome scale. AP/MS is neither superior nor equivalent in providing binary information.

Moreover, the overlap between Combined-AP/MS (~9000 interactions) and Y2H-union (~3000) consists of 260 interactions. This low overlap impressively reaffirms the distinct nature of the data delivered by the two methods -- Y2H does much better in finding transient, condition-specific interactions and those between complexes (SOM XI); whereas AP/MS finds stable complexes, This distinction is also made evident by analyzing functional correlations between interacting pairs (kinase-substrate pairs, transcription factor pairs, and date and party hub analysis).

(SOM VII) Generating a high-quality proteome-scale yeast binary interactome map

To generate a protein interaction dataset as unbiased as possible, we need to eliminate possible biases inherent in different datasets. As shown, co-complex membership datasets are not suitable to be included in the binary interactome map. Despite their high quality, both Uetz-array and LC-multiple datasets have biases which make them unsuitable for deciphering general properties of yeast protein interaction network. As discussed in the main text, bait proteins in Uetz-array are enriched with essential ones. Literature curated datasets combine the information from reported small-scale interaction studies. Therefore, these datasets are prone to sociological and other inspection biases. For instance, a protein not often studied would have a lower degree in this dataset regardless of its actual number of interactors. We plotted the degree of a protein versus number of publications that an interaction involving this protein was reported, and saw a clear correlation in the LC-multiple dataset (fig. S25). However, it is hard to determine whether the higher degree stems from the higher number of publications or higher number of publications result from the degree, or the physiological importance, of the protein. We concluded that the literature-based interaction datasets are not suitable for the analysis requiring unbiased datasets.

To obtain a more comprehensive map of the binary yeast interactome we combined the three unbiased high-throughput Y2H datasets available so far.

"Y2H-union", the union of Uetz-screen, Ito-core, and CCSB-YI1, contains 2,930 binary interactions among 2,018 proteins.

Overlaps between Y2H datasets:

CCSB-YI1 has significant overlaps with both Ito-core (35%, $P<10^{-10}$) and Uetz-screen (27%, $P<10^{-10}$) (Fig. 2D), which are comparable to that between the two most recent high-throughput AP/MS datasets (25% between Krogan and Gavin; fig. S5B). These significant yet partial overlaps are explained by combination of several factors: 1. differences in interrogated protein space, 2. sampling effects, 3. distinct profiles of detected interactions by different Y2H implementations, and 4. use of different ORFs for the experiments.

1. **Search space.** Although the search space of the previous screens was not explicitly documented, 228 interactions from Uetz-screen and 262 interactions from Ito-core datasets could not possibly be detected in our screen because the corresponding ORFs were not present in our starting ORF collection. Adjusting for these increases the overlaps to 27% for Uetz-screen and 35% for Ito-core.
2. **Sampling effects.** For the CCSB-Y2H screen we documented 85% sampling-sensitivity (2 to 3-fold higher than previous attempts; 29% and 35% for Uetz-screen and Ito-core, respectively; SOM VI). Thus, a fraction of the non-reproduced interactions is likely to stem from this still incomplete sampling. The confirmation rates in the small-scale pair-wise test experiment (Fig. 1C) (32% for Uetz-screen, 34% for Ito-core,) match the

overlaps of the overall datasets very well, taking completeness and sampling-sensitivity into account (fig. S26).

3. **Distinct profiles of detected interactions.** Different implementations of any assay lead to detection of distinct sets of interactions. For Y2H, the choice of vectors, yeast strains, and LexA versus Gal4-based transcription factors significantly affects which particular interactions score positive. The very same problems also apply to AP/MS methodologies, where the choice and placement of affinity-tags, cell lines, separation techniques for proteins and peptides, and the instruments and algorithms used for peptide identification can create differences in the final data. We have demonstrated experimentally that not all Y2H systems are identical, and that different interactions can be detected by alternative Y2H implementations. More specifically, we carried out Y2H experiments with two different sets of AD/DB vectors and Y2H strains [CCSB-Y2H and MDC-Y2H (*56*)]. Using the same ORF clones for human PRS, 45% of CCSB-Y2H identified PRS interactions were detected by MDC-Y2H. Such effects are partly responsible for the observed confirmation rates of Uetz-screen and Ito-core in our small-scale (Fig. 1C) and large-scale experiments (Fig. 2D).
4. **ORF collections.** Lastly, even small differences in the tested ORFs can affect whether an interaction is detected. Loss of a single amino acid at either terminus can enable detection of interactions that were previously not detectable. We used a full-length ORF collection that is different from those

used in previous reports, so it is likely that many interactions were not recapitulated as a consequence of such differences.

After removing overlaps with Ito-core, Uetz-screen, LC-multiple and Combined-AP/MS, CCSB-YI1 contains 1,366 novel interactions.

(SOM VIII) Topological analyses and their robustness

Degree distributions of Y2H-union, Combined-AP/MS and LC-multiple

As previously found for many macromolecular and other networks, the degree distribution of Y2H-union is best approximated by a power law (*57*), as are those of Combined-AP/MS and LC-multiple (fig. S6). To investigate the robustness of these fits, we added an exponential cut-off term. Our results indicate that the exponential cut-off term is not significant, confirming the scale-free nature of these datasets (fig. S27).

Other topological features of Y2H-union, Combined-AP/MS and LC-multiple

One common feature of interactome networks is their “small-world” property, characterized by both high clustering coefficient and low characteristic path length (*58*). We calculated these two parameters for Y2H-union, Combined-AP/MS and LC-multiple (fig. S28). As expected, the binary network appears to display the typical small-world property. In contrast**,** the co-complex and literature-curated networks show characteristic path lengths larger than expected for randomized networks with the same degree distribution.

The notion that hubs tend not to interact with each other (*59*), the property of “negative assortativity”, is now clearly re-demonstrated with our new binary map from the negative correlation between degrees of connected nodes observed in Y2H-union (fig. S29). The assortativity of Combined-AP/MS network appears positive, showing that hubs tend to interact with each other in co-complex networks. This is not surprising as most proteins within a complex have similar degrees, and all are represented to interact with each other.

Robustness of the topological analysis

Y2H-union contains 2,930 binary interactions among 2,018 proteins, corresponding to ~20% of all possible binary interactions in yeast cells. It is possible but unlikely that the topological features we observe change as more interactions are reported in the future. To address this concern and demonstrate the robustness of the results obtained with an estimated 20% of interactions, we followed three independent lines of evidence:

1. **Gradual growth of the yeast binary interactome dataset.** The Y2H-union dataset has been compiled using data from three independent experiments that were performed and published sequentially by Uetz *et al.*, Ito *et al*., and our group. When the network analyses were repeated using the individual datasets we found similar topological properties as were described for Y2H-union. One example is the relationship between degree and essentiality shown for the individual datasets in fig. S9. The retention of similar topological properties with gradual growth in binary interactions is strong

evidence that the network properties will remain unchanged as more data are added.

2. **Systematic analysis of sampling effects on topological parameters.** We analyzed potential sampling effects on the degree distribution as previously reported by our group (*60*). In Y2H-union are 2,930 binary interactions among 2,018 proteins, which have an average degree of ~3 and a "node coverage" of ~34%. Given the estimated yeast binary interactome size of 18,000±9000 (95% confidence interval), the average degree of a protein in the full network will be 6±3. Hence, in a network covering ~34% of the nodes an average degree of 2±1 should be expected, which agrees well with the average observed degree. Thus, it is likely that most edges in the subspace of 2,018 nodes have been detected (high "edge coverage"). From Fig. 2 of Han *et al*. (*60*), we can confirm the scale-free nature of the full yeast interactome network with an R-square value greater than 0.8 (R-square value is obtained for a power-law fit).
3. **Re-sampling simulations confirm the robustness of topological parameters.** To further confirm the validity of our results, we performed re-sampling analyses on the calculations of topological parameters (characteristic path length, clustering coefficient, and assortativity) by randomly adding or deleting 5-20% of edges. The results remain statistically equivalent (fig. S30).

   We employed the assortativity measure developed by Newman (*61*).

$$r = \frac{M^{-1}\sum_i j_i k_i - \left[M^{-1}\sum_i \frac{1}{2}(j_i + k_i)\right]^2}{M^{-1}\sum_i \frac{1}{2}(j_i^2 + k_i^2) - \left[M^{-1}\sum_i \frac{1}{2}(j_i + k_i)\right]^2}$$

Where r is the assortativity, j_i and k_i are the degrees of the nodes at the ends of the i th edge, with $i = 1...M$. The assortativity measure r is the Pearson correlation coefficient for the degrees of all directly interacting nodes and can assume values of $-1 \le r \le 1$. For our original Y2H-union network, the measured assortativity was negative (-0.0836) and remained negative even after adding an additional 60% of edges (fig. S30B).

(SOM IX) Essentiality analysis

Possible biases in the datasets towards essentiality

The relation between essentiality and degree in protein-protein interaction (PPI) network was first observed by Jeong *et al*. (*62*) (fig. S9A). The PPI dataset used in that analysis was composed of two sources. First, a literature-curated interaction set collected from Database of Interacting Proteins (DIP) (*24*) (fig. S9B) cannot be used for making reliable predictions for organism level conclusions (SOM VII). Second, the large-scale Y2H assay reported by Uetz *et al*. (*9*) was included. Although there is a correlation between degree and essentiality in the combined Uetz dataset, most of this positive correlation stems from biased bait selection for the Uetz-array dataset (SOM VII, fig. S9C).

The three unbiased datasets (Uetz-screen, Ito-core and CCSB-YI1) show either no or a small positive correlation between degree and essentiality (fig. S9D-

F). This observation is consistent with a lack of correlation noted for unbiased *C. elegans* (unpublished data) and human protein-protein interaction datasets (fig. S9G, H) (*1, 56*).

Clustering of essential proteins

Essential proteins are clustered in the Y2H-union network (fig. S10, S31A). Such a striking interconnectivity between essential proteins might relate to the evolution of the interactome as a whole. In the Combined-AP/MS and LC-multiple networks we also observed such clustering (fig. S31B, C). Moreover, for both datasets, we observed a larger giant component size than expected from random proteins for the network obtained by interactions only between essential proteins. For Combined-AP/MS this is expected because most constituents of an essential complex are essential as well, and these proteins are connected in Combined-AP/MS due to nature of this dataset. However, this high amount of clustering compared to Y2H-union is a signature of a potential bias in LC-multiple. In LC-multiple biases could result from sociological tendencies to study the interactors of essential proteins, which in turn are essential as well, inflating the degrees of essential proteins.

Essentiality and distance analysis

We took each protein as a reference and calculated the fraction of essential proteins among the proteins whose distance to the reference protein is d (d = 1,

2…8). Then we took the average of these fractions for essential, non-essential and all yeast proteins (Fig. 4A).

Giant component size analysis

We selected the same number of nodes as essential proteins (that is 449 proteins) randomly from the Y2H-union dataset 100,000 times. We calculated the giant component size of the network constructed by considering the interactions only between proteins in each randomized protein set (Fig. 4B).

Same complex membership analysis

We selected the same number of edges as the number of edges between essential proteins (242 edges) from Y2H-union dataset 10,000 times. We measured how many of the protein pairs that are connected by an edge are also present in the same complex for each randomization (Fig. 4C). Here, we take the union of all complexes reported by MIPS, Gavin *et al.* (2006) (*13*) or Krogan *et al.* (2006) (*14*), since Collins *et al.* (Combined-AP/MS) did not report any complexes (*16*).

(SOM X) Calculation of fold enrichment

The expected number of overlaps between two genome-wide screens can be estimated using a hypergeometric model as:

$$overlap_{expected} = \frac{m \times n}{N}$$

where *m* is number of pairs in one dataset, *n* is the number of pairs in another dataset, and *N* is the total number of pairs in the genome (18×10^6).

The fold enrichment is therefore:

$$\text{fold enrichment} = \frac{overlap_{observed}}{overlap_{expected}}$$

Note that because we do not know the exact search space for any of the datasets (*i.e.*, Y2H-union, Combined-AP/MS, Phosphorylome, and the regulatory network), it is impossible to calculate the exact $overlap_{expected}$. Our modeling choice is to consider the whole protein-coding genome as the search space, since all of these datasets are genome-wide screens (or combinations of different genome-wide screens).

The recently generated phosphorylome network describes transient biochemical interactions between kinases and their substrates (*17*). We also observed a significant overlap between interactome and phosphorylome data, with the binary interactome more related to the phosphorylome than the co-complex membership network (fig. S13). Thus, combining high-quality Y2H-union with phosphorylome data would generate numerous valuable hypotheses and may lead to a significant growth of knowledge.

(SOM XI) Properties of the merged network

Calculation of the fraction of bottlenecks

We merged the three networks (MIPS, Y2H-union, and Combined-AP/MS) into one network. The betweenness of each edge in this combined network was calculated (*63*). For Fig. 5D, the top 10% of the edges with the highest betweenness are considered as bottlenecks. Changing the specific cutoff does not change the results much (fig. S32). For each dataset:

$$Fraction = \frac{N_{bottleneck}}{N_d}$$

where $N_{bottlenck}$ is the number of bottlenecks in a dataset that are not within MIPS complexes, and N_d is the number of edges in the dataset.

Fraction of edges connecting different MIPS complexes

$$Fraction = \frac{N_{MIPS}}{N_d}$$

where N_{MIPS} is the number of edges in a dataset that connect two MIPS complexes, while N_d is the number of edges in the dataset that are in the space of MIPS complexes, *i.e.*, both end nodes of the edges are within MIPS complexes (not necessarily the same complex though).

Generating a MIPS complexes - Y2H map

We examined the interactions between the constituents of MIPS complexes using Y2H data (fig. S14). We excluded proteins that are constituents of two different

complexes. Several examples of such complex-to-complex connectivity are evident in the resulted complete map of MIPS complexes connected by Y2H interactions (fig. S14). One example is the dynactin complex, which together with the dynein complex is involved in partitioning the mitotic spindle during anaphase B (*64*). The two complexes are known to be connected through an interaction between Nip100 and Pac11 (*65*). We recovered this interaction plus one other connection between the two complexes: the interaction between Arp1 and Pac11 (fig. S14). The dynactin complex can be completely reconstituted with Y2H interactions, whereas four AP/MS experiments failed to detect any interaction within this complex. Another interesting example is the triad of three complexes connected to each other by Y2H interactions: the cyclin-dependent kinase Srb10 and Pho85 complexes (*66, 67*), involved in transcriptional regulation during the cell cycle, connected to the TFIIH complex (a general transcription factor for RNA polymerase II) (*68*) (fig. S14). Pho85 is connected to both the Srb10 complex and TFIIH complex (*69*). The Srb10 and TFIIH complexes are both part of the RNA polymerase II holoenzyme. The Kin28-Ccl1 kinase-cyclin pair in the TFIIH complex is a positive regulator of transcription, whereas the Srb10 complex negatively regulates transcription. The integrated interactome map delineates a connection between the two complexes, providing a starting point for future investigations of the mechanism by which these complexes work together to regulate transcription.

Interactions between complexes

We found that Y2H experiments reveal more inter-complex interactions than intra-complex ones proportionally compared to AP/MS (fig. S13). This does not mean that AP/MS datasets lack interactions connecting different MIPS complexes. Although AP/MS datasets contain many protein pairs that directly contact each other within complexes, such information is mixed with indirect co-complex associations. Furthermore, it is possible that the edges connecting MIPS complexes in the AP/MS datasets indicate alternative complexes with additional subunits rather than true interactions between distinct complexes. We find that more than 60% of AP/MS protein pairs connecting different MIPS complexes are actually assigned to a common complex by the authors (*13, 14*) describing the AP/MS experiments, in contrast to only 10% of such Y2H protein pairs (fig. S33A). Hence, it is likely that protein pairs found in two different MIPS complexes that are connected with an AP/MS edge are mostly subunits of an another complex which is not catalogued in MIPS.

To further explore the differences between the Y2H and AP/MS based edges connecting different complexes, we examined the expression profiles of these protein pairs. Over 80% of AP/MS protein pairs connecting MIPS complexes are also co-expressed (fig. S33A), suggesting that they are likely constituents of the same complex rather than connecting two different complexes. On the contrary, the enrichment of co-expressed Y2H pairs is not as extreme (fig. S33B), indicating that they are connecting different cellular modules/complexes. Our results also demonstrate the dynamic nature of the network: different complexes come

together under specific conditions to perform a certain function via these connections discovered by Y2H experiments.

Other than enrichment of interactions between MIPS complexes, we have other evidence indicating that indeed Y2H interrogates a different subspace within the whole interactome: enrichment of date hubs in the Y2H based interactions (Fig. 3E), differences in the co-expression patterns (Fig. 5C), enrichment of protein pairs supported by transcriptional regulation or phosphorylation (fig. S13) and fraction of bottleneck proteins in the combined network (Fig. 5D).

(SOM XII) Topological and biological features of LC-multiple

We showed potential biases associated with LC-multiple in the main text. Here we examine the properties of this dataset and contrast them with Y2H-union and Combined-AP/MS. In LC-multiple, just as in Y2H-union, we observed a positive correlation between the degree of a protein and number of phenotypes observed when this protein is deleted (fig. S34A). In LC-multiple, just as in Y2H-union and Combined-AP/MS, hubs tend to evolve more slowly than less connected proteins (*44, 70*), in support of the hypothesis that hub proteins contribute to robustness (fig. S34B). Although “negative assortativity”, the concept that hubs tend not to interact with each other (*59*), is clearly demonstrated in Y2H-union from the negative correlation between degrees of connected nodes, in LC-multiple the positive correlation is small, probably stemming from the bias in this dataset (fig. S34C). In LC-multiple the ratio between date and party hubs is drastically different than Y2H-

union and Combined-AP/MS, which suggests that proteins in a coherent sub-modules are preferentially studied (fig. S34D).

Turning to biological features, LC-multiple shows significant enrichment (all $P<10^{-10}$) for functionally similar pairs in all three GO branches (fig. S35A). As GO annotations are based on the literature, the better enrichment in LC-multitple could result from this bias. There is significant enrichment of positive correlations of phenotypic profiles (*20*) between interacting pairs in LC-multiple (fig. S11, S35B), and LC-multiple is also significantly enriched with co-expressed pairs (fig. S12, S35C). The LC-multiple interactions appear slightly more co-expressed than those in Y2H-union, possibly due to a greater fraction of interactions within highly co-expressed complexes (fig. S35C). Interestingly, Y2H-union is enriched in both co-expressed pairs and anti-correlated pairs. An example of anti-correlation is the clear negative correlation between the expression profiles of *YIG1* and *GPP1* (fig. S35D). *GPP1*, together with *GPP2*, encodes glycerol 3-phosphatase (Gpp) (*71*). Overexpression of *YIG1* strongly decreases the activity of Gpp, possibly explaining the anti-correlation (*72*). Strikingly, LC-multiple also exhibited the strongest enrichment of co-regulating TF pairs, indicating a bias towards studying transcription factors (fig. S35E). Likewise, LC-multiple exhibited the strongest enrichment for kinase-substrate pairs, reflective of a bias towards signaling pathways (fig. S35F). However, in the merged network of Y2H-union, Combined-AP/MS, LC-multiple and MIPS, there is significant proportion of bottleneck edges or edges connecting different complexes (fig. S35G, H).

Figure Legends

Supporting Online Material Fig. S1. Illustration of the matrix model interactions for the 20S proteasome complex to show that not all such co-complex associations are direct physical interactions.

Supporting Online Material Fig. S2. Illustration of the biased sampling issue in MIPS for binary interactions.

Supporting Online Material Fig. S3. Schematic of the CCSB high-throughput Y2H screening pipeline.

Supporting Online Material Fig. S4. (**A**) Fraction of protein pairs in PRS, PRS-Y2H (subset of PRS interactions with Y2H evidence), RRS, and CCSB-YI1 that tested positive by PCA, MAPPIT and Y2H. (**B**) Precision of CCSB-YI1 interactome when measured against PRS or PRS-Y2H using PCA, MAPPIT and the combined average.

Supporting Online Material Fig. S5. (**A**) Completeness of Gavin *et al.* (2006) AP/MS experiment. (**B**) Overlap between Krogan and Gavin.

Supporting Online Material Fig. S6. Fitting the degree distributions with a power law distribution for (**A**) Y2H-union, (**B**) Combined-AP/MS, and (**C**) LC-multiple.

Supporting Online Material Fig. S7. Data quality assessment of all currently available yeast interactome datasets. (**A**) Number of interactions reported in various large-scale *S. cerevisiae* protein-protein interaction datasets. (**B**) Fraction of a random sample of interactions from each dataset confirmed by Y2H. (**C**) Fraction of the same samples confirmed by PCA. (**D**) Fraction of positives in each dataset calculated using MIPS. (**E**) Fraction of positives in each dataset calculated

using Binary-GS. Error bars in all figures indicate one SE above and below the value. The color scheme in all figures is: red, Y2H datasets; green, AP/MS datasets; blue: literature-curated datasets; orange, positive reference and GS sets.

Supporting Online Material Fig. S8. Fraction of bait and prey proteins among the proteins with a particular degree in the Uetz-array dataset.

Supporting Online Material Fig. S9. Degree versus essentiality for (**A**) Interaction dataset used in Jeong *et al.* (*62*) (**B**) Literature based portion of Jeong *et al.* **(C**) Uetz-array dataset. (**D**) Uetz-screen dataset. (**E**) Ito-core dataset. (**F**) CCSB-YI1 dataset. (**G**) Y2H-based worm interactome. (**H**) Y2H-based human interactions dataset (*1, 56*).

Supporting Online Material Fig. S10. Interaction network formed by only essential genes. Red edges have only been identified in Y2H-union, green edges were also detected by Combined-AP/MS.

Supporting Online Material Fig. S11. Fraction of pairs with correlated phenotypic profiles (*PCC* cutoff is 0.5).

Supporting Online Material Fig. S12. Fraction of pairs with correlated expression profiles (*PCC* cutoff is 0.5).

Supporting Online Material Fig. S13. Left panel: enrichment of kinase-substrate pairs in protein-protein interaction datasets. Right panel: fraction of edges that connect different MIPS complexes in each network. (Asterisks indicate statistical significance over random expectation).

Supporting Online Material Fig. S14. MIPS complexes connected by Y2H interactions. Thickness of the edges correlates with the number of interacting

protein pairs between the constituents of the complexes. Expanded are the details of interactions between and within dynein and dynactin complexes and Srb10, TFIIH and Pho85 complexes.

Supporting Online Material Fig. S15. Positive and random reference sets (PRS, RRS) are used to optimize assay performance by selecting an assay stringency that increases detection of interactions in PRS and minimizes detection of interactions in RRS.

Supporting Online Material Fig. S16. Precision of high-throughput interaction datasets measured against alternative binary GS sets. (**A**) The binary GS interactions derived from low-throughput experiments recorded in at least two of five interaction databases MIPS, BIND, IntAct, MINT and DIP. (**B**) The binary GS interactions derived from small MIPS complexes of four or less subunits. (**C**) The binary GS interactions derived from co-crystallized proteins recorded in the PDB. (**D**) The interactions in Structure Interaction Network (SIN) dataset. (**E**) The binary GS interactions derived from the highest confidence interactions in the LC-multiple dataset reported by at least five different publications. (**F**) 50% of Binary-GS.

Supporting Online Material Fig. S17. Different measurements of data quality using MIPS and Binary-GS.

Supporting Online Material Fig. S18. Illustration to show the difference in computer-science and biological classification schemes.

Supporting Online Material Fig. S19. False positive rates of all datasets.

Supporting Online Material Fig. S20. Different scoring metrics of data quality using biological data.

Supporting Online Material Fig. S21. The search space of our high-throughput Y2H screen.

Supporting Online Material Fig. S22. Principles of three used interaction assays: Y2H, restoration of the Gal4 transcription factor; MAPPIT, reconstitution of a signaling cascade, activation of STAT3 dependent transcription; PCA, reconstitution of Yellow Fluorescent Protein (YFP).

Supporting Online Material Fig. S23. Datasets can be empirically evaluated by testing a subset of interactions and comparing the results against PRS (positive controls) and RRS (negative controls).

Supporting Online Material Fig. S24. (**A**) Fraction confirmed by PCA for samples from Y2H-union, Combined-AP/MS, and AP/MS-union. *P*-values report the statistical significance of differences in the confirmation rate of each dataset with the detection level of RRS. (**B**) Lower bound estimation of precision using PCA confirmation results. (**C**) Estimated (lower bound) number of binary interactions in each dataset. Pie charts: estimated fraction of binary interactions in each dataset.

Supporting Online Material Fig. S25. Relationships between degree and the average number of publications associated with proteins of the corresponding degree for interactions reported in Y2H-union and LC-multiple.

Supporting Online Material Fig. S26. Overlap between CCSB-YI1 and Ito-core (Uetz-screen).

Supporting Online Material Fig. S27. (**A**) Fitting the degree distributions with a power law with exponential cut-off function without binning the data. (**B**) Fitting the

degree distributions with a power law with exponential cut-off function after log-binning the data.

Supporting Online Material Fig. S28. Characteristic path length (*L*) and clustering coefficient (*C*) of the three networks compared with those of random networks with the same degree-distribution and associated *P*-values.

Supporting Online Material Fig. S29. The relationships between increasing degree of a gene product and the average degree of its immediate neighbors.

Supporting Online Material Fig. S30. (**A**) Robustness of topological parameters (characteristic path length and clustering coefficient) with random addition of edges. (**B**) Robustness of the negative assortativity result with random addition of edges.

Supporting Online Material Fig. S31. Essential proteins in Y2H-union, Combined AP/MS and LC-multiple networks. Nodes corresponding to essential proteins are labeled by filled circles. In the bottom, giant component size of the networks formed by essential proteins and their random controls obtained by selecting same number of nodes randomly 100,000 times from the corresponding datasets.

Supporting Online Material Fig. S32. Fraction of bottlenecks in each dataset with different cut-offs to define bottlenecks.

Supporting Online Material Fig. S33. (**A**) For interactions between MIPS complexes, left panel: fraction of protein pairs reported as being in the same complex; right panel: fraction of co-expressed protein pairs (with *PCC* > 0.5). (**B**) Distribution of Pearson correlation coefficients of protein pairs connecting different MIPS complexes.

Supporting Online Material Fig. S34. Topological properties of LC-multiple compared to Y2H-union and Combined-AP/MS. The relationships between increasing degree of a gene product and (**A**) the number of phenotypes associated with deletion of the encoding gene; (**B**) the average mutation rate of the encoding gene (*dN/dS*); and (**C**) the average degree of its immediate neighbors. **(D**) Contribution of date hubs and party hubs to the LC-multiple interaction networks, as measured by change in the characteristic path length after simulated removal of edges by deleting the indicated types of nodes. Inset: fraction of date hubs and party hubs.

Supporting Online Material Fig. S35. Biological features of yeast interactome datasets with the addition of LC-multiple. (**A**) Enrichment of interacting protein pairs (measured relative to random) that share GO annotations in the biological process, cellular component and molecular function branches of the GO ontology. (**B**) Pearson correlation coefficient (*PCC*) of phenotypic profiles between interacting pairs in different datasets. (**C**) Co-expression correlation between interacting pairs. (**D**) Expression profiles of the interacting proteins Yip1 and Gpp1 show a clear negative correlation. (**E**) Enrichment of interacting proteins as targets of a common TF (co-regulated), and enrichment of interacting TFs in a common MIM (co-regulating). (**F**) Enrichment of kinase-substrate pairs in protein-protein interaction datasets. (Asterisks indicate statistical significance over random expectation). (**G**) Fraction of bottlenecks from each dataset in the combined network which consists of interactions from MIPS, Y2H-union, Combined-AP/MS,

and LC-multiple datasets. (**H**) Fraction of edges that connect different MIPS complexes in each network.

SOM References

1. J. F. Rual *et al.*, *Nature* **437**, 1173 (2005).
2. D. M. Gelperin *et al.*, *Genes Dev.* **19**, 2816 (2005).
3. P. James, J. Halladay, E. A. Craig, *Genetics* **144**, 1425 (1996).
4. A. J. Walhout, M. Vidal, *Genome Res.* **9**, 1128 (1999).
5. M. Vidal, P. Braun, E. Chen, J. D. Boeke, E. Harlow, *Proc. Natl. Acad. Sci. USA* **93**, 10321 (1996).
6. M. Vidal, R. K. Brachmann, A. Fattaey, E. Harlow, J. D. Boeke, *Proc. Natl. Acad. Sci. USA* **93**, 10315 (1996).
7. I. Lemmens, S. Lievens, S. Eyckerman, J. Tavernier, *Nat. Protoc.* **1**, 92 (2006).
8. I. Remy, S. W. Michnick, *Methods Mol. Biol.* **261**, 411 (2004).
9. P. Uetz *et al.*, *Nature* **403**, 623 (2000).
10. T. Ito *et al.*, *Proc. Natl. Acad. Sci. USA* **98**, 4569 (2001).
11. A. C. Gavin *et al.*, *Nature* **415**, 141 (2002).
12. Y. Ho *et al.*, *Nature* **415**, 180 (2002).
13. A. C. Gavin *et al.*, *Nature* **440**, 631 (2006).
14. N. J. Krogan *et al.*, *Nature* **440**, 637 (2006).
15. T. Reguly *et al.*, *J. Biol.* **5**, 11 (2006).
16. S. R. Collins *et al.*, *Mol. Cell. Proteomics* **6**, 439 (2007).
17. J. Ptacek *et al.*, *Nature* **438**, 679 (2005).
18. H. Yu, M. Gerstein, *Proc. Natl. Acad. Sci. USA* **103**, 14724 (2006).
19. D. P. Wall *et al.*, *Proc. Natl. Acad. Sci. USA* **102**, 5483 (2005).
20. A. M. Dudley, D. M. Janse, A. Tanay, R. Shamir, G. M. Church, *Mol. Syst. Biol.* **1**, 0001 (2005).
21. R. J. Marinelli *et al.*, *Nucleic Acids Res.* **36**, D871 (2008).
22. Gene Ontology Consortium, *Nucleic Acids Res.* **36**, D440 (2008).
23. H. W. Mewes *et al.*, *Nucleic Acids Res.* **34**, D169 (2006).
24. I. Xenarios *et al.*, *Nucleic Acids Res.* **30**, 303 (2002).
25. G. D. Bader, D. Betel, C. W. Hogue, *Nucleic Acids Res.* **31**, 248 (2003).
26. A. Chatr-aryamontri *et al.*, *Nucleic Acids Res.* **35**, D572 (2007).
27. H. Hermjakob *et al.*, *Nucleic Acids Res.* **32**, D452 (2004).
28. R. Jansen, M. Gerstein, *Curr. Opin. Microbiol.* **7**, 535 (2004).
29. I. Remy, S. W. Michnick, *Nat. Methods* **3**, 977 (2006).
30. G. MacBeath, S. L. Schreiber, *Science* **289**, 1760 (2000).
31. M. L. Goodson, B. Farboud, M. L. Privalsky, *Nucl. Recept. Signal.* **5**, e002 (2007).
32. S. F. Martin, M. H. Tatham, R. T. Hay, I. D. Samuel, *Protein Sci.* **17**, 777 (2008).
33. A. Ben-Hur, W. S. Noble, *BMC Bioinformatics* **7 Suppl 1**, S2 (2006).
34. A. Gomez, N. Domedel, J. Cedano, J. Pinol, E. Querol, *Bioinformatics* **19**, 895 (2003).
35. R. Jansen *et al.*, *Science* **302**, 449 (2003).
36. C. von Mering *et al.*, *Nature* **417**, 399 (2002).
37. G. D. Bader, C. W. Hogue, *Nat. Biotechnol.* **20**, 991 (2002).
38. M. Groll *et al.*, *Nature* **386**, 463 (1997).
39. P. Aloy, R. B. Russell, *Trends Biochem. Sci.* **27**, 633 (2002).
40. S. A. Teichmann, *J. Mol. Biol.* **324**, 399 (2002).
41. H. Yu *et al.*, *Genome Res.* **14**, 1107 (2004).
42. A. Kouranov *et al.*, *Nucleic Acids Res.* **34**, D302 (2006).
43. J. S. Bader, A. Chaudhuri, J. M. Rothberg, J. Chant, *Nat. Biotechnol.* **22**, 78 (2004).

44. P. M. Kim, L. J. Lu, Y. Xia, M. B. Gerstein, *Science* **314**, 1938 (2006).
45. I. Lee, S. V. Date, A. T. Adai, E. M. Marcotte, *Science* **306**, 1555 (2004).
46. S. Suthram, T. Shlomi, E. Ruppin, R. Sharan, T. Ideker, *BMC Bioinformatics* **7**, 360 (2006).
47. S. Li *et al.*, *Science* **303**, 540 (2004).
48. L. Giot *et al.*, *Science* **302**, 1727 (2003).
49. C. A. Stanyon *et al.*, *Genome Biol.* **5**, R96 (2004).
50. E. Formstecher *et al.*, *Genome Res.* **15**, 376 (2005).
51. S. Fields, *FEBS J.* **272**, 5391 (2005).
52. H. Yu, R. Jansen, G. Stolovitzky, M. Gerstein, *Bioinformatics* **23**, 2163 (2007).
53. C. J. Jeffery, *Trends Genet.* **19**, 415 (2003).
54. E. L. Hong *et al.*, *Nucleic Acids Res.* **36**, D577 (2008).
55. S. Ghaemmaghami *et al.*, *Nature* **425**, 737 (2003).
56. U. Stelzl *et al.*, *Cell* **122**, 957 (2005).
57. A. L. Barabási, R. Albert, *Science* **286**, 509 (1999).
58. D. J. Watts, S. H. Strogatz, *Nature* **393**, 440 (1998).
59. S. Maslov, K. Sneppen, *Science* **296**, 910 (2002).
60. J. D. Han, D. Dupuy, N. Bertin, M. E. Cusick, M. Vidal, *Nat. Biotechnol.* **23**, 839 (2005).
61. M. E. Newman, *Phys. Rev. Lett.* **89**, 208701 (2002).
62. H. Jeong, S. P. Mason, A. L. Barabasi, Z. N. Oltvai, *Nature* **411**, 41 (2001).
63. H. Yu, P. M. Kim, E. Sprecher, V. Trifonov, M. Gerstein, *PLoS Comput. Biol.* **3**, e59 (2007).
64. J. A. Kahana *et al.*, *Mol. Biol. Cell* **9**, 1741 (1998).
65. B. L. Drees *et al.*, *J. Cell Biol.* **154**, 549 (2001).
66. A. S. Carroll, E. K. O'Shea, *Trends Biochem. Sci.* **27**, 87 (2002).
67. S. Kuchin, P. Yeghiayan, M. Carlson, *Proc. Natl. Acad. Sci. USA* **92**, 4006 (1995).
68. G. Orphanides, T. Lagrange, D. Reinberg, *Genes Dev.* **10**, 2657 (1996).
69. V. Measday *et al.*, *Mol. Cell. Biol.* **17**, 1212 (1997).
70. H. B. Fraser, D. P. Wall, A. E. Hirsh, *BMC Evol. Biol.* **3**, 11 (2003).
71. A. K. Pahlman, K. Granath, R. Ansell, S. Hohmann, L. Adler, *J. Biol. Chem.* **276**, 3555 (2001).
72. K. Granath, T. Modig, A. Forsmark, L. Adler, G. Liden, *Yeast* **22**, 1257 (2005).

SUPPLEMENTARY FIGURE S1

20S proteasome

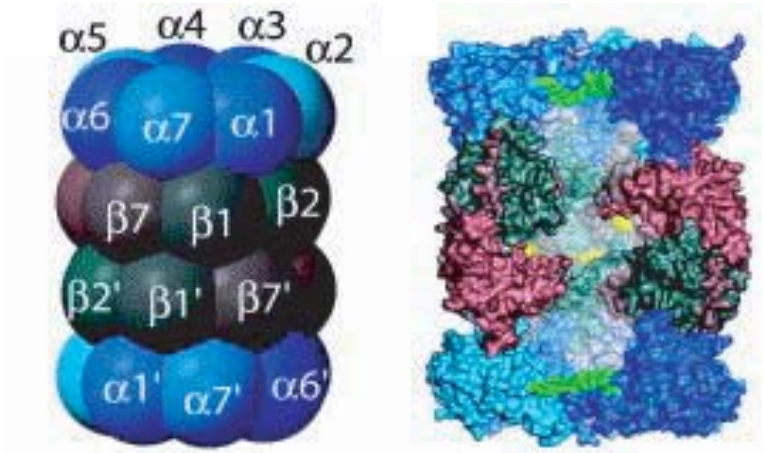

In reality, each subunit interacts with 6 neighboring proteins and each subunit interacts with 4 neighboring proteins

70 interactions

Matrix Model

Each protein has 27 interacting partners

378 interactions

(The figure of 20S proteasome structure is adapted from M. Rechsteiner, C.P. Hill, *Trends Cell Biol*, 15:27–33, 2005)

SUPPLEMENTARY FIGURE S2

A. Binary GSs explore the binary interaction space the same way as Y2H

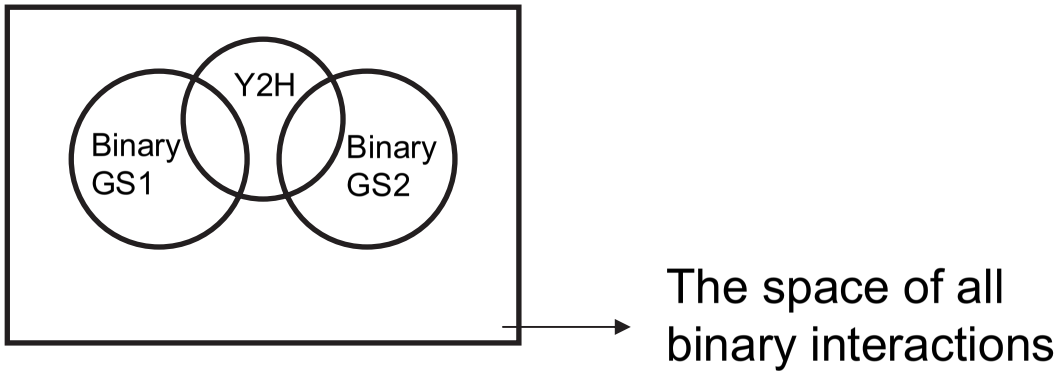

B. MIPS as a gold standard set explores the space differently and therefore has an artificially smaller overlap with Y2H

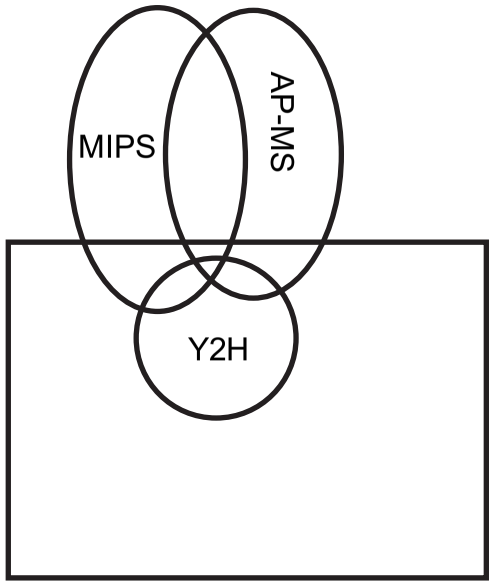

SUPPLEMENTARY FIGURE S3

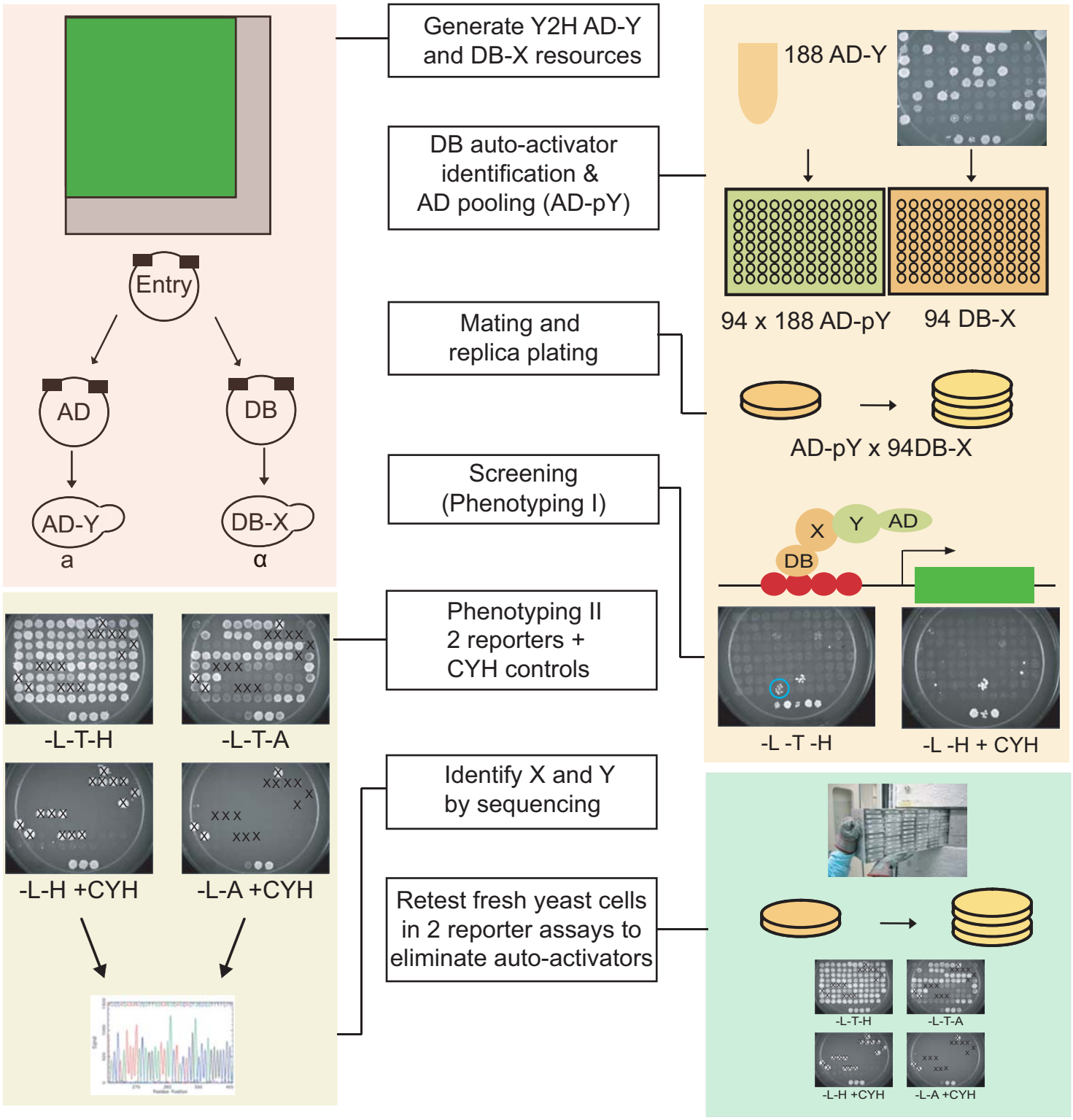

SUPPLEMENTARY FIGURE S4

A

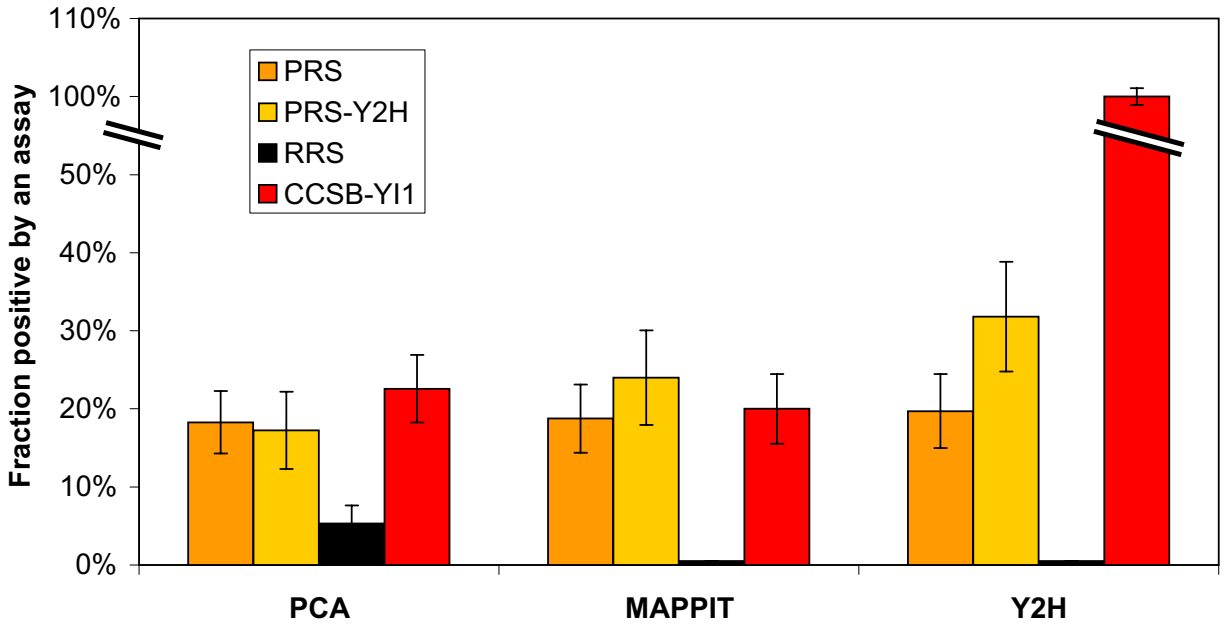

B

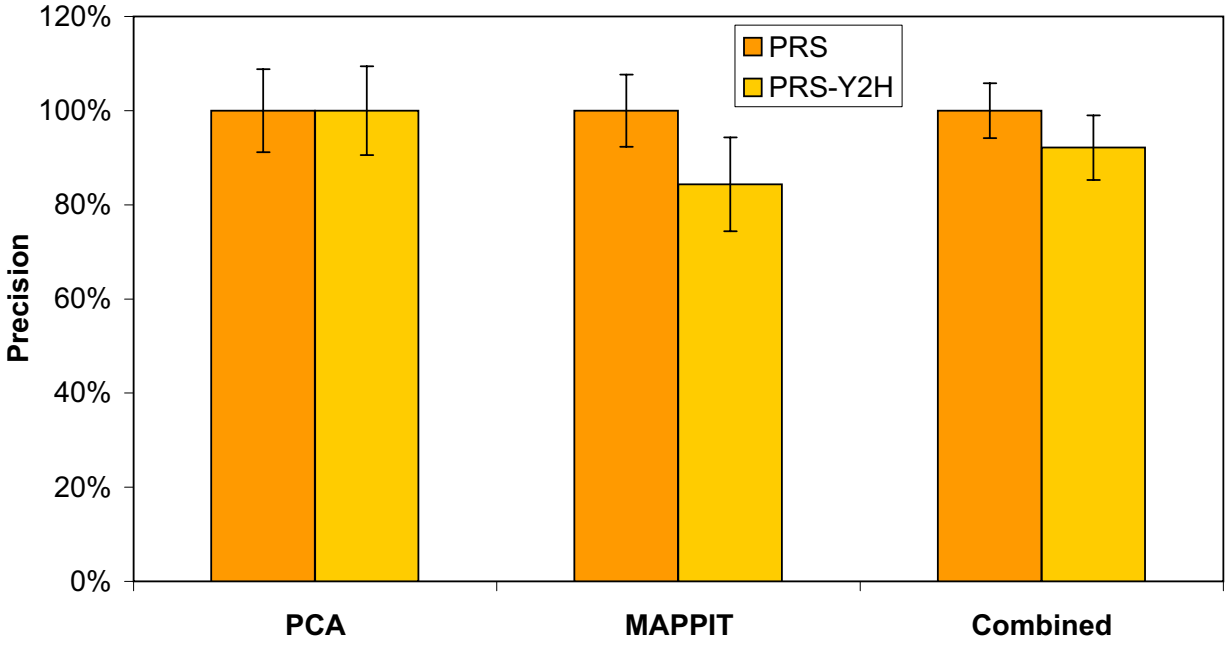

SUPPLEMENTARY FIGURE S5

A

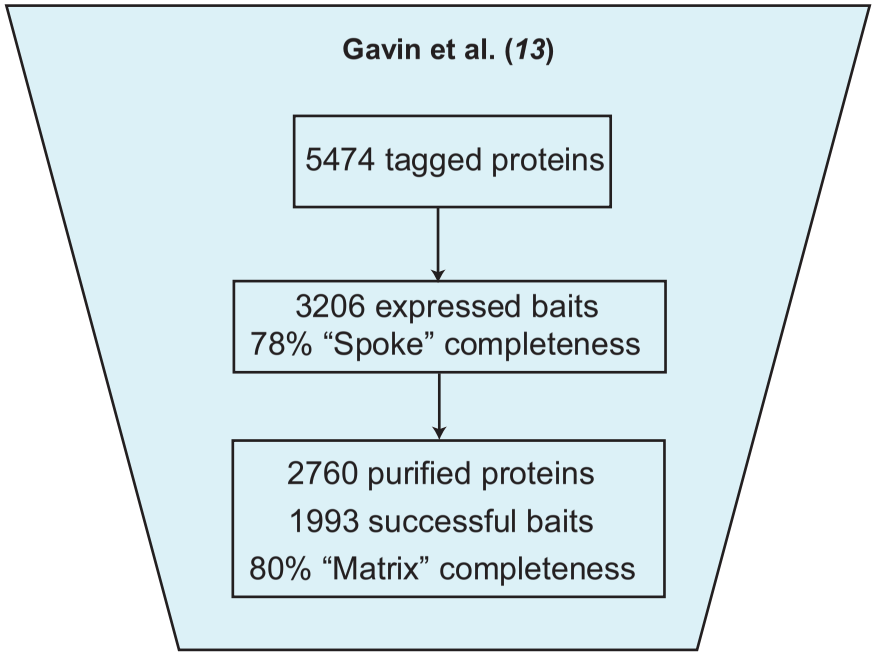

B

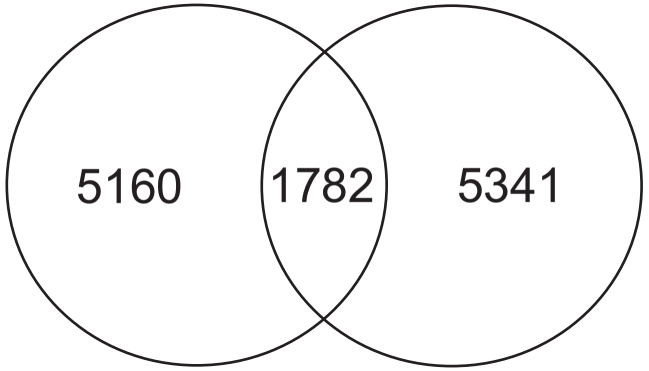

Gavin *et al.* (2006)
Overlap: 26%

Krogan *et al.* (2006)
Overlap: 25%

SUPPLEMENTARY FIGURE S6

A

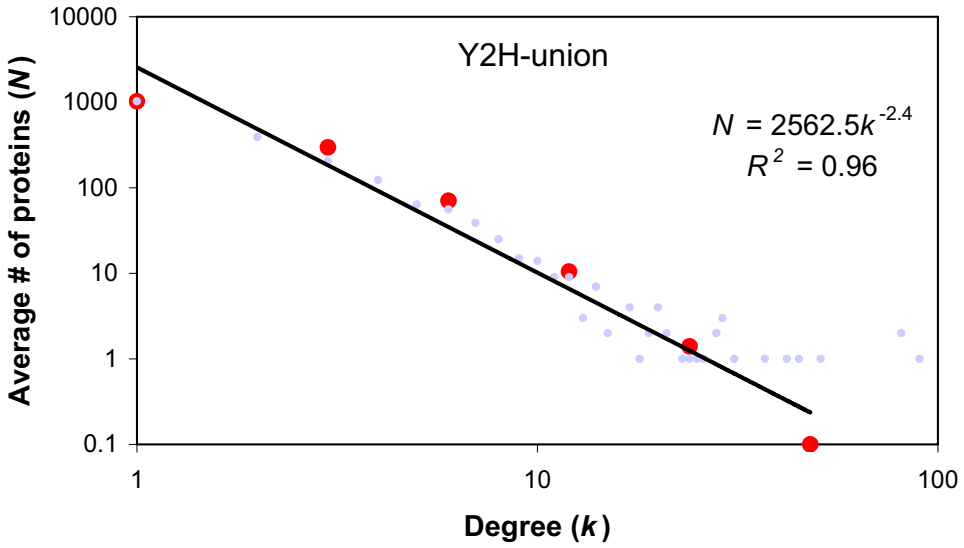

B

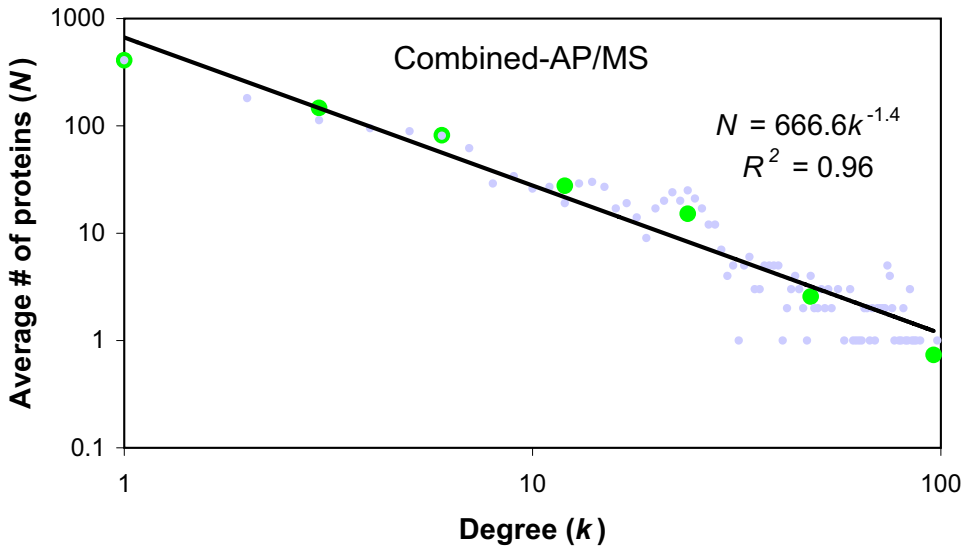

C

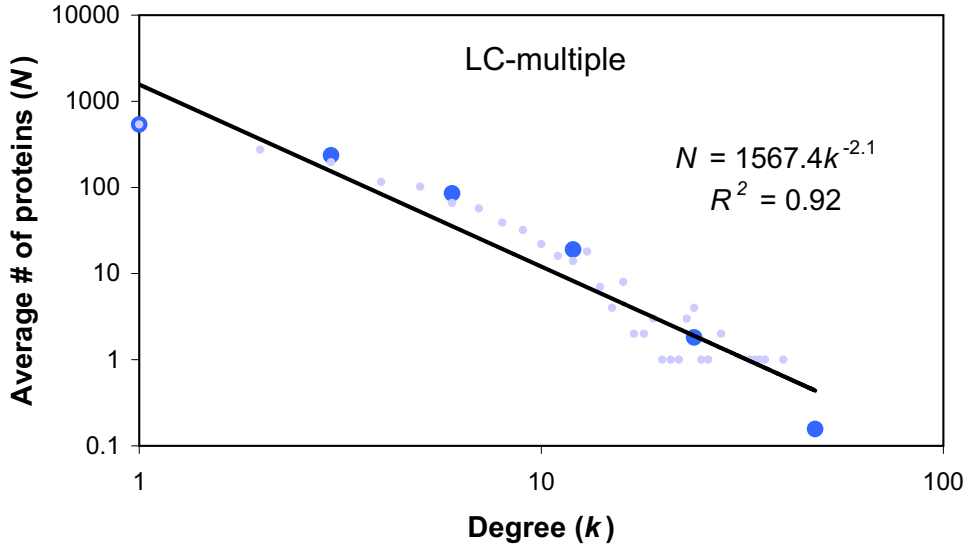

SUPPLEMENTARY FIGURE S7

A

Reference	Uetz *et al.* (9)		Ito *et al.* (10)		Gavin *et al.* (11)	Ho *et al.* (12)	Gavin *et al.* (13)	Krogan *et al.* (14)	Reguly *et al.* (15)	
Dataset name	Uetz-screen	Uetz-array	Ito-core	Ito-noncore	Gavin2002-spoke	Ho-spoke	Gavin	Krogan	LC-multiple	LC-one
# of interactions	682	281	843	3632	3210	3597	6942	7123	2925	8933

Binary Co-complex Literature

B

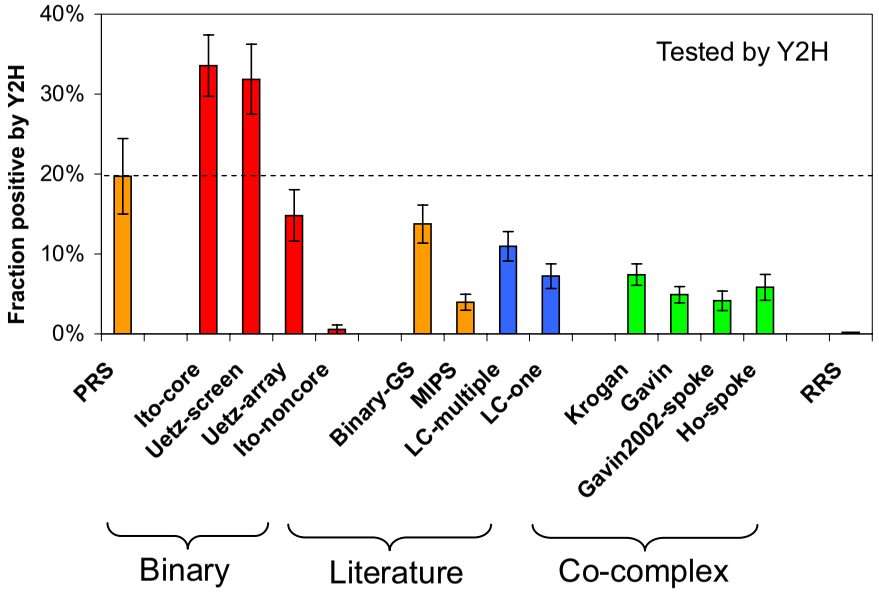

C

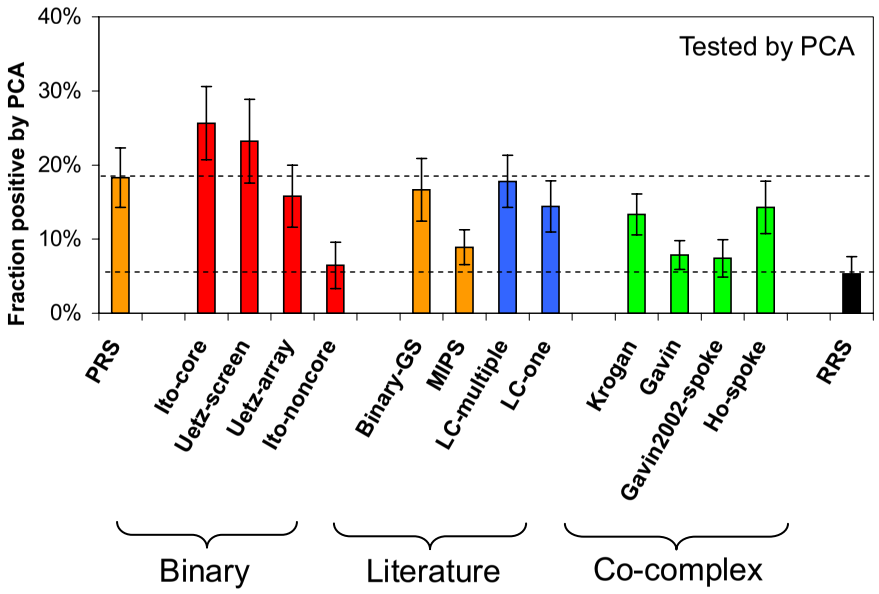

D

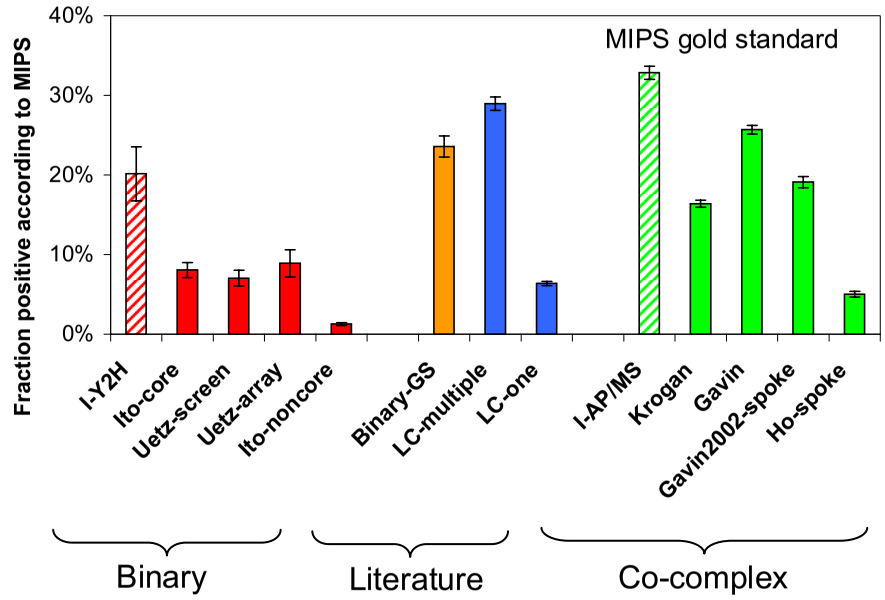

E

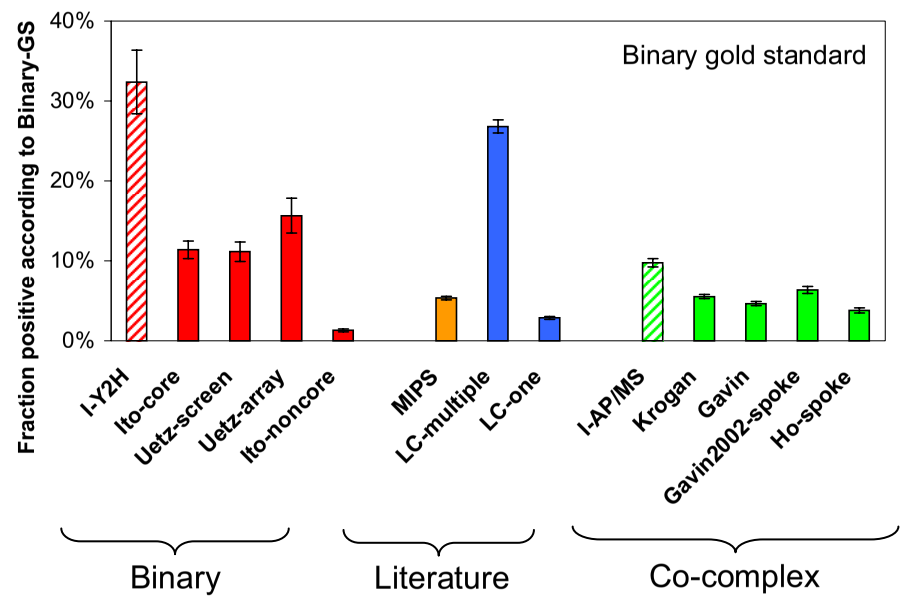

SUPPLEMENTARY FIGURE S8

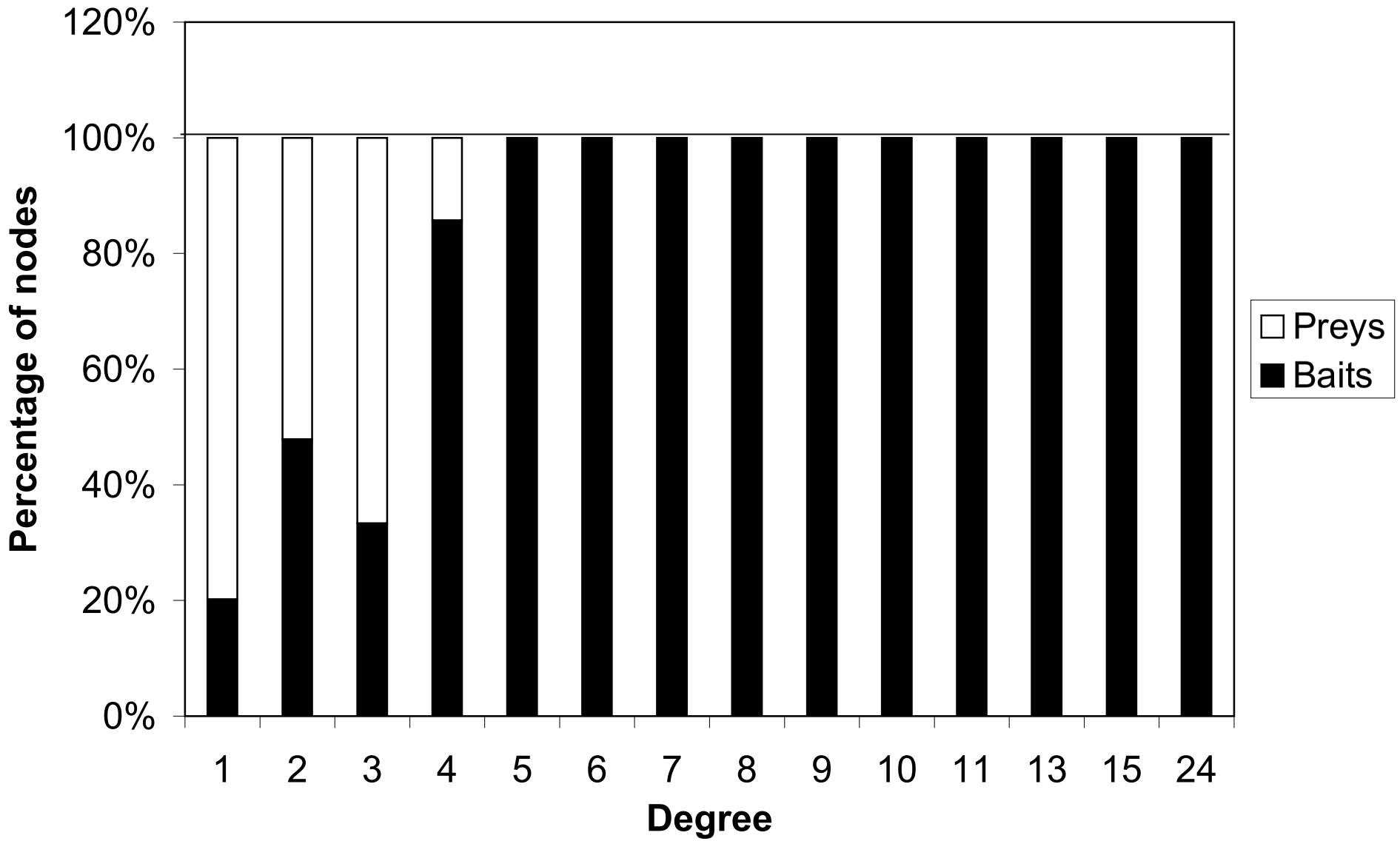

SUPPLEMENTARY FIGURE S9

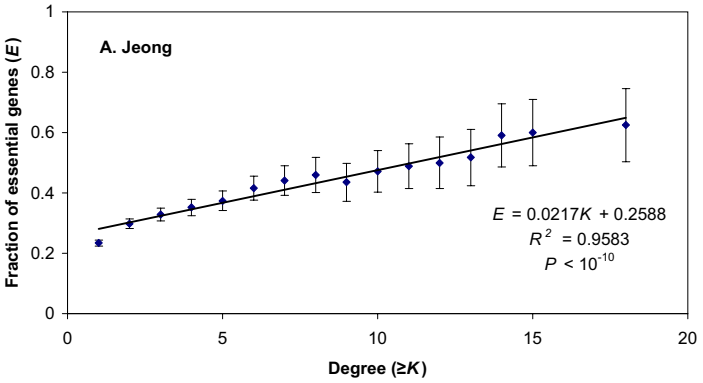

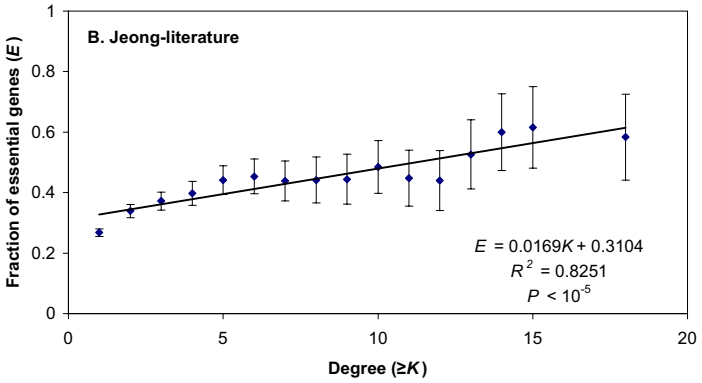

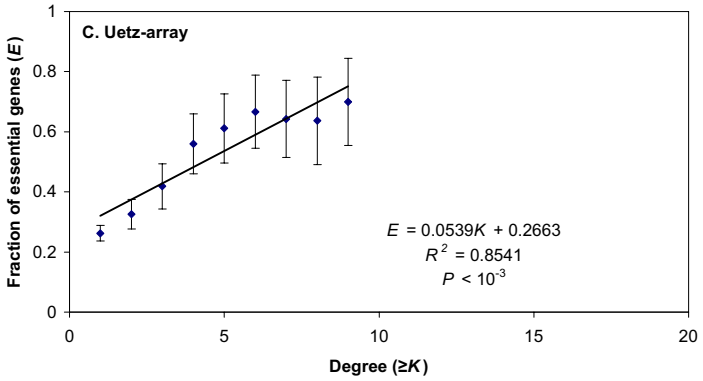

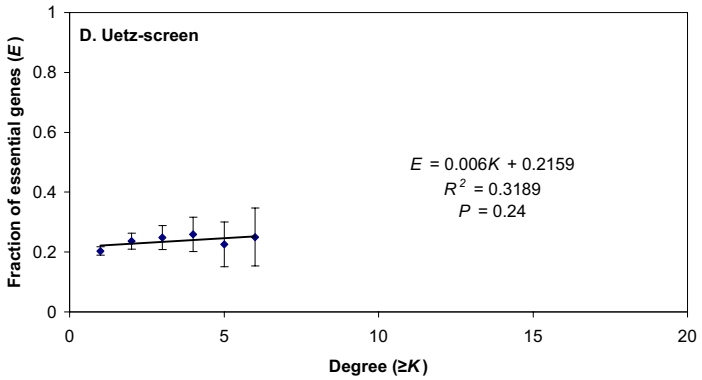

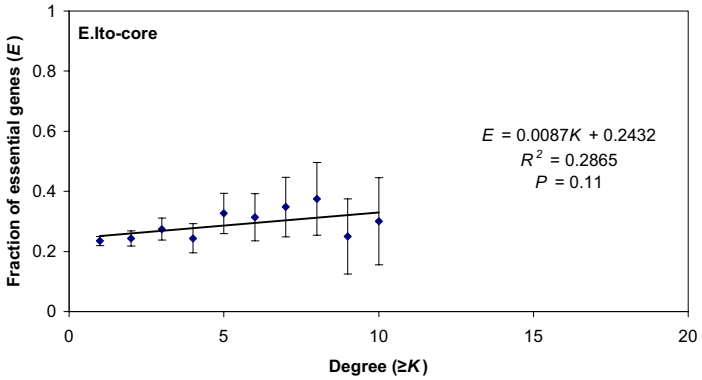

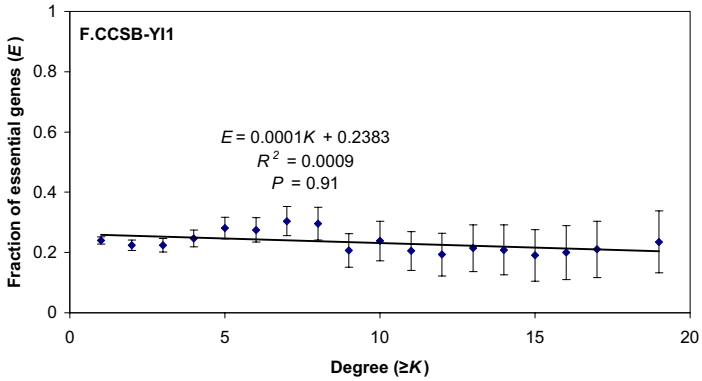

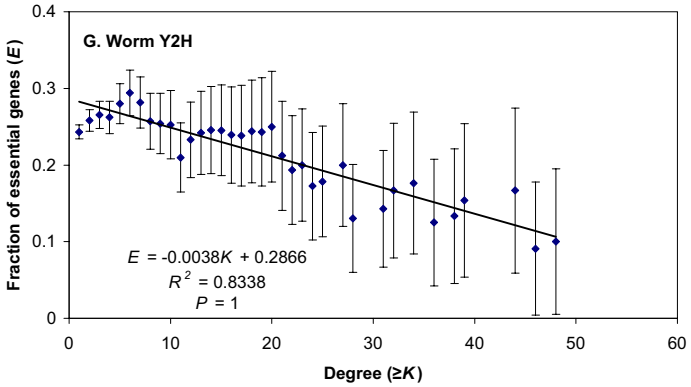

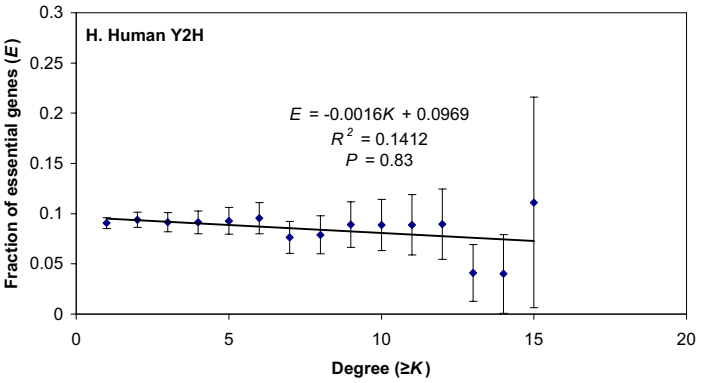

SUPPLEMENTARY FIGURE S10

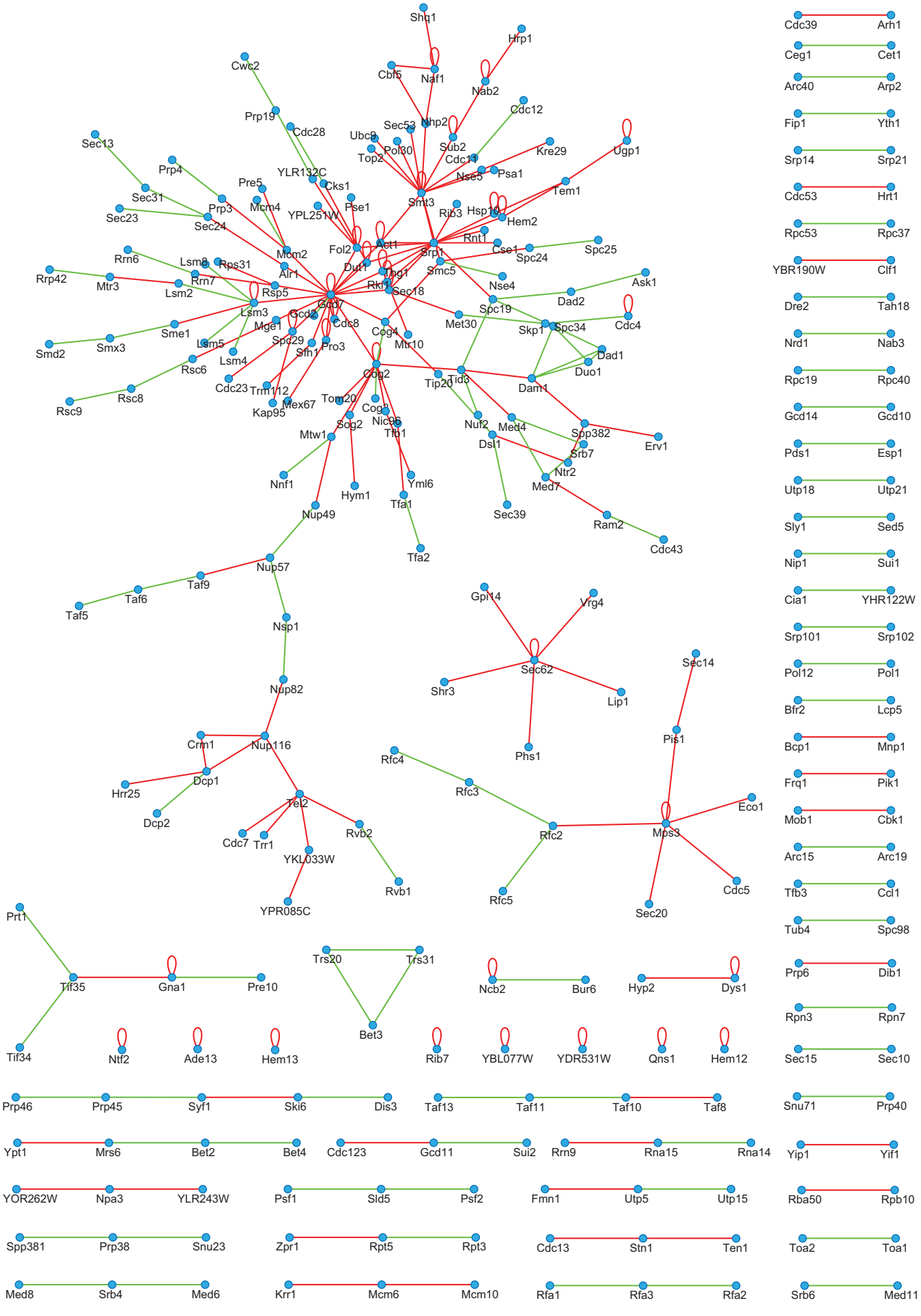

SUPPLEMENTARY FIGURE S11

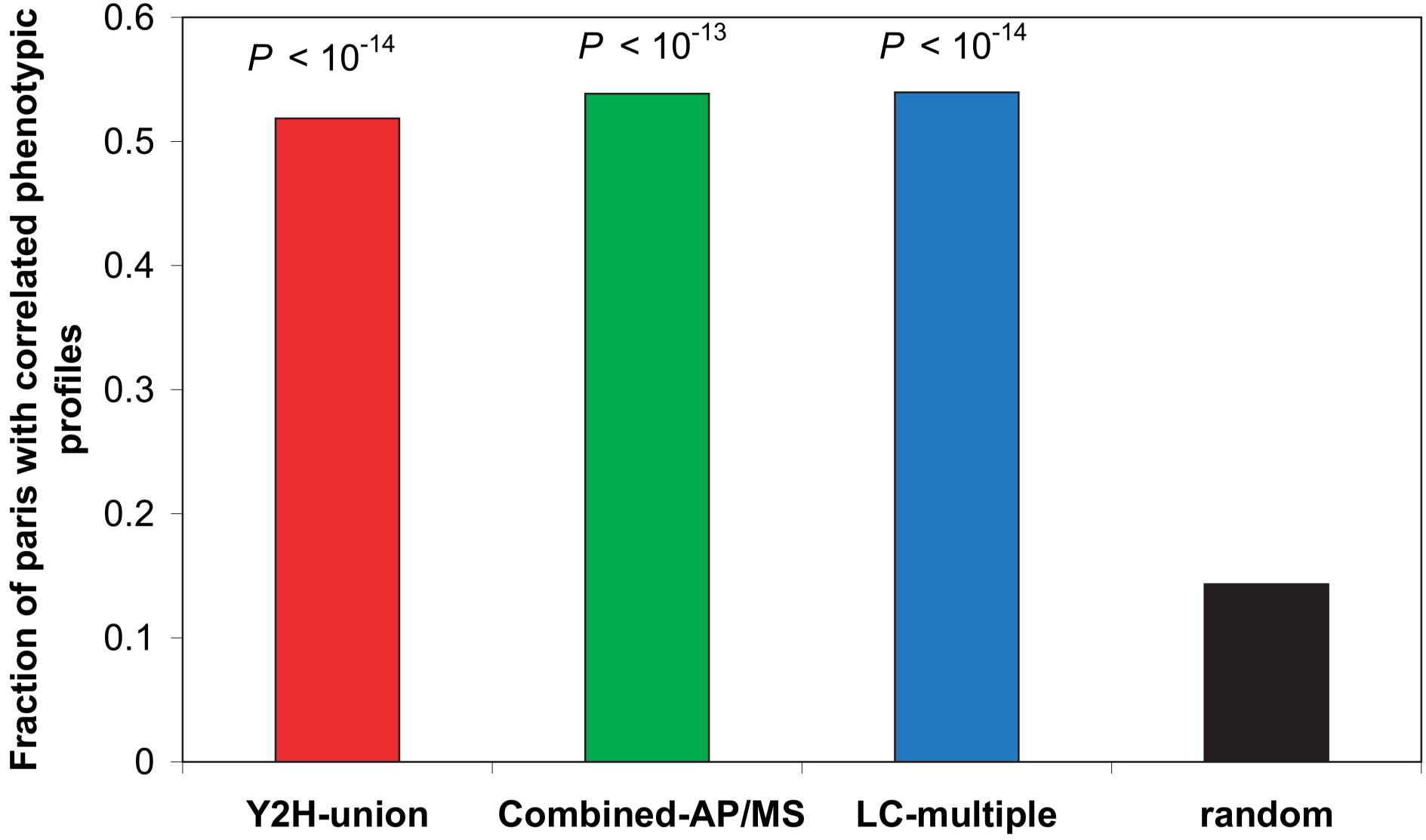

SUPPLEMENTARY FIGURE S12

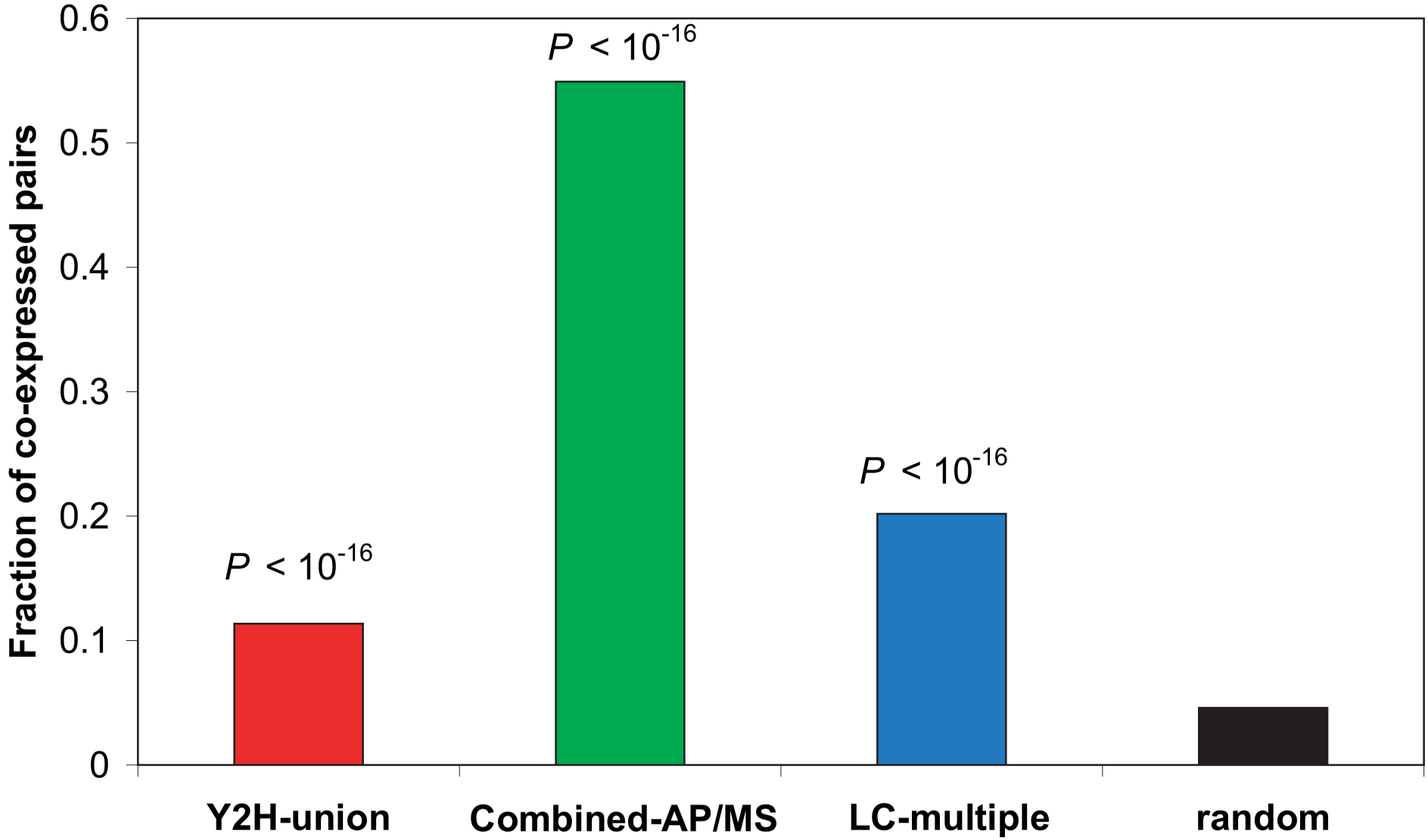

SUPPLEMENTARY FIGURE S13

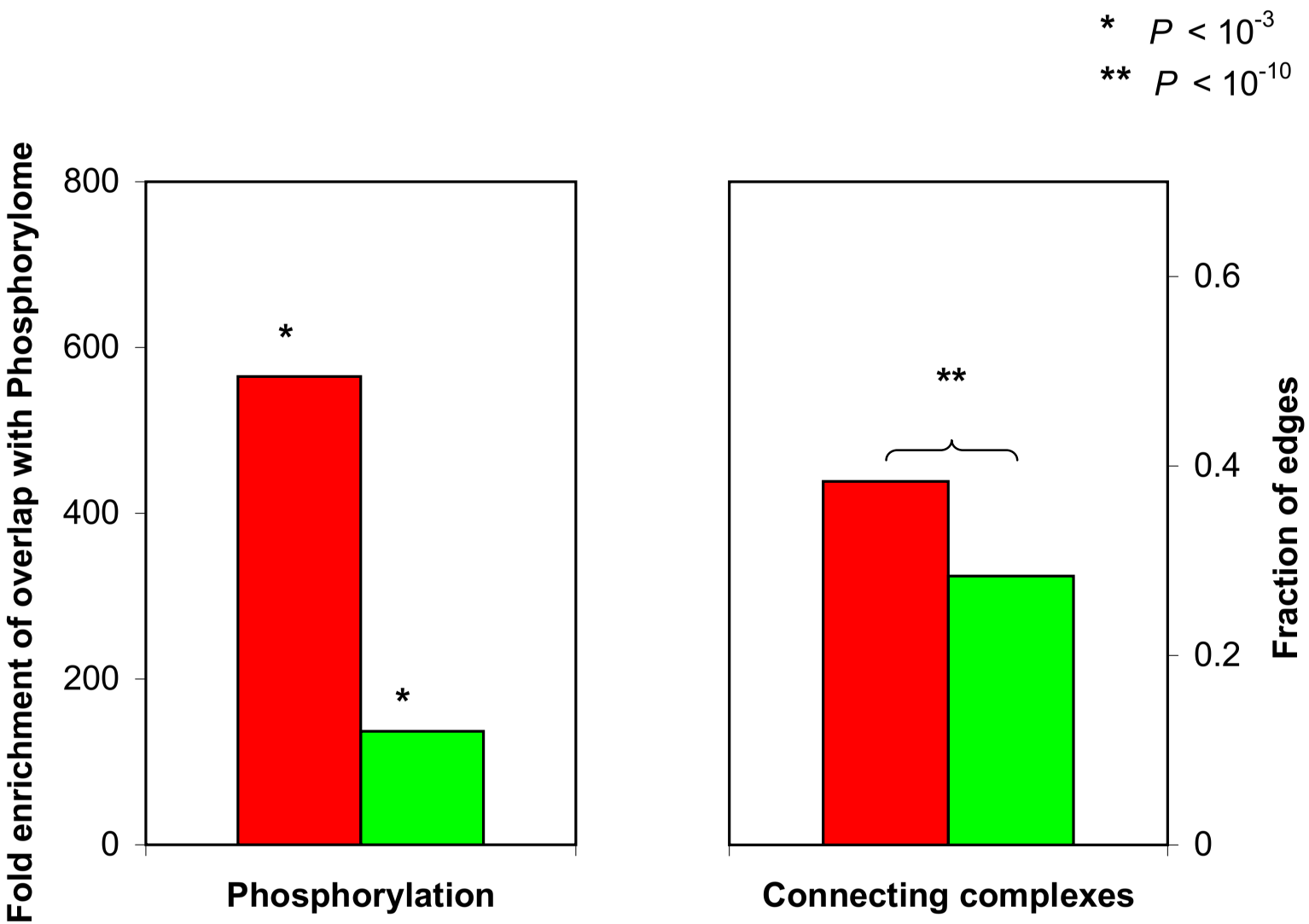

SUPPLEMENTARY FIGURE S14

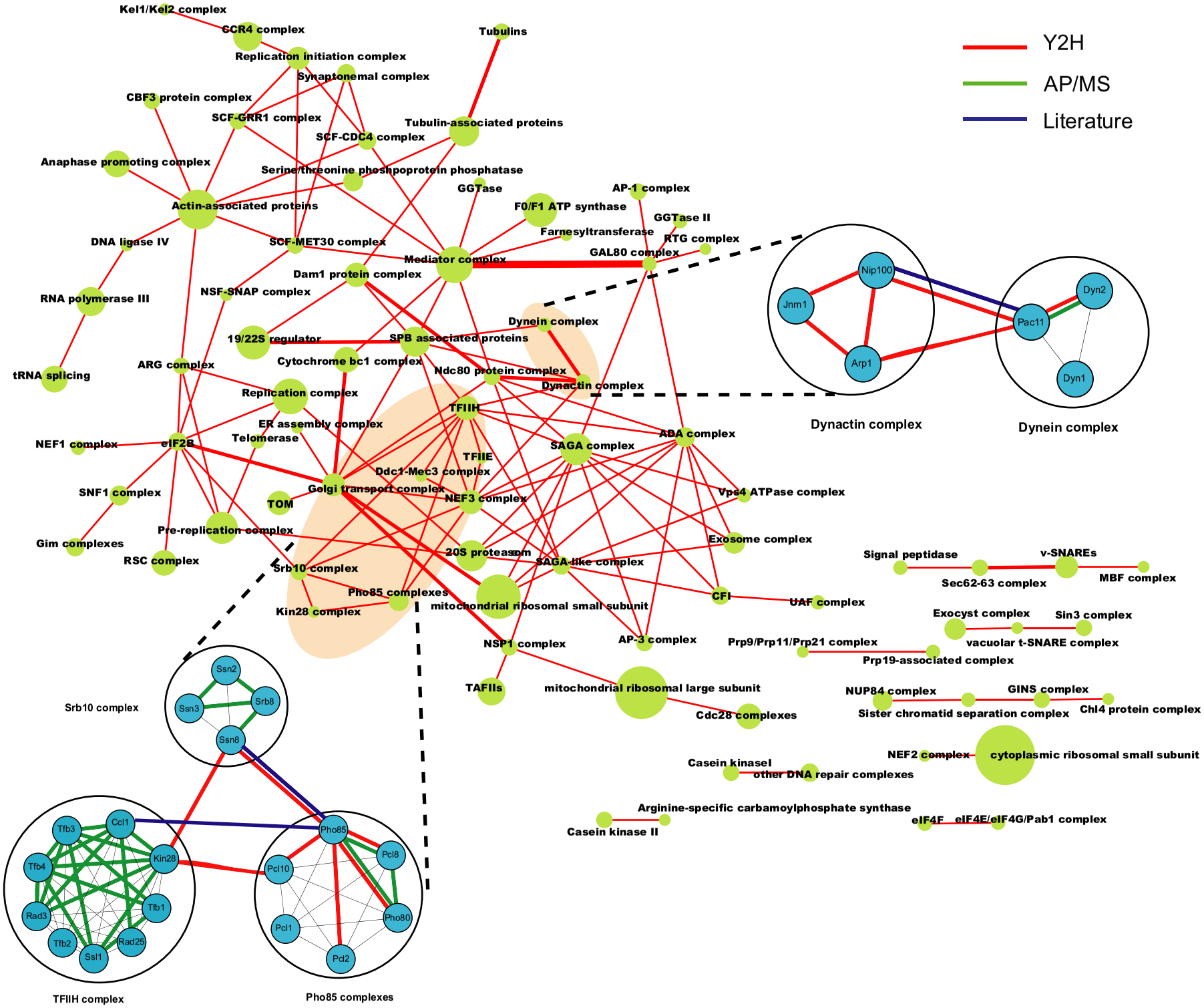

SUPPLEMENTARY FIGURE S15

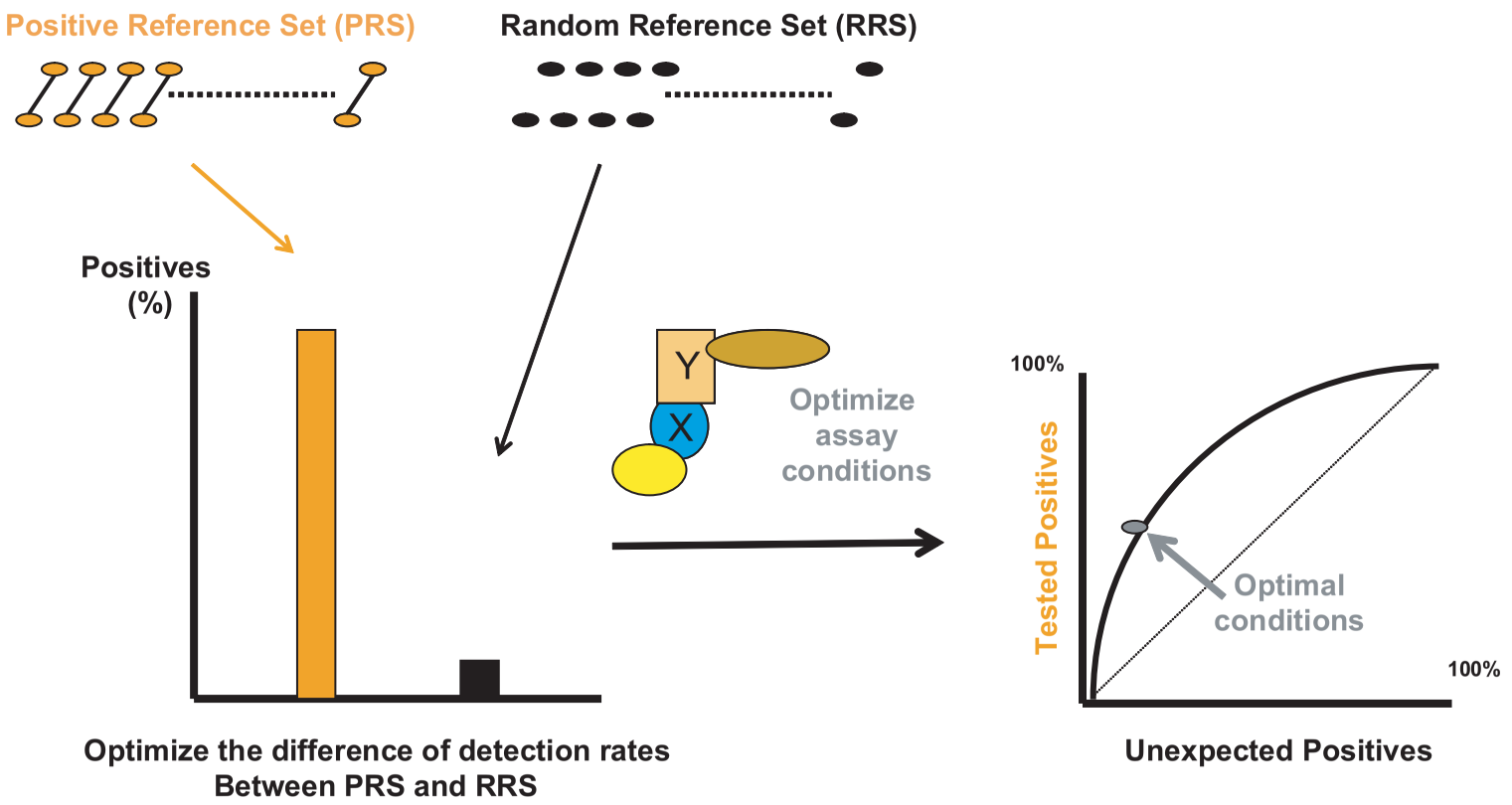

SUPPLEMENTARY FIGURE S16

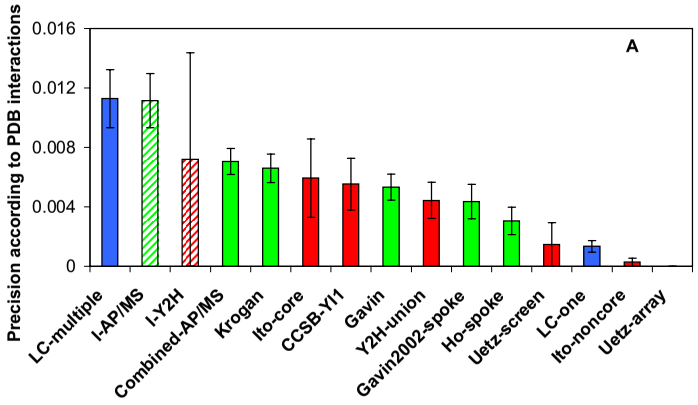

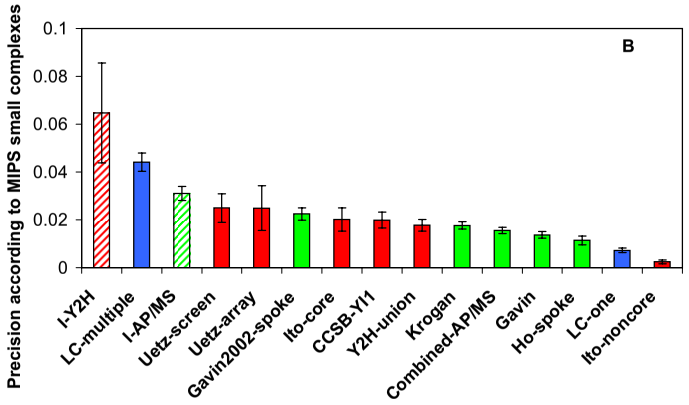

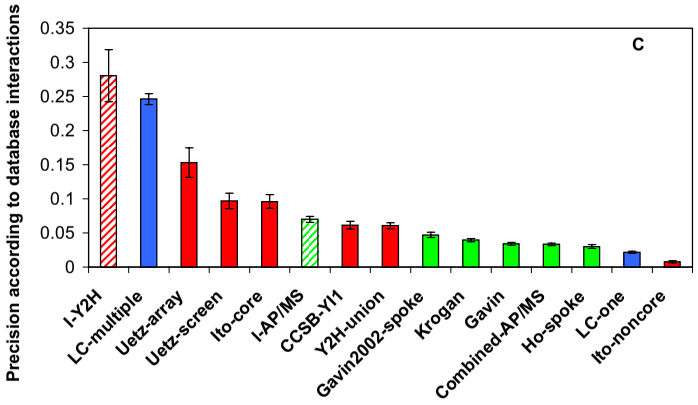

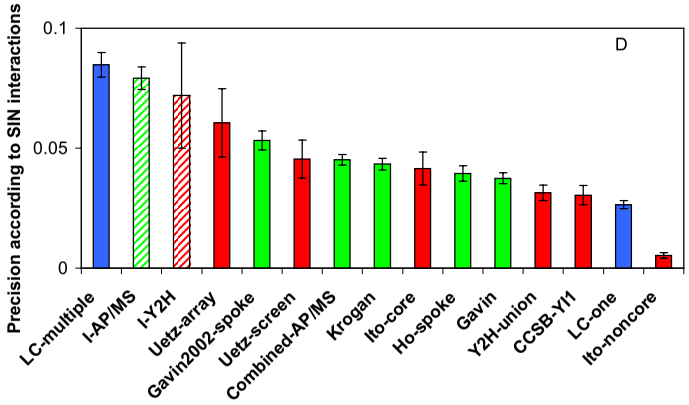

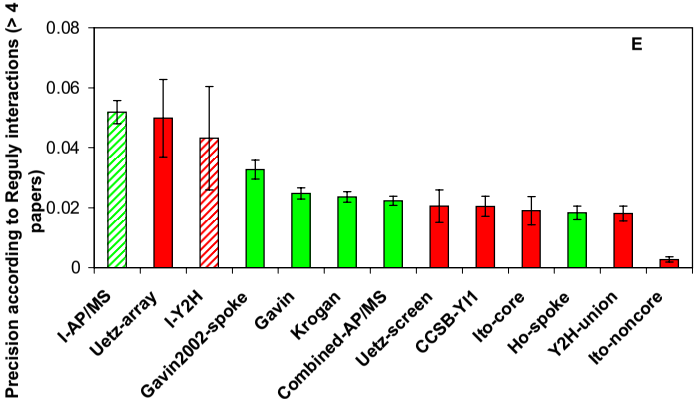

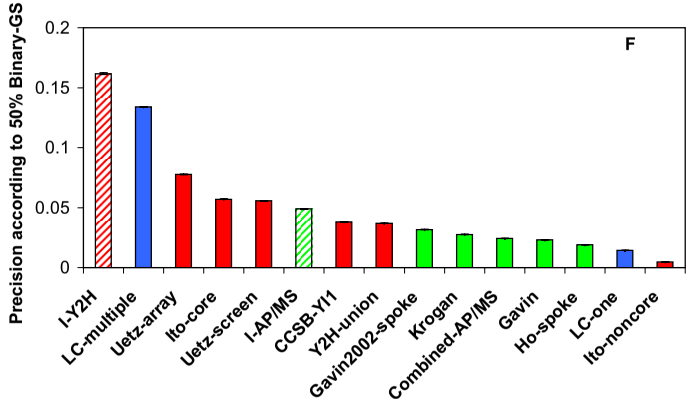

SUPPLEMENTARY FIGURE S17

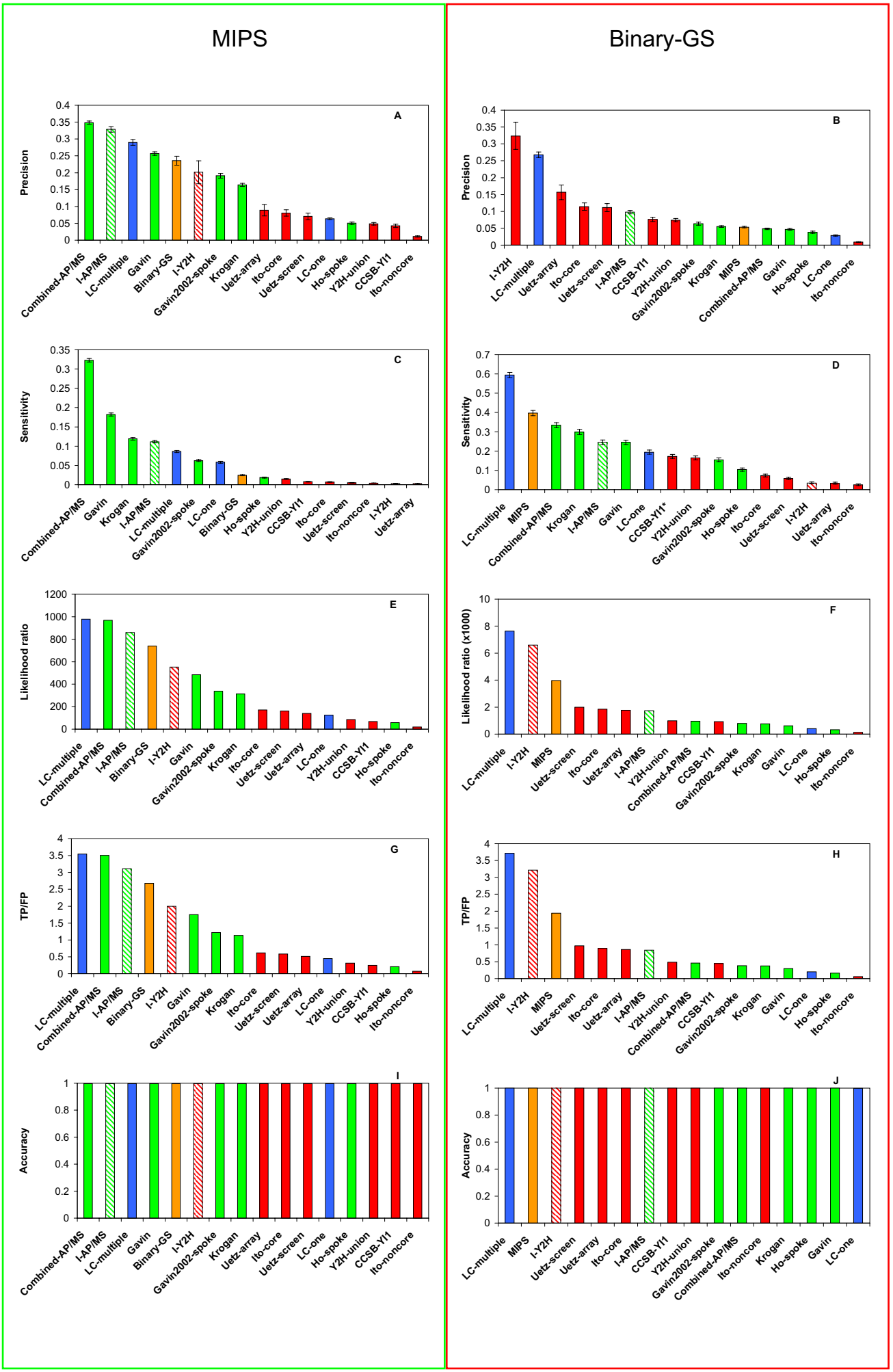

SUPPLEMENTARY FIGURE S18

A. Ideal classification scheme

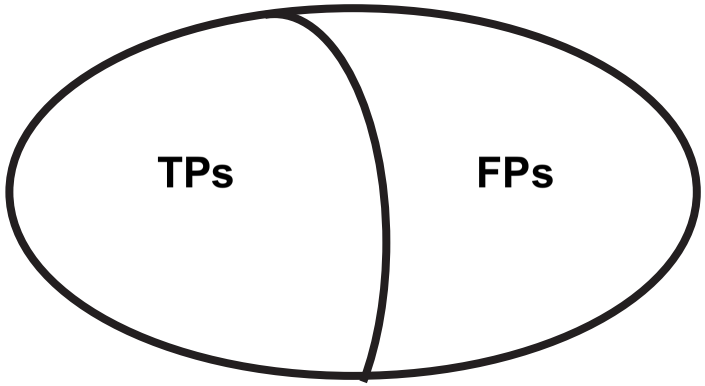

B. Classification scheme based on incomplete knowledge

(Usually faced in biological classification problems)

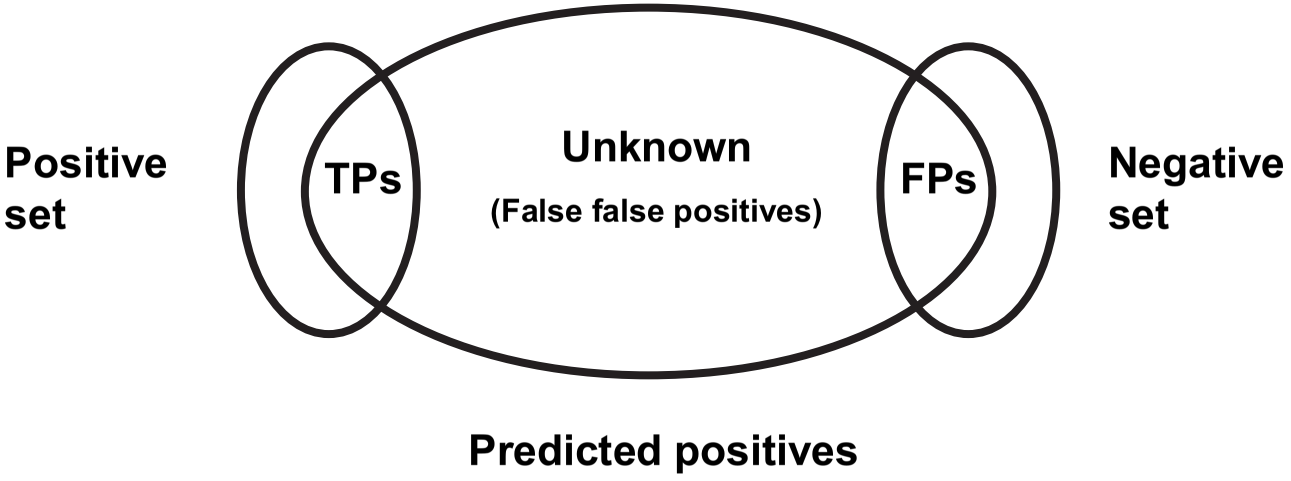

SUPPLEMENTARY FIGURE S19

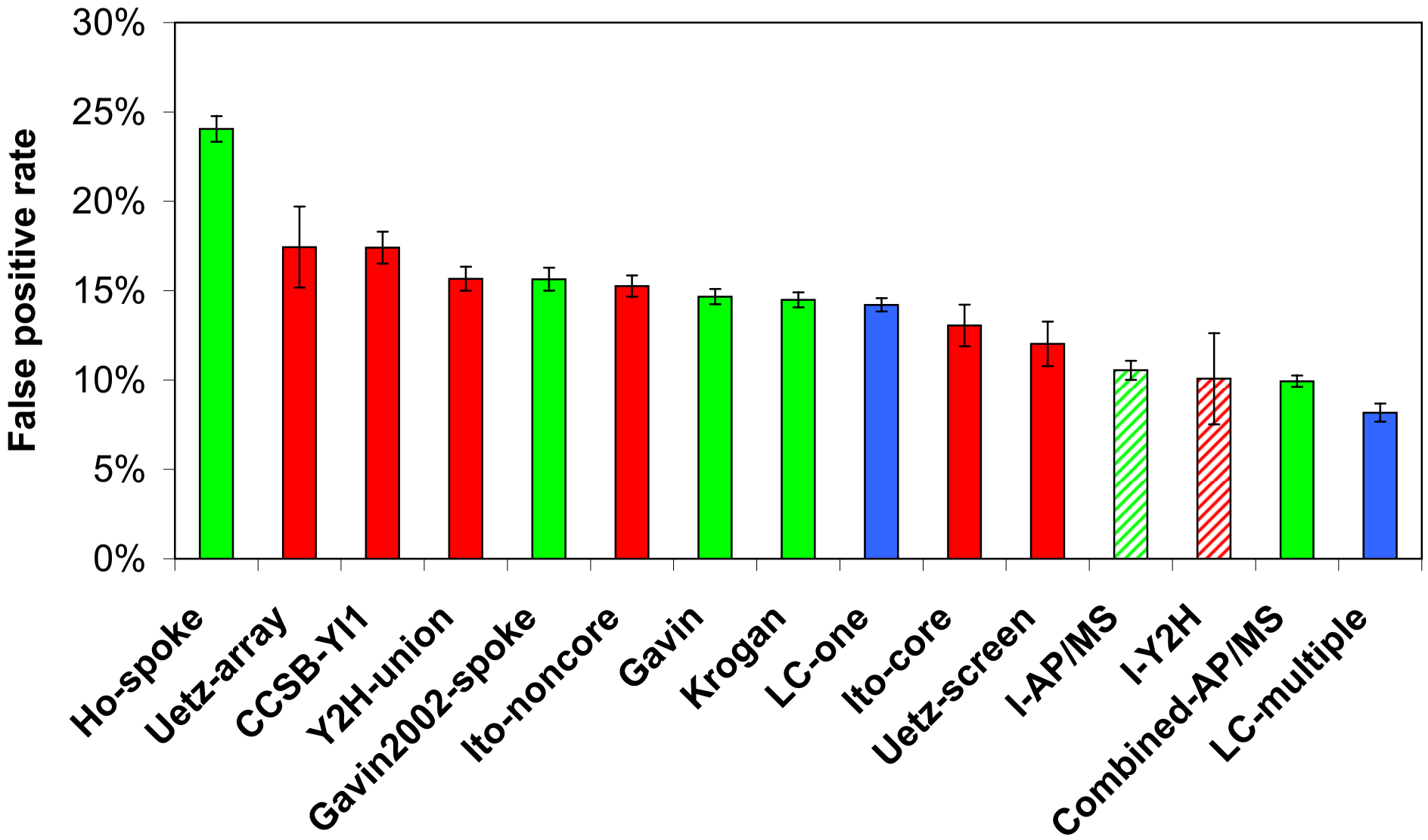

SUPPLEMENTARY FIGURE S20

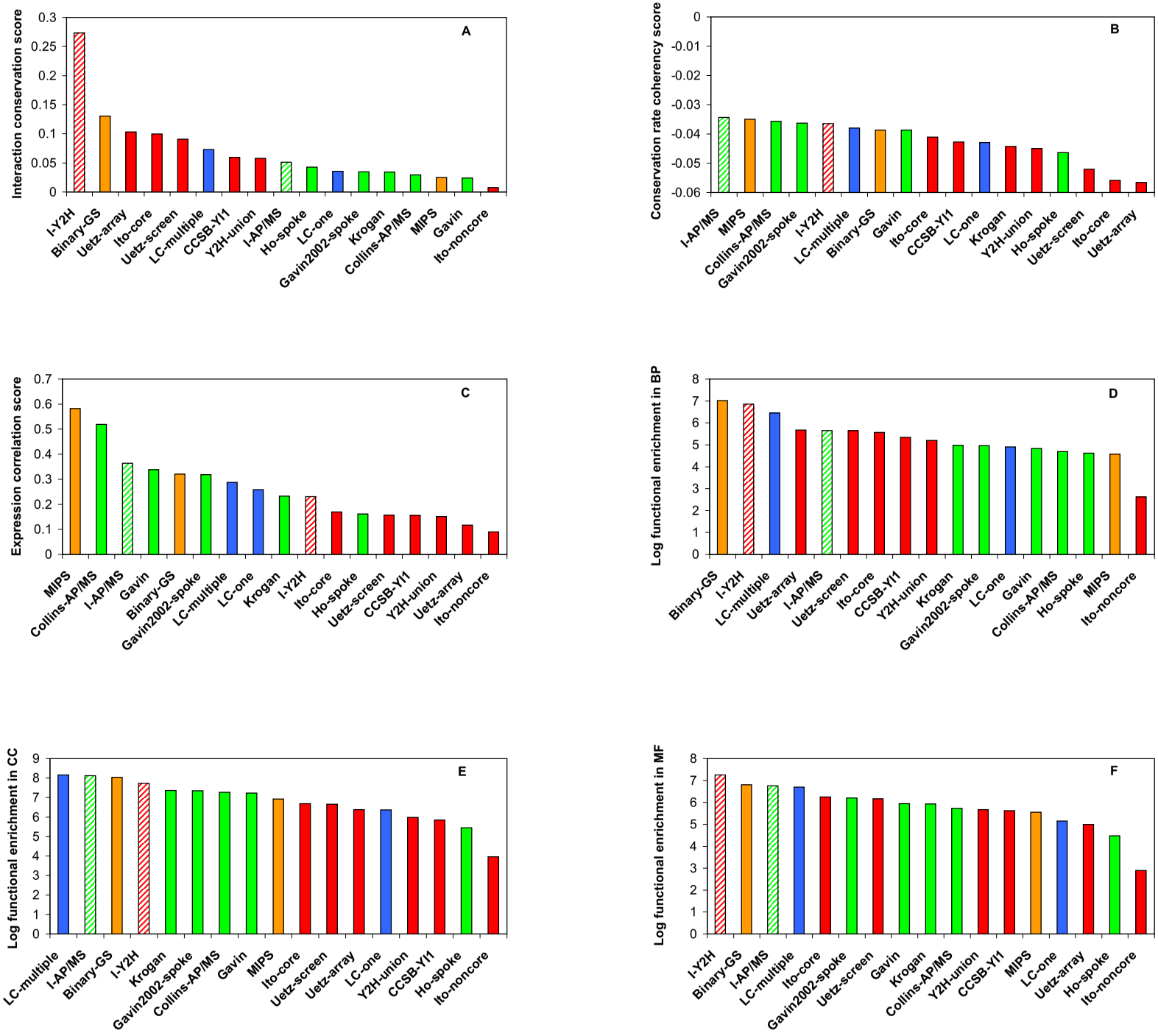

SUPPLEMENTARY FIGURE S21

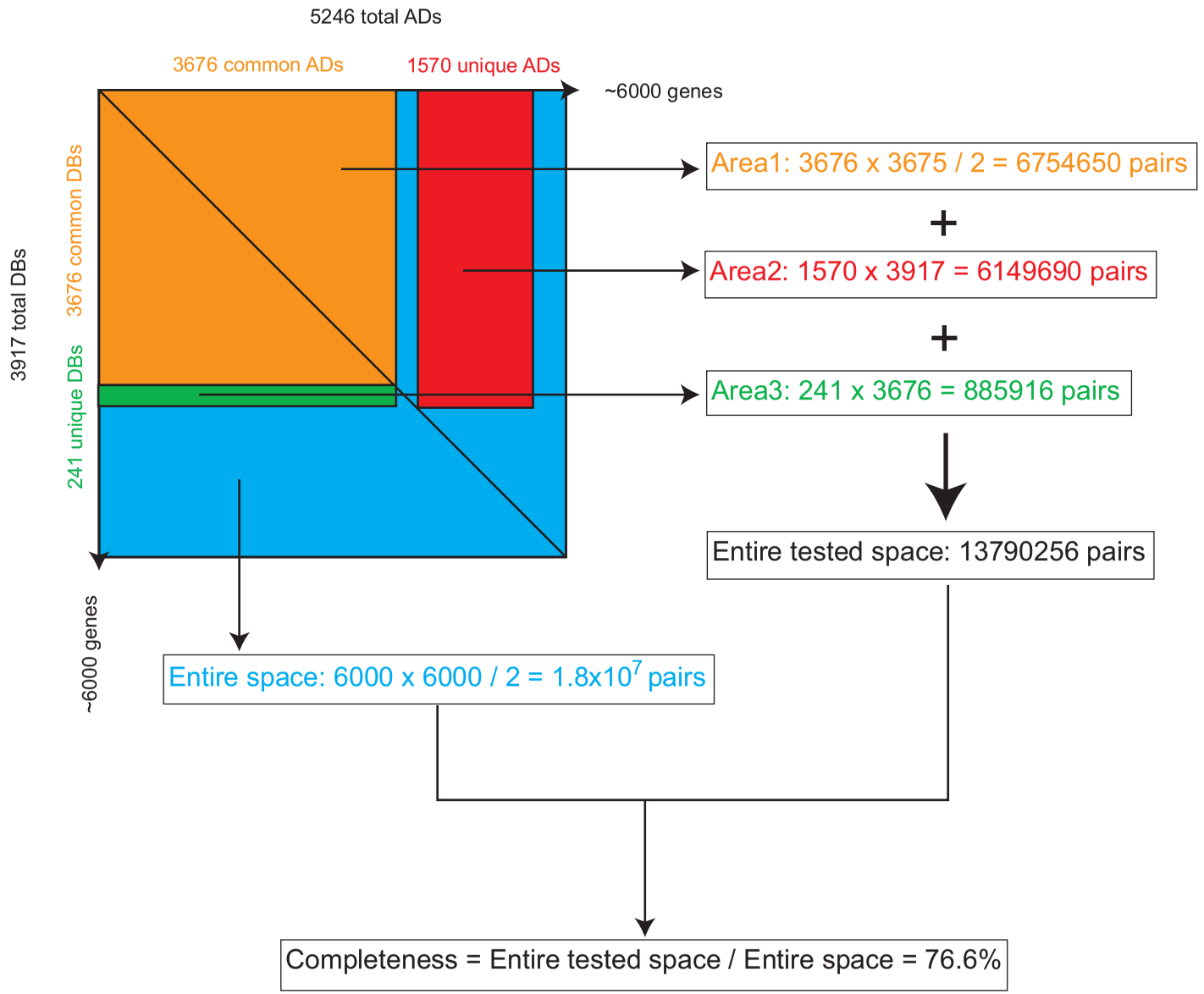

SUPPLEMENTARY FIGURE S22

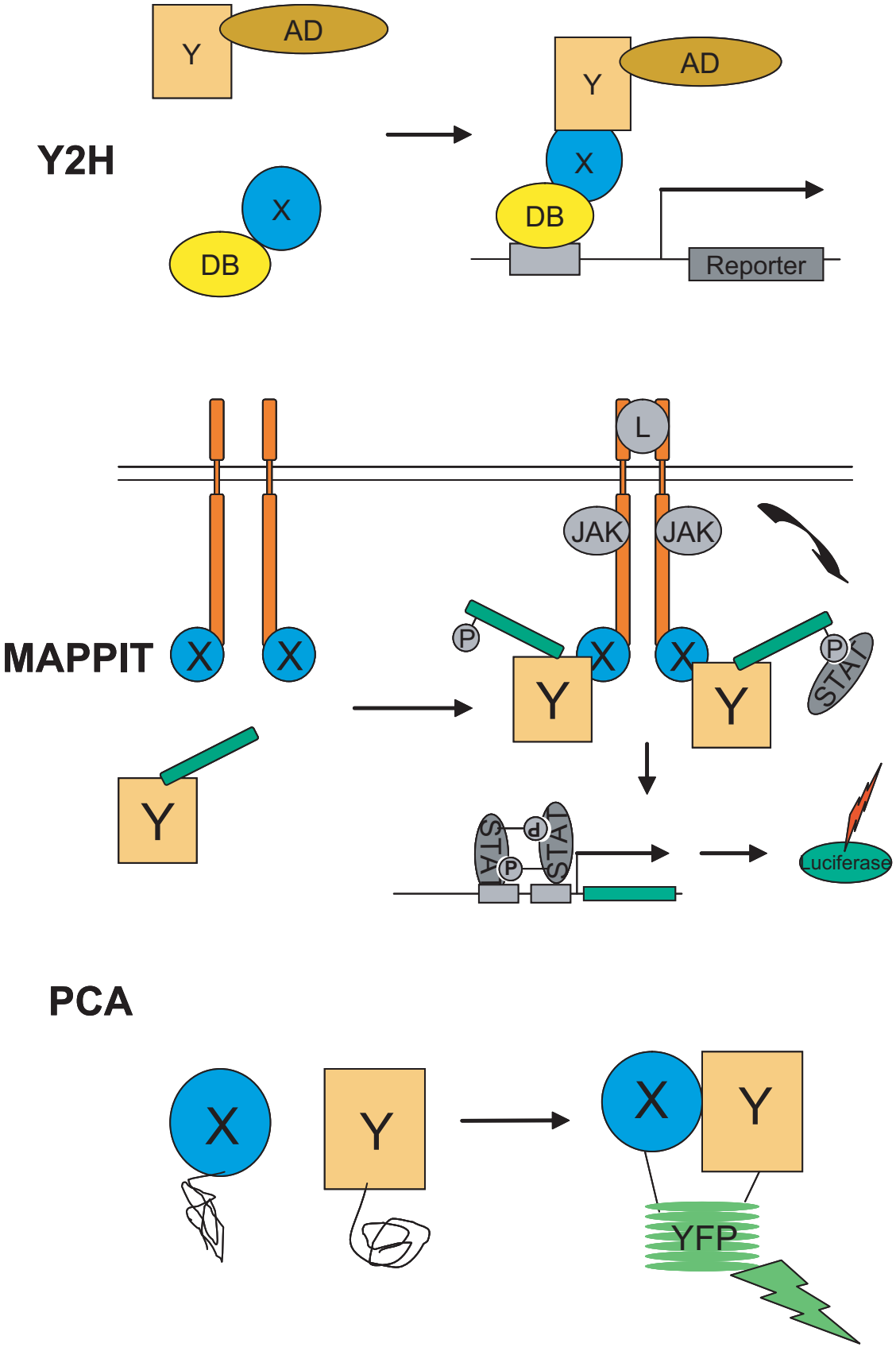

SUPPLEMENTARY FIGURE S23

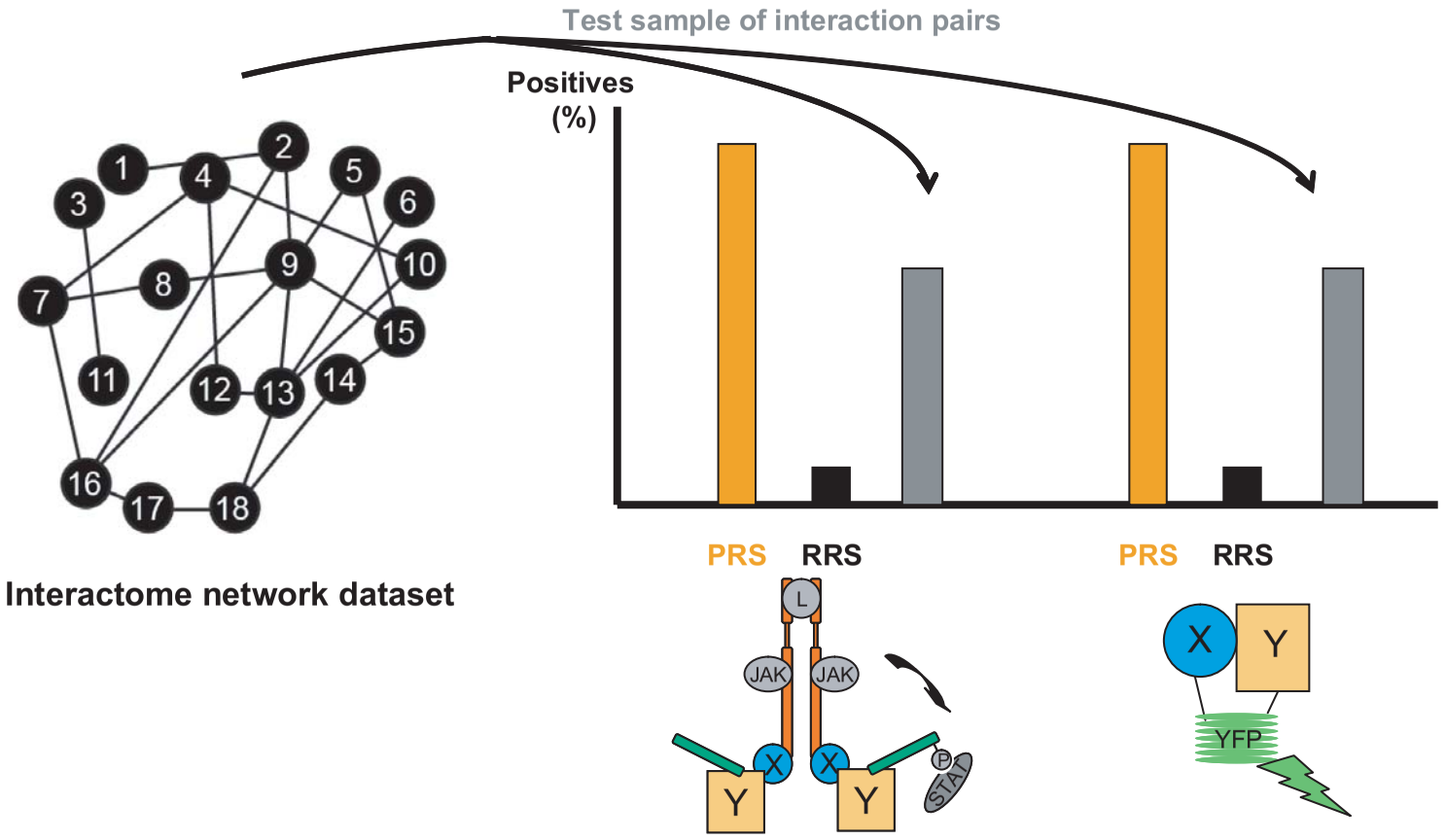

SUPPLEMENTARY FIGURE S24

A

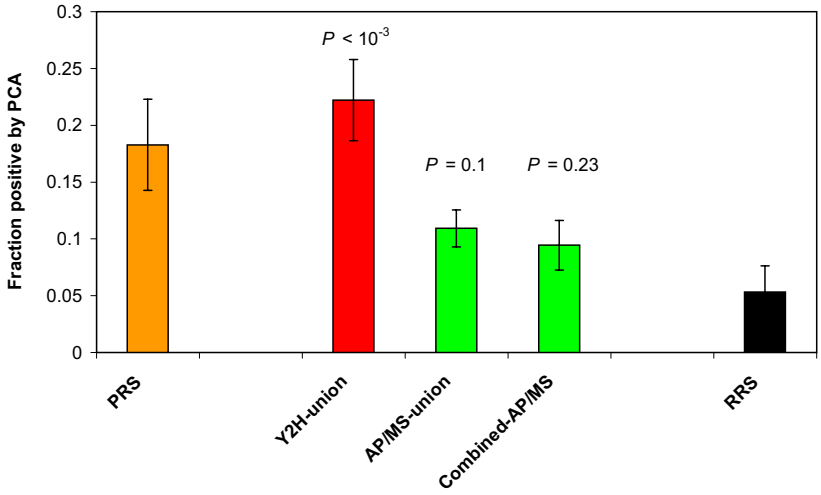

B

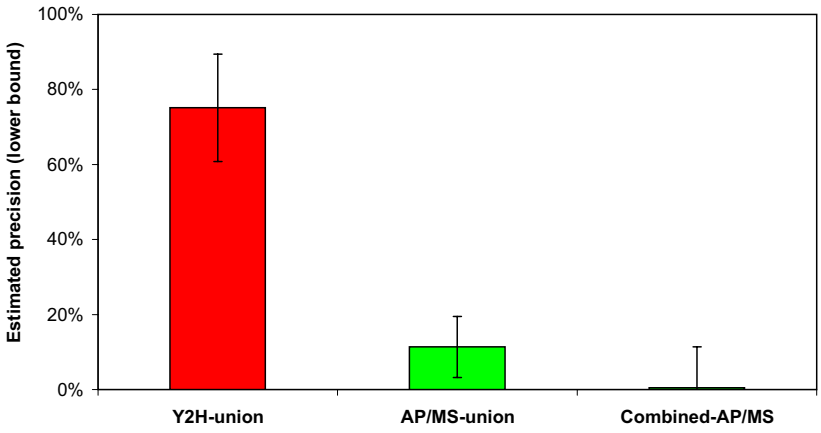

C

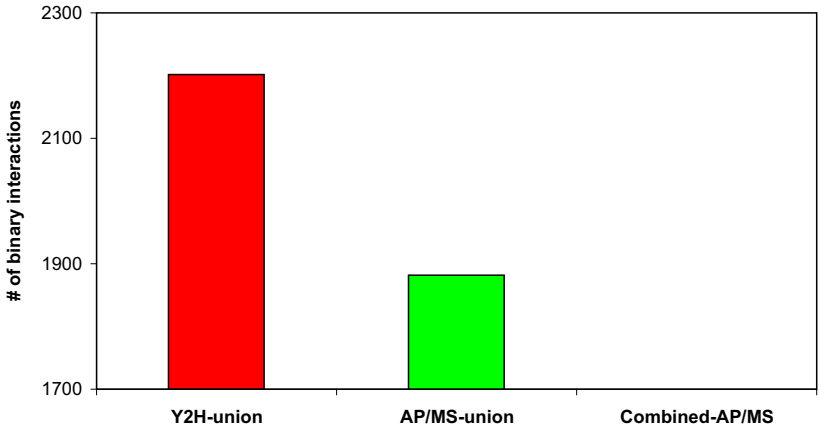

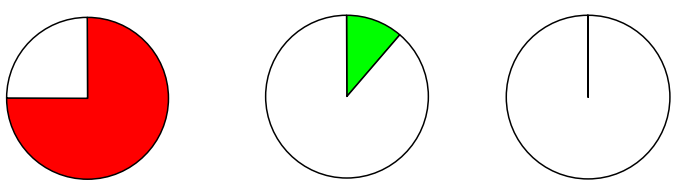

SUPPLEMENTARY FIGURE S25

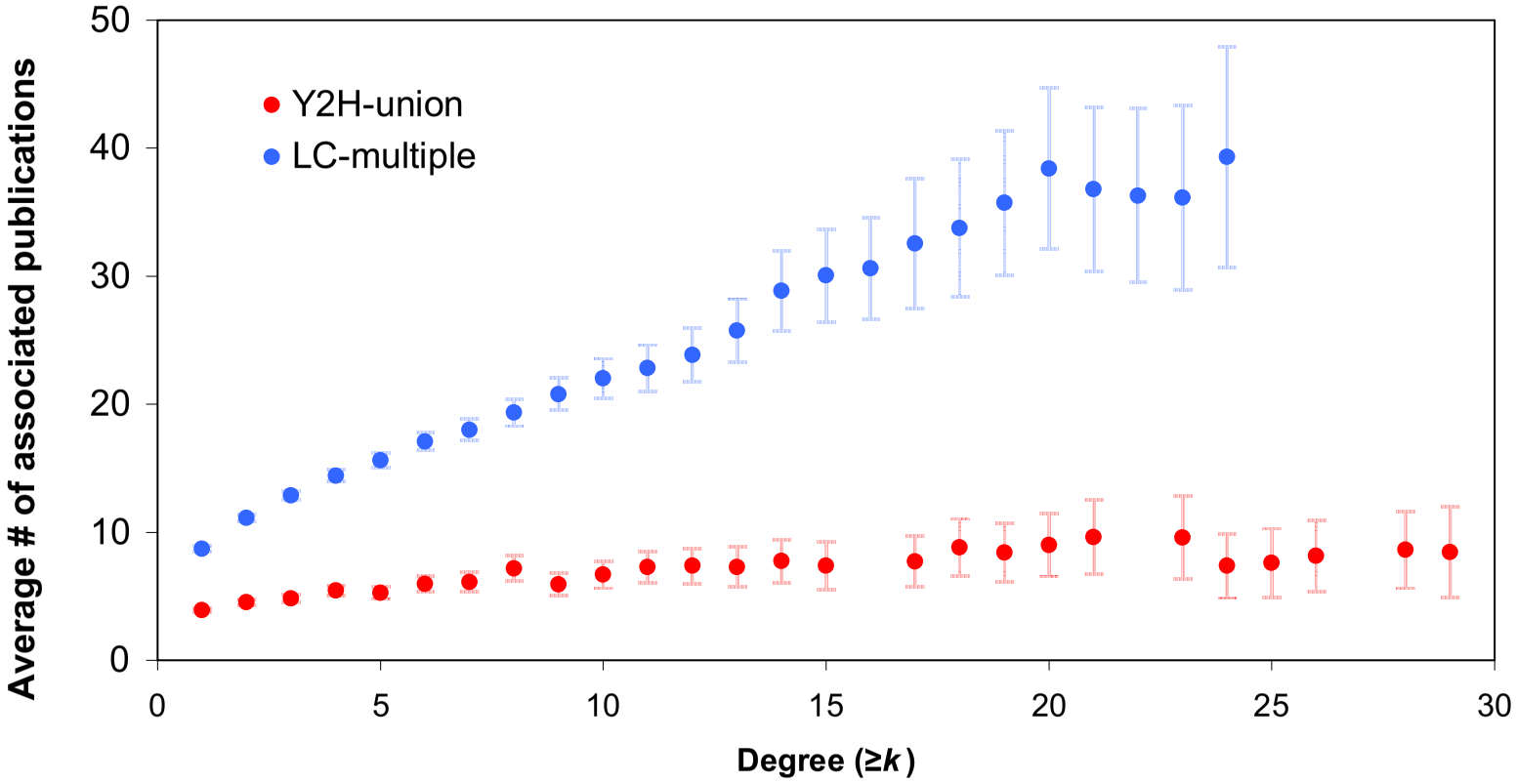

SUPPLEMENTARY FIGURE S26

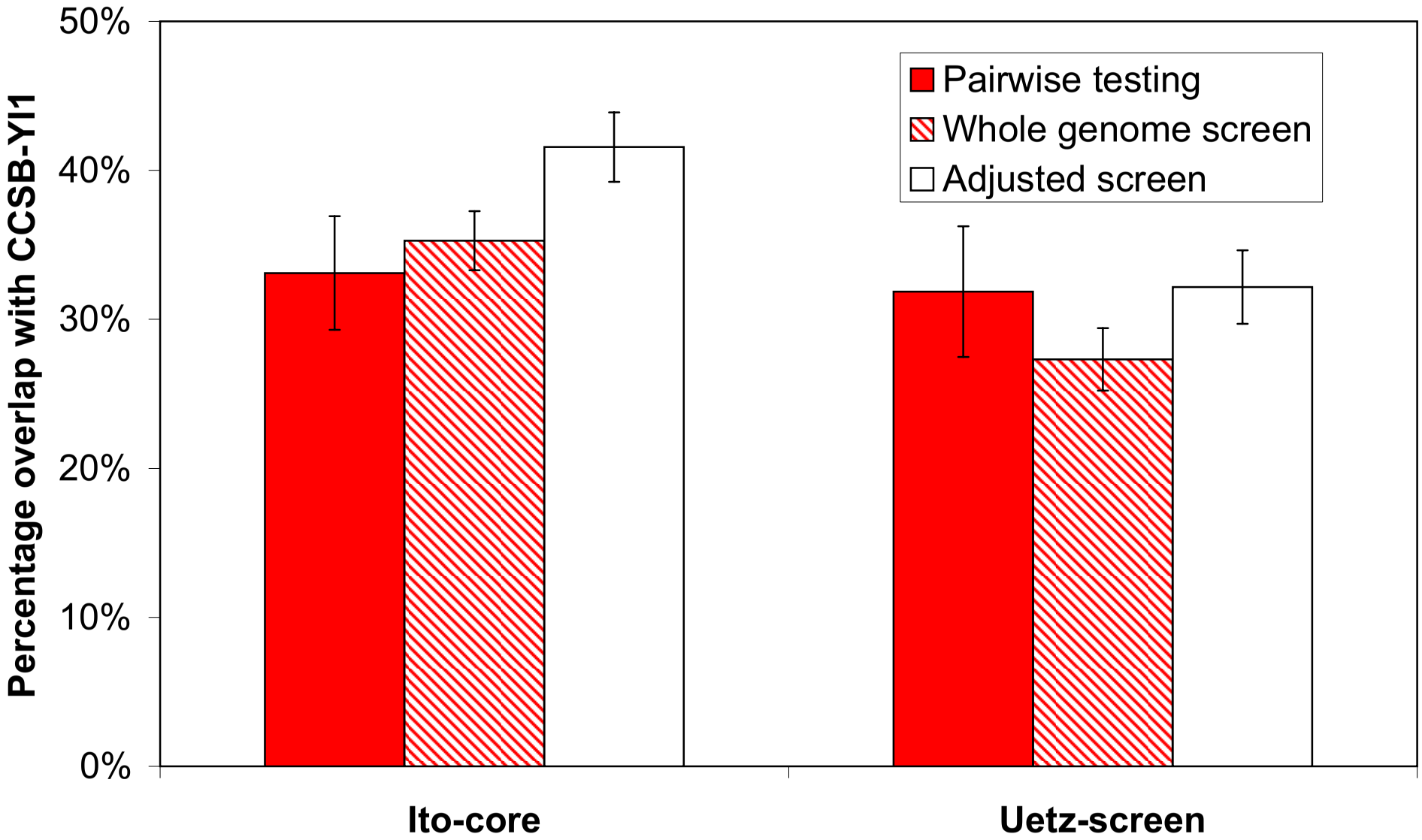

SUPPLEMENTARY FIGURE S27

A. Normal fitting

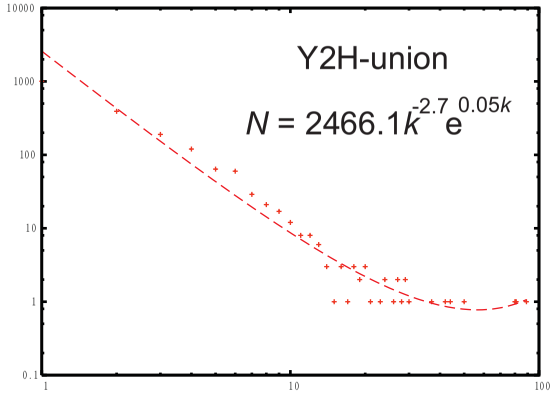

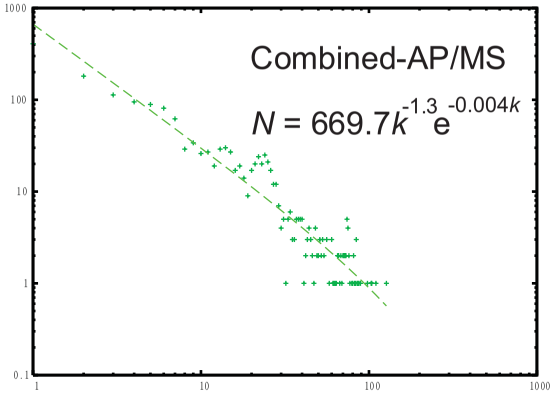

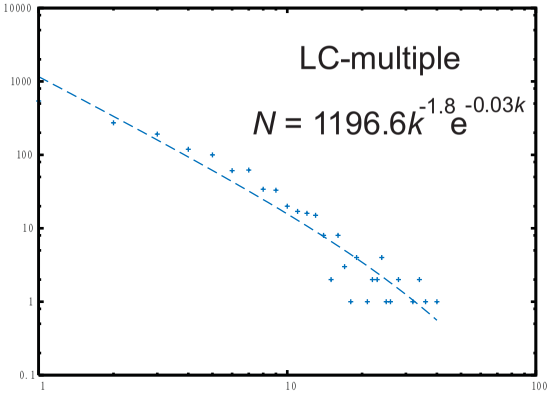

B. Log-binned fitting

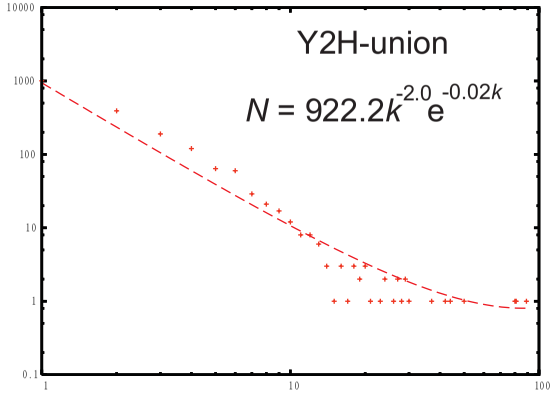

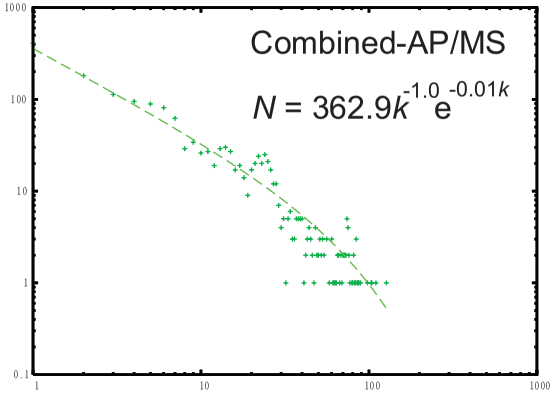

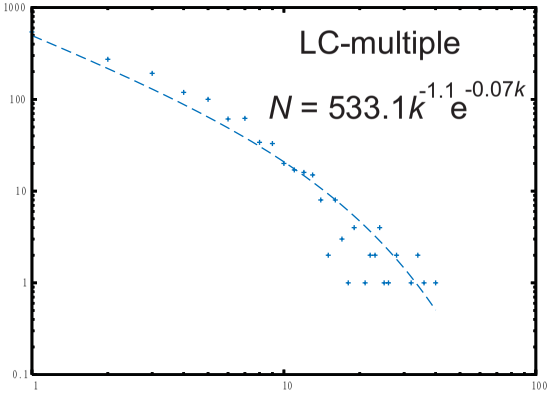

SUPPLEMENTARY FIGURE S28

	L_{actual}	L_{random}	P	C_{actual}	C_{random}	P
Y2H-union	5.61	5.08±0.041	10^{-37}	0.046	0.0073±0.0014	10^{-200}
Combined-AP/MS	5.54	3.34±0.013	10^{-200}	0.55	0.041±0.0017	10^{-200}
LC-multiple	7.54	4.81±0.025	10^{-200}	0.29	0.0059±0.0018	10^{-200}

SUPPLEMENTARY FIGURE S29

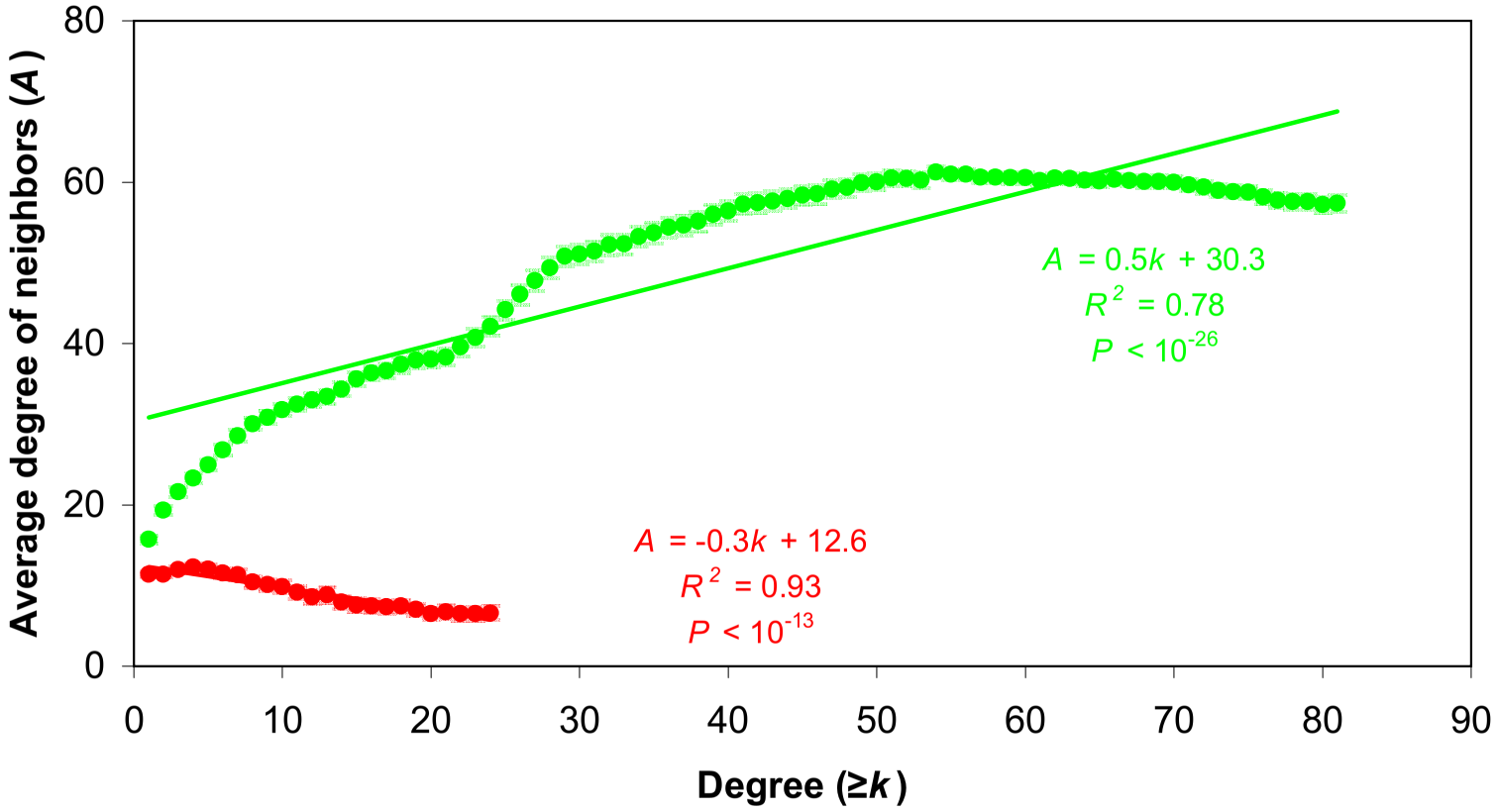

SUPPLEMENTARY FIGURE S30

A

	Observed value	5% added		10% added		15% added		20% added	
		Average	*P*	Average	*P*	Average	*P*	Average	*P*
L	5.61±0.0014	5.64±0.030	0.16	5.64±0.039	0.22	5.61±0.045	0.46	5.59±0.045	0.33
C	0.046±0.0039	0.046±0.00090	0.45	0.044±0.0011	0.27	0.042±0.0014	0.17	0.040±0.0013	0.069

B

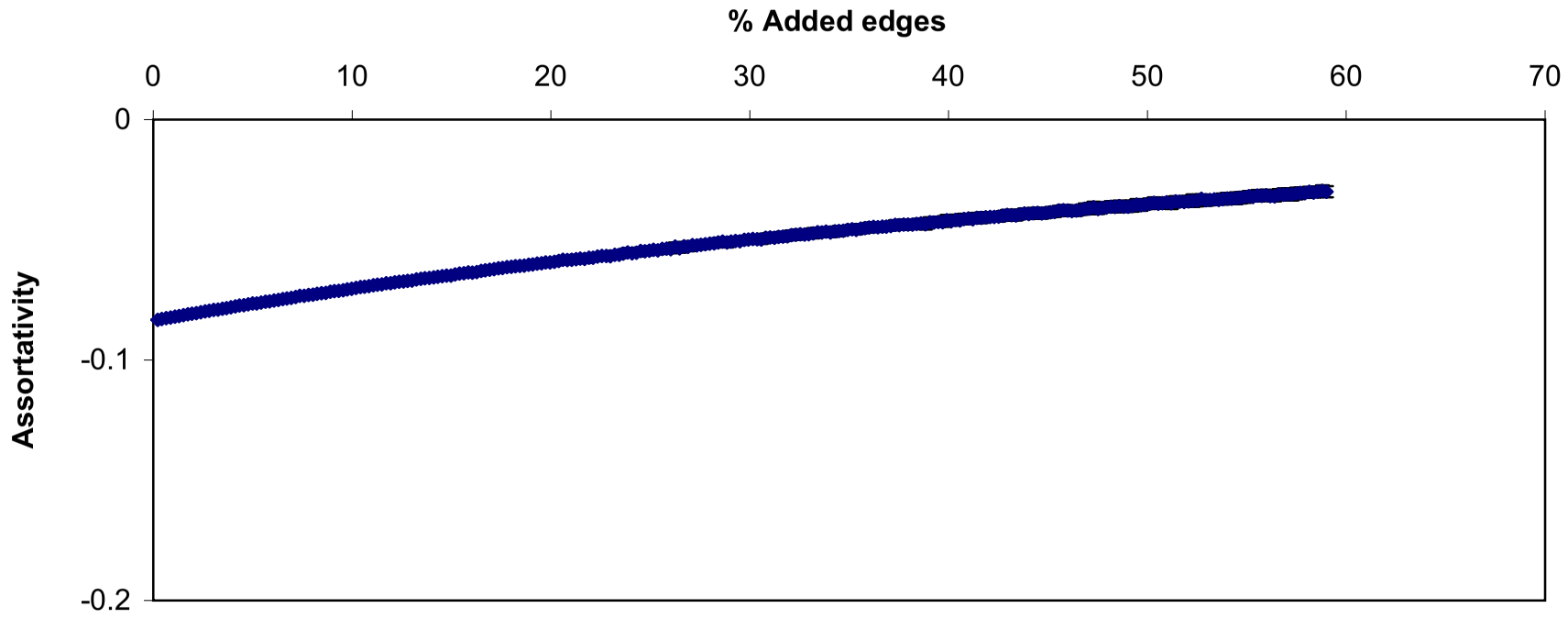

SUPPLEMENTARY FIGURE S31

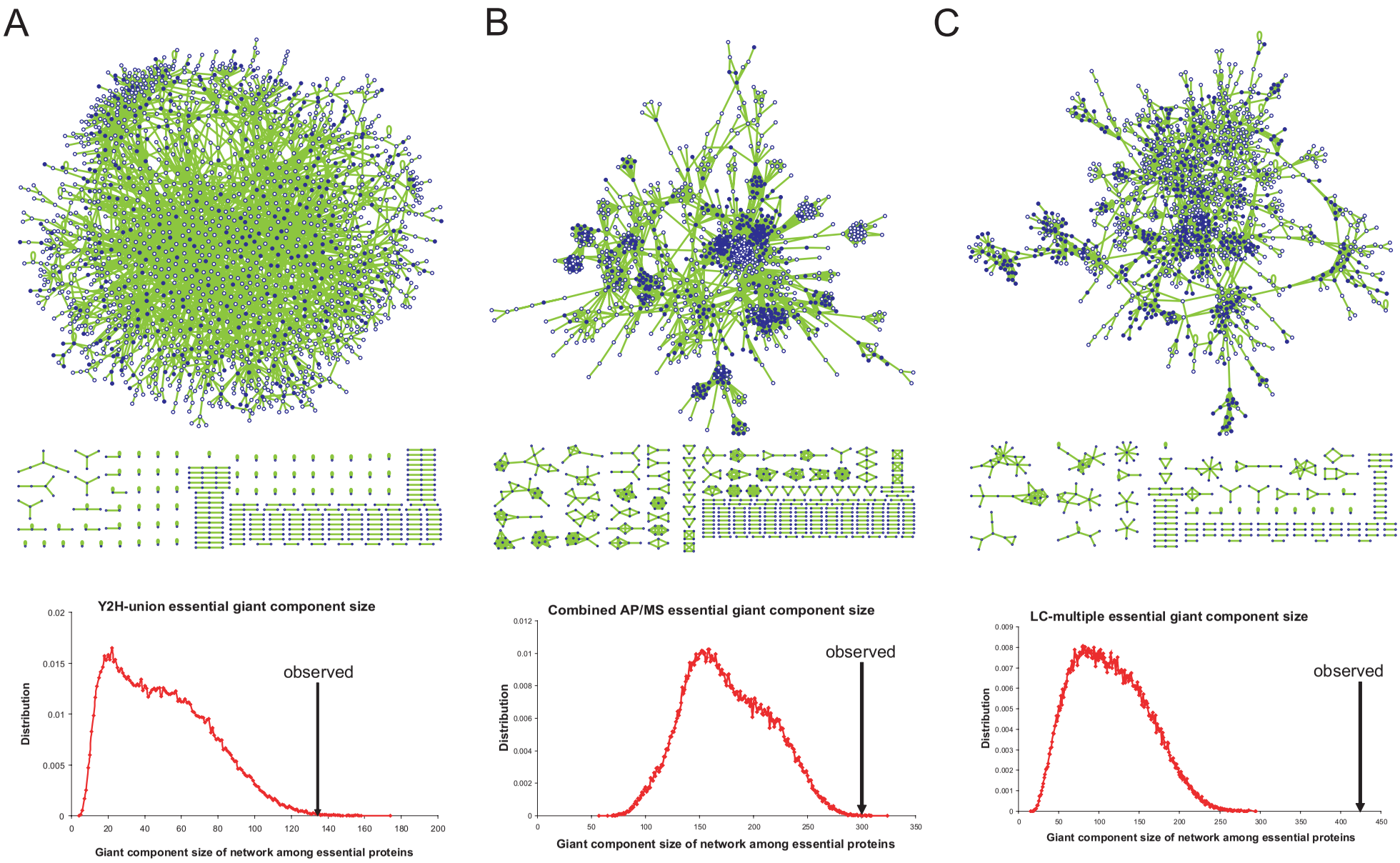

SUPPLEMENTARY FIGURE S32

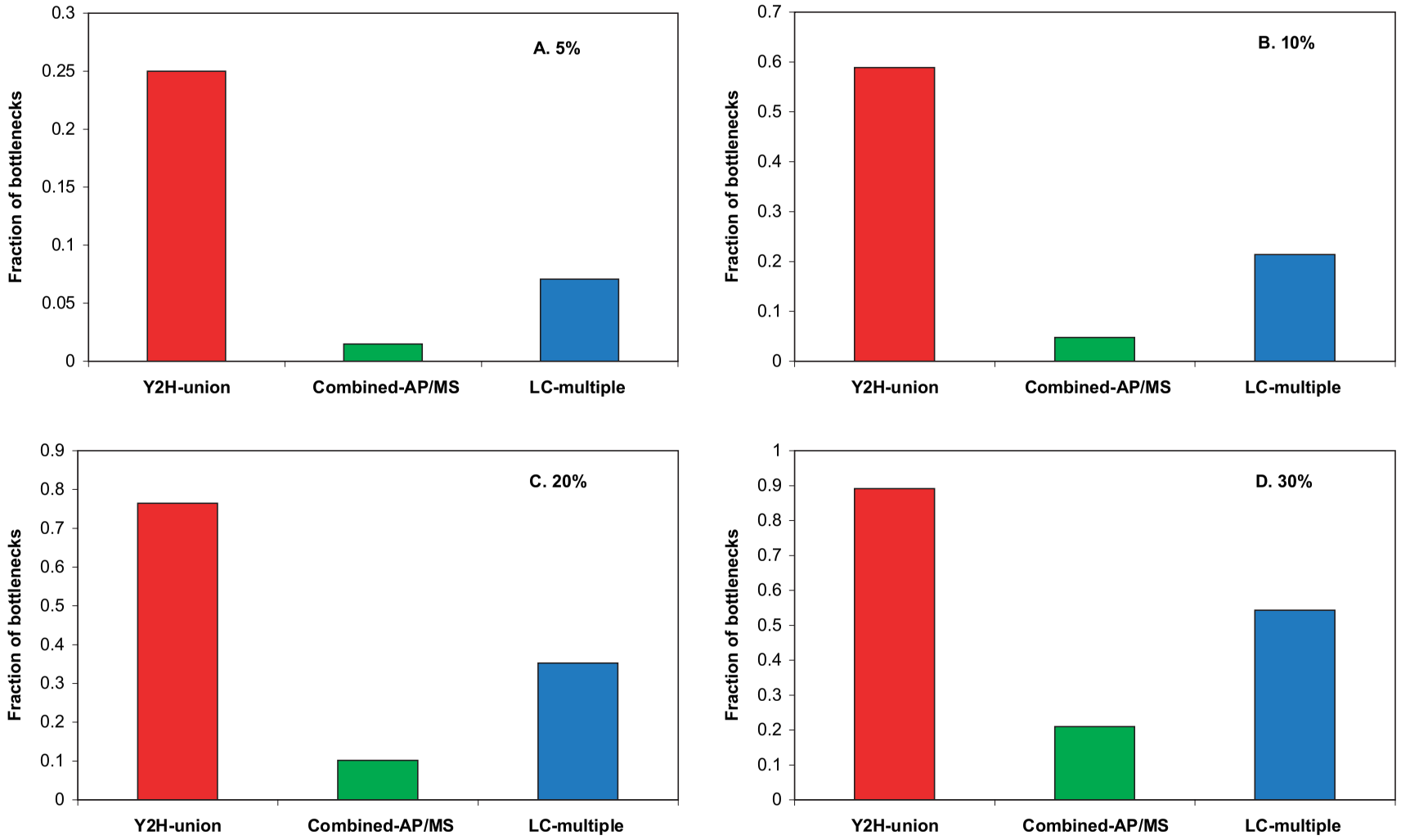

SUPPLEMENTARY FIGURE S33

A

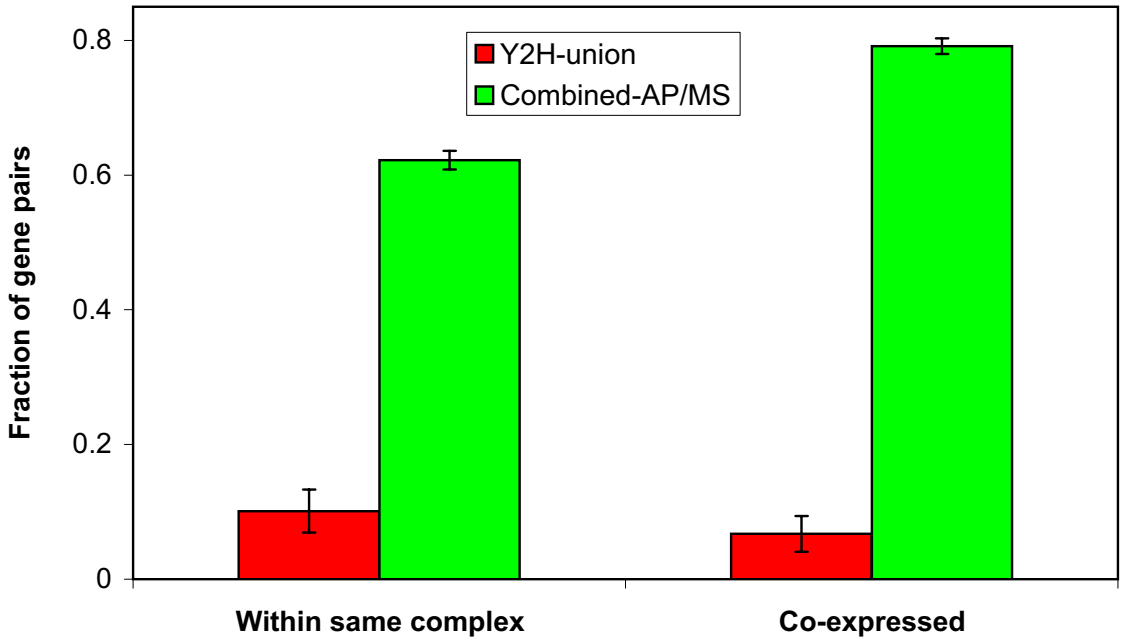

B

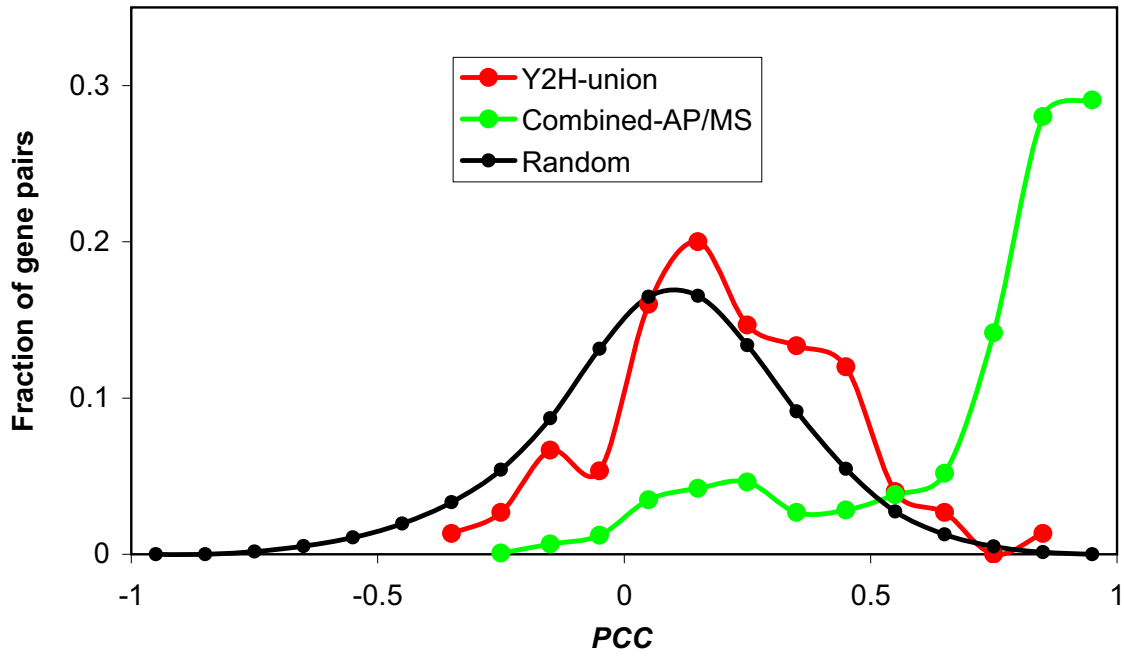

SUPPLEMENTARY FIGURE S34

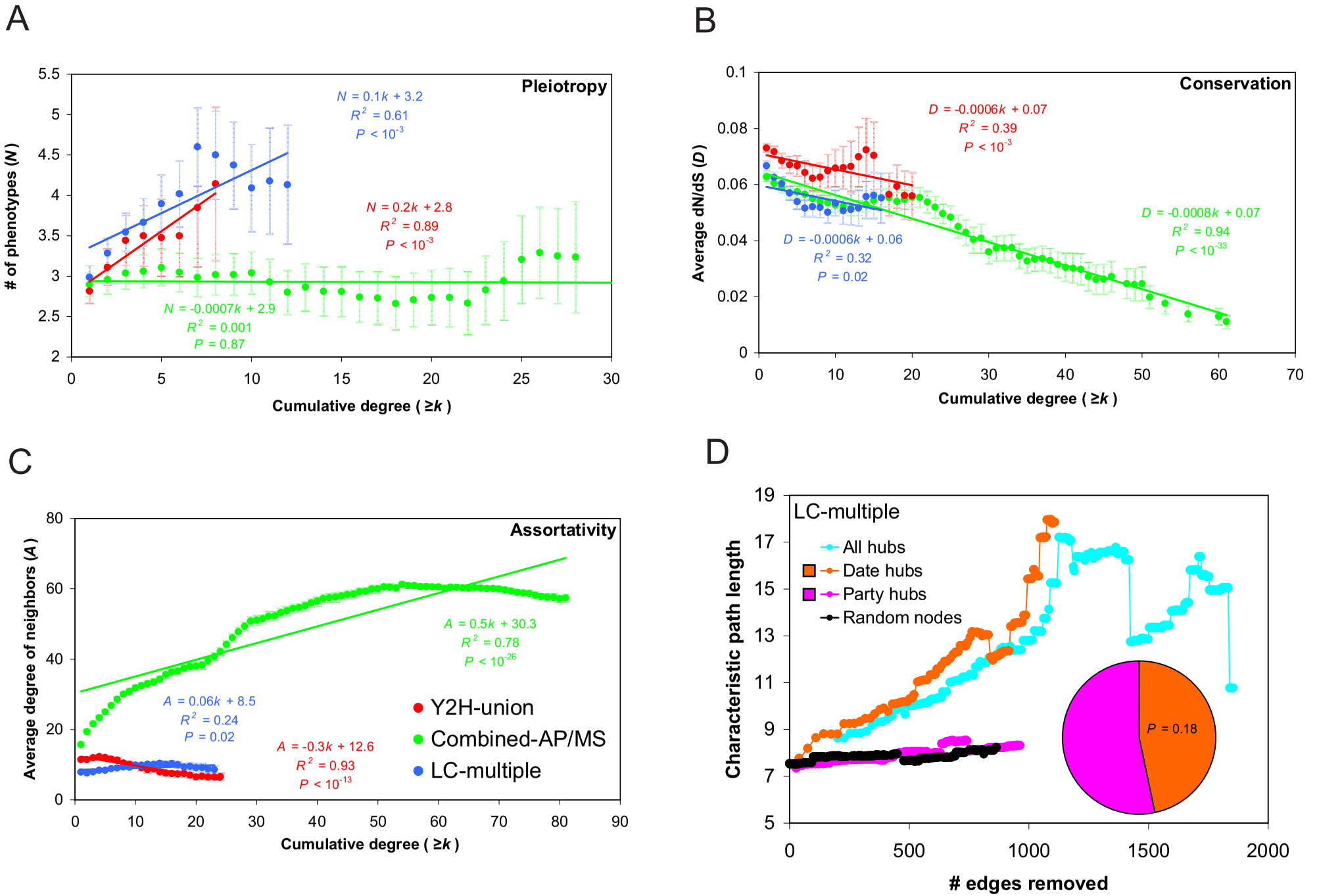

SUPPLEMENTARY FIGURE S35

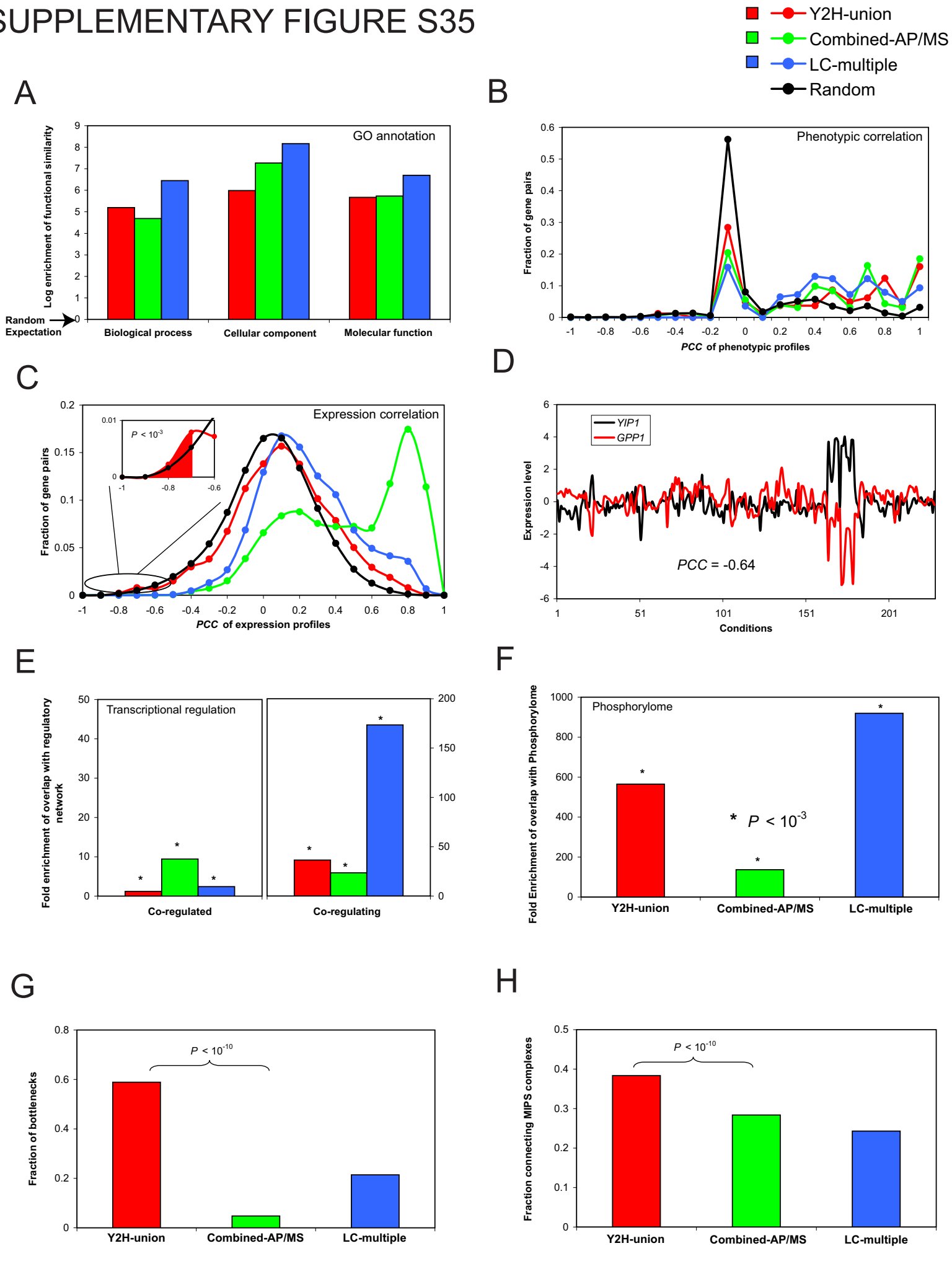

Supporting Online Material Table S1. The Binary-GS set

Interactions		Interactions		Interactions		Interactions	
Protein A	**Protein B**	**Protein A**	**Protein B**	**Protein A**	**Protein B**	**Protein A**	**Protein B**
YCL067C	YCR097W	YCR039C	YCR097W	YCR096C	YCR097W	YMR174C	YPL154C
YDR510W	YPL020C	Q0105	YEL024W	YBL045C	YEL024W	YBL045C	Q0105
YPR191W	YBL045C	YOR065W	YEL024W	YOR065W	Q0105	YOR065W	YBL045C
YOR065W	YFR033C	YGR183C	YEL024W	YGR183C	YBL045C	YGR183C	YOR065W
YJL166W	YEL024W	YJL166W	Q0105	YJL166W	YBL045C	YJL166W	YFR033C
YJL166W	YOR065W	YAL003W	YBR118W	YAL003W	YPR080W	YBL041W	YGR253C
YMR314W	YGR253C	YMR314W	YBL041W	YER012W	YFR050C	YPR103W	YGR253C
YPR103W	YBL041W	YPR103W	YER012W	YER094C	YBL041W	YER094C	YER012W
YER094C	YPR103W	YOR157C	YFR050C	YML092C	YER094C	YJL001W	YFR050C
YJL001W	YER012W	YOL038W	YER012W	YGR135W	YOR157C	YGL011C	YER012W
YGL011C	YML092C	YGL011C	YJL001W	YOR362C	YMR314W	YFR050C	YMR314W
YFR050C	YOR362C	YFR050C	YBL041W	YOR157C	YBL041W	YGR253C	YGR135W
YGL011C	YGR135W	YBR154C	YOL005C	YOR151C	YOL005C	YOR151C	YBR154C
YOR151C	YOR210W	YOR224C	YOL005C	YGL070C	YOR151C	YPR187W	YBR154C
YPR187W	YOR151C	YIL021W	YOL005C	YIL021W	YOR210W	YIL021W	YOR151C
YIL021W	YOR224C	YDR092W	YGL087C	YJL026W	YGR180C	YJR104C	YMR038C
YOR326W	YGL106W	YKL058W	YOR194C	YOR194C	YOR194C	YDR292C	YKL154W
YPL169C	YKL186C	YKL090W	YIL148W	YKL090W	YKR094C	YKL090W	YLL039C
YKL090W	YLR167W	YER148W	YKL058W	YHL015W	YDL061C	YGR214W	YDL061C
YLR048W	YDL061C	YGR214W	YGL123W	YLR048W	YGL123W	YJL190C	YDL061C
YLR367W	YDL061C	YJL190C	YGL123W	YLR367W	YGL123W	YJL190C	YGR214W
YJL190C	YLR048W	YLR367W	YGR214W	YLR367W	YLR048W	YDL083C	YGR214W
YDL083C	YLR048W	YMR143W	YGR214W	YMR143W	YLR048W	YJR123W	YGR214W
YJR123W	YLR048W	YJR123W	YDL083C	YJR123W	YMR143W	YDR450W	YOL040C
YML026C	YOL040C	YNL178W	YDL061C	YNL178W	YHL015W	YGR118W	YDL061C
YPR132W	YDL061C	YDR500C	YKL180W	YLR185W	YKL180W	YHL033C	YKL180W
YLL045C	YKL180W	YBR191W	YPL131W	YPL079W	YPL131W	YIL133C	YGL147C
YIL133C	YNL067W	YNL069C	YGL147C	YNL069C	YNL067W	YOR063W	YGL031C
YOR063W	YGR148C	YOR063W	YIL133C	YOR063W	YNL069C	YLR029C	YHR141C
YLR029C	YNL162W	YMR121C	YHR141C	YMR121C	YNL162W	YLR029C	YHL033C
YLR029C	YLL045C	YMR121C	YHL033C	YMR121C	YLL045C	YGL135W	YHR141C
YGL135W	YNL162W	YPL220W	YHR141C	YPL220W	YNL162W	YNL301C	YDR500C
YNL301C	YLR185W	YOL120C	YDR500C	YOL120C	YLR185W	YNL301C	YGL103W
YOL120C	YGL103W	YBL087C	YGL031C	YBL087C	YGR148C	YER117W	YGL031C
YER117W	YGR148C	YBL087C	YOR063W	YER117W	YOR063W	YKR066C	YJR048W
YJR068W	YBR087W	YNL290W	YOL094C	YNL290W	YJR068W	YJR102C	YLR417W
YPL002C	YLR417W	YPL002C	YJR102C	YER136W	YFL038C	YLR335W	YNL189W
YMR186W	YDR214W	YPL240C	YDR214W	YMR297W	YLR178C	YOR005C	YGL090W
YML065W	YKR101W	YGR254W	YGR254W	YGR254W	YHR174W	YHR174W	YHR174W
YKL190W	YLR433C	YKL190W	YML057W	YLR433C	YML057W	YIL033C	YJL164C
YIL033C	YKL166C	YIL033C	YPL203W	YJL164C	YKL166C	YJL164C	YPL203W
YKL166C	YPL203W	YER123W	YHR135C	YER123W	YNL154C	YER123W	YPL204W
YHR135C	YNL154C	YHR135C	YPL204W	YNL154C	YPL204W	YGL019W	YIL035C
YGL019W	YOR039W	YGL019W	YOR061W	YIL035C	YOR039W	YIL035C	YOR061W
YOR039W	YOR061W	YLR288C	YPL194W	YDL108W	YPR025C	YCR081W	YDR443C

YCR081W	YNL025C	YCR081W	YPL042C	YDR443C	YNL025C	YDR443C	YPL042C
YNL025C	YPL042C	YJL006C	YKL139W	YJL006C	YML112W	YKL139W	YML112W
YKL182W	YPL231W	YDL090C	YKL019W	YGL155W	YKL019W	YJL031C	YOR370C
YJL031C	YPR176C	YOR370C	YPR176C	YCR034W	YGR032W	YCR034W	YLR342W
YGR032W	YLR342W	YGR143W	YPR159W	YAL044C	YDR019C	YAL044C	YFL018C
YAL044C	YMR189W	YDR019C	YFL018C	YDR019C	YMR189W	YFL018C	YMR189W
YCR024CA	YEL017CA	YCR024CA	YGL008C	YCR024CA	YPL036W	YEL017CA	YGL008C
YEL017CA	YPL036W	YGL008C	YPL036W	YEL056W	YPL001W	YHR099W	YOR244W
YMR263W	YNL330C	YMR263W	YOL004W	YNL330C	YOL004W	YNL037C	YOR136W
YGL206C	YGR167W	YBL078C	YNL223W	YKL135C	YLR170C	YKL135C	YPL259C
YKL135C	YPR029C	YLR170C	YPL259C	YLR170C	YPR029C	YPL259C	YPR029C
YBL037W	YJR005W	YBL037W	YJR058C	YBL037W	YOL062C	YJR005W	YJR058C
YJR005W	YOL062C	YJR058C	YOL062C	YBR288C	YGR261C	YBR288C	YJL024C
YBR288C	YPL195W	YGR261C	YJL024C	YGR261C	YPL195W	YJL024C	YPL195W
YHR012W	YJL053W	YHR012W	YJL154C	YJL053W	YJL154C	YOR069W	YOR132W
YBL050W	YBR080C	YKL041W	YLR025W	YKL041W	YPR173C	YLR025W	YPR173C
YLR148W	YLR396C	YLR148W	YMR231W	YLR148W	YPL045W	YLR396C	YMR231W
YLR396C	YPL045W	YMR231W	YPL045W	YGR238C	YHR158C	YDR328C	YGR140W
YDR328C	YMR094W	YDR328C	YMR168C	YGR140W	YMR094W	YGR140W	YMR168C
YMR094W	YMR168C	YBR115C	YGL154C	YJL143W	YNR017W	YEL020WA	YHR005CA
YAL009W	YHR004C	YCL009C	YMR108W	YGR072W	YHR077C	YGR072W	YMR080C
YHR077C	YMR080C	YFR002W	YGL172W	YFR002W	YGR119C	YFR002W	YJL041W
YGL172W	YGR119C	YGL172W	YJL041W	YGR119C	YJL041W	YJL041W	YJL061W
YFL022C	YLR060W	YFL022C	YPR047W	YLR060W	YPR047W	YGR240C	YMR205C
YER017C	YMR089C	YMR035W	YMR150C	YHR024C	YLR163C	YDL040C	YHR013C
YAL038W	YOR347C	YGL032C	YNR044W	YBR278W	YNL262W	YBR278W	YPR175W
YNL262W	YPR175W	YIL139C	YPL167C	YAR007C	YJL173C	YAR007C	YNL312W
YJL173C	YNL312W	YER176W	YHR164C	YBL035C	YIR008C	YBL035C	YKL045W
YBL035C	YNL102W	YIR008C	YKL045W	YIR008C	YNL102W	YKL045W	YNL102W
YDL102W	YJR006W	YDL102W	YJR043C	YJR006W	YJR043C	YIL009CA	YLR233C
YIL009CA	YLR318W	YLR233C	YLR318W	YDR178W	YKL141W	YDR178W	YKL148C
YDR178W	YLL041C	YKL141W	YKL148C	YKL141W	YLL041C	YKL148C	YLL041C
YER070W	YGR180C	YER070W	YIL066C	YER070W	YJL026W	YGR180C	YIL066C
YIL066C	YJL026W	YDR301W	YLR115W	YDR301W	YLR277C	YLR115W	YLR277C
YAL043C	YJR093C	YAL043C	YLR277C	YJR093C	YLR277C	YDL014W	YLR197W
YDL014W	YOR310C	YLR197W	YOR310C	YJL203W	YLL036C	YJL203W	YPR101W
YLL036C	YPR101W	YDL030W	YDL043C	YDL132W	YDR054C	YDL132W	YDR328C
YDL132W	YFL009W	YDR054C	YDR328C	YDR054C	YFL009W	YDR328C	YFL009W
YDL132W	YJR090C	YDR054C	YJR090C	YDR328C	YJR090C	YDL132W	YIL046W
YDR054C	YIL046W	YDR328C	YIL046W	YHR005C	YJR086W	YHR005C	YOR212W
YJR086W	YOR212W	YDR113C	YGR098C	YHR172W	YLR212C	YHR172W	YNL126W
YLR212C	YNL126W	YGR244C	YOR142W	YDR285W	YIL072W	YDR285W	YLR263W
YIL072W	YLR263W	YBR126C	YDR074W	YBR126C	YML100W	YBR126C	YMR261C
YDR074W	YML100W	YDR074W	YMR261C	YML100W	YMR261C	YEL034W	YJR047C
YER165W	YGR162W	YER165W	YOL139C	YGR162W	YOL139C	YER025W	YJR007W
YER025W	YPL237W	YJR007W	YPL237W	YJL138C	YKR059W	YGL049C	YGR162W
YGL049C	YOR276W	YGR162W	YOR276W	YDR385W	YOR133W	YGL023C	YMR023C
YER148W	YGR246C	YER148W	YNL039W	YGR246C	YNL039W	YBL021C	YGL237C
YBL021C	YKL109W	YBL021C	YOR358W	YGL237C	YKL109W	YGL237C	YOR358W

YKL109W	YOR358W	YGL130W	YPL228W	YML095C	YMR201C	YML095C	YPL022W
YMR201C	YPL022W	YEL037C	YER162C	YBR114W	YJR052W	YMR106C	YMR284W
YDR369C	YMR224C	YDR369C	YNL250W	YMR224C	YNL250W	YCR092C	YNL082W
YCR092C	YOL090W	YNL082W	YOL090W	YDR097C	YOL090W	YAL051W	YOR363C
YDR173C	YML099C	YDR173C	YMR042W	YDR173C	YMR043W	YML099C	YMR042W
YML099C	YMR043W	YMR042W	YMR043W	YBL103C	YOL067C	YBR112C	YCR084C
YMR053C	YNL309W	YMR053C	YNL330C	YMR053C	YOL004W	YNL309W	YNL330C
YNL309W	YOL004W	YIR017C	YJR060W	YIR017C	YNL103W	YJR060W	YNL103W
YIR017C	YPL038W	YNL103W	YPL038W	YDR253C	YIR017C	YDR253C	YNL103W
YDR397C	YER159C	YDR207C	YJR094C	YHR193C	YPL037C	YER001W	YLR182W
YDL056W	YLR182W	YDR009W	YML051W	YDR009W	YPL248C	YML051W	YPL248C
YNL199C	YPL075W	YBL014C	YER148W	YBL014C	YJL025W	YBL014C	YML043C
YER148W	YJL025W	YER148W	YML043C	YJL025W	YML043C	YBL025W	YLR141W
YBL025W	YMR270C	YLR141W	YMR270C	YKL028W	YKR062W	YGR005C	YGR186W
YGR005C	YPL129W	YGR186W	YPL129W	YDR086C	YER087CA	YDR086C	YLR378C
YER087CA	YLR378C	YBR171W	YLR292C	YBR171W	YOR254C	YBR171W	YPL094C
YLR292C	YOR254C	YLR292C	YPL094C	YOR254C	YPL094C	YIR022W	YJR010CA
YIR022W	YML055W	YJR010CA	YML055W	YER090W	YKL211C	YJR109C	YOR303W
Q0085	YPL078C	Q0250	YBR037C	YAL005C	YNL007C	YAL005C	YNL064C
YAL005C	YPL240C	YAL030W	YGR009C	YAL040C	YBR160W	YAL040C	YJL157C
YAL041W	YBR200W	YAL041W	YGR152C	YAL041W	YJL157C	YAL041W	YLR229C
YAL041W	YOR212W	YAL042W	YML067C	YAL043C	YLR115W	YAL047C	YAL047C
YAL047C	YHR172W	YAL047C	YLR045C	YAL047C	YNL126W	YAL056W	YER020W
YAR019C	YML064C	YBL007C	YCL034W	YBL007C	YCR088W	YBL007C	YDR388W
YBL007C	YER133W	YBL007C	YFR024CA	YBL007C	YGR268C	YBL007C	YHR016C
YBL007C	YIR006C	YBL007C	YNL094W	YBL007C	YOR181W	YBL007C	YPR171W
YBL008W	YJL115W	YBL016W	YDR480W	YBL016W	YHR084W	YBL016W	YPL049C
YBL023C	YDL017W	YBL026W	YCR077C	YBL026W	YDR378C	YBL026W	YER146W
YBL026W	YGL173C	YBL026W	YJL124C	YBL026W	YJR022W	YBL026W	YLR438CA
YBL026W	YNL147W	YBL050W	YDR468C	YBL050W	YLR268W	YBL050W	YMR197C
YBL050W	YOL018C	YBL050W	YOR106W	YBL078C	YHR171W	YBL078C	YNR007C
YBL085W	YBR200W	YBL085W	YDR239C	YBL085W	YER124C	YBL085W	YER158C
YBL085W	YLR086W	YBL085W	YML109W	YBL099W	YDR322CA	YBL105C	YPR165W
YBR003W	YJR022W	YBR009C	YBR010W	YBR009C	YDR225W	YBR010W	YDR225W
YBR010W	YPL209C	YBR017C	YDR192C	YBR017C	YGR119C	YBR045C	YER133W
YBR050C	YER133W	YBR060C	YLL004W	YBR077C	YKR007W	YBR087W	YMR078C
YBR087W	YOR144C	YBR088C	YCR092C	YBR088C	YDR097C	YBR088C	YJR043C
YBR088C	YKL113C	YBR088C	YNL290W	YBR088C	YOL094C	YBR088C	YOR217W
YBR091C	YHR005CA	YBR091C	YOR297C	YBR097W	YLR240W	YBR102C	YDR166C
YBR102C	YGL233W	YBR102C	YHR165C	YBR102C	YLR166C	YBR107C	YDR254W
YBR108W	YDR388W	YBR108W	YHR016C	YBR109C	YDR356W	YBR109C	YFR014C
YBR109C	YGL043W	YBR109C	YLR433C	YBR109C	YML057W	YBR109C	YNR035C
YBR109C	YOL016C	YBR109C	YOR326W	YBR114W	YMR190C	YBR118W	YLR249W
YBR127C	YDR202C	YBR127C	YJR033C	YBR128C	YPL120W	YBR130C	YPL240C
YBR133C	YJL187C	YBR133C	YKL101W	YBR135W	YBR160W	YBR136W	YDR499W
YBR136W	YPL153C	YBR143C	YDR172W	YBR152W	YGR075C	YBR154C	YDL140C
YBR154C	YOR116C	YBR154C	YOR341W	YBR155W	YJR032W	YBR155W	YMR186W
YBR155W	YPL240C	YBR156C	YGR113W	YBR156C	YPL209C	YBR160W	YDL155W
YBR160W	YFL029C	YBR160W	YGR108W	YBR160W	YGR109C	YBR160W	YIL050W

YBR160W	YJL194W	YBR160W	YLR079W	YBR160W	YLR210W	YBR160W	YMR199W
YBR160W	YNL309W	YBR160W	YPL256C	YBR160W	YPR119W	YBR160W	YPR120C
YBR167C	YHR062C	YBR170C	YGR048W	YBR172C	YLR116W	YBR188C	YDR416W
YBR188C	YLL036C	YBR188C	YLR117C	YBR188C	YMR213W	YBR188C	YPL151C
YBR193C	YER022W	YBR195C	YPR018W	YBR200W	YDR103W	YBR200W	YER114C
YBR200W	YHL007C	YBR200W	YJL157C	YBR200W	YLR229C	YBR202W	YEL032W
YBR202W	YLR274W	YBR207W	YFL041W	YBR217W	YHR171W	YBR217W	YMR159C
YBR217W	YPL149W	YBR239C	YHR016C	YBR253W	YER022W	YBR254C	YKR068C
YBR274W	YDR113C	YBR279W	YOL145C	YBR289W	YOR290C	YBR290W	YPL240C
YCL008C	YHL002W	YCL027W	YER118C	YCL032W	YDR103W	YCL032W	YDR309C
YCL032W	YHR061C	YCL032W	YLR362W	YCL034W	YOR181W	YCR002C	YDL225W
YCR002C	YDR507C	YCR009C	YDR388W	YCR009C	YMR232W	YCR042C	YER148W
YCR052W	YFR037C	YCR052W	YLR321C	YCR060W	YPL240C	YCR066W	YGL058W
YCR077C	YDR378C	YCR077C	YER112W	YCR077C	YER146W	YCR077C	YJL124C
YCR077C	YJR022W	YCR077C	YLR438CA	YCR077C	YNL147W	YCR086W	YDR309C
YCR086W	YFL008W	YCR086W	YHR061C	YCR088W	YDR388W	YCR088W	YFL039C
YCR088W	YFR024CA	YCR088W	YHR016C	YCR088W	YIL095W	YCR088W	YIR003W
YCR088W	YNL020C	YCR088W	YNL094W	YCR088W	YNL106C	YCR088W	YNL138W
YCR088W	YNL298W	YCR088W	YOR284W	YCR096C	YCR096C	YCR096C	YMR043W
YDL003W	YFL008W	YDL017W	YDR052C	YDL029W	YJR065C	YDL029W	YOR181W
YDL030W	YJL203W	YDL035C	YER020W	YDL042C	YDR227W	YDL042C	YFR028C
YDL042C	YJL076W	YDL042C	YLR442C	YDL043C	YJL203W	YDL047W	YMR028W
YDL064W	YDR510W	YDL077C	YDR080W	YDL077C	YLR396C	YDL077C	YPL045W
YDL101C	YKL025C	YDL101C	YML058W	YDL101C	YPL153C	YDL106C	YFR034C
YDL106C	YKR099W	YDL111C	YGR158C	YDL113C	YJL036W	YDL126C	YDL190C
YDL126C	YGR048W	YDL126C	YLR207W	YDL126C	YOL013C	YDL127W	YDR388W
YDL127W	YPL031C	YDL132W	YML088W	YDL132W	YOL133W	YDL134C	YMR028W
YDL140C	YDR228C	YDL140C	YDR301W	YDL140C	YGL043W	YDL140C	YGL070C
YDL140C	YGL130W	YDL140C	YOL005C	YDL140C	YOR151C	YDL140C	YOR210W
YDL140C	YOR224C	YDL140C	YPR187W	YDL147W	YDR179C	YDL150W	YKR025W
YDL156W	YFR024CA	YDL161W	YGL206C	YDL179W	YPL031C	YDL185W	YOR270C
YDL188C	YMR028W	YDL192W	YER122C	YDL199C	YPL240C	YDL207W	YDR192C
YDL207W	YMR255W	YDL207W	YOR046C	YDL208W	YNL124W	YDL209C	YJR050W
YDL209C	YLL036C	YDL217C	YHR005CA	YDL217C	YJL054W	YDL220C	YDR082W
YDL220C	YLR233C	YDL220C	YNL102W	YDL225W	YDR507C	YDL225W	YHR016C
YDL225W	YHR107C	YDL225W	YJR076C	YDL225W	YLR314C	YDL226C	YDR264C
YDL235C	YIL147C	YDL235C	YLR006C	YDL240W	YPR165W	YDL246C	YPL240C
YDR016C	YDR201W	YDR016C	YGL061C	YDR016C	YGR113W	YDR016C	YKL052C
YDR016C	YKR037C	YDR016C	YKR083C	YDR027C	YDR484W	YDR027C	YJL029C
YDR052C	YPL153C	YDR054C	YLL039C	YDR076W	YER095W	YDR078C	YHL006C
YDR080W	YLR396C	YDR085C	YHR107C	YDR088C	YGR006W	YDR099W	YDR130C
YDR103W	YOR212W	YDR121W	YPR175W	YDR123C	YOL108C	YDR129C	YFL039C
YDR142C	YGL153W	YDR142C	YGR239C	YDR142C	YHR160C	YDR142C	YLR191W
YDR145W	YMR005W	YDR162C	YHL007C	YDR167W	YDR167W	YDR167W	YER148W
YDR167W	YML114C	YDR167W	YMR005W	YDR168W	YPL240C	YDR171W	YDR171W
YDR172W	YDR172W	YDR181C	YJL115W	YDR181C	YMR127C	YDR181C	YOR213C
YDR189W	YLR026C	YDR190C	YPL235W	YDR192C	YMR255W	YDR195W	YER032W
YDR201W	YKR037C	YDR207C	YMR139W	YDR213W	YHR165C	YDR216W	YPR086W
YDR217C	YPL153C	YDR225W	YJL081C	YDR227W	YDR227W	YDR227W	YLR442C

YDR227W	YNL216W	YDR228C	YJR022W	YDR239C	YER114C	YDR244W	YGL153W
YDR244W	YGR077C	YDR244W	YLR191W	YDR244W	YNL214W	YDR246W	YKR068C
YDR264C	YOR212W	YDR267C	YHR122W	YDR270W	YNL259C	YDR277C	YJR022W
YDR283C	YPL240C	YDR301W	YKR002W	YDR301W	YNL317W	YDR309C	YHR061C
YDR309C	YHR107C	YDR309C	YKL082C	YDR309C	YLR229C	YDR309C	YML109W
YDR309C	YNL298W	YDR310C	YOL068C	YDR310C	YOR279C	YDR320C	YGR167W
YDR328C	YJL149W	YDR328C	YJL204C	YDR328C	YLR097C	YDR328C	YML088W
YDR328C	YOL133W	YDR356W	YHR172W	YDR356W	YKL042W	YDR356W	YNL126W
YDR359C	YGR002C	YDR377W	YPL078C	YDR378C	YER112W	YDR378C	YER146W
YDR378C	YJL124C	YDR378C	YJR022W	YDR378C	YLR438CA	YDR378C	YNL147W
YDR381W	YDR381W	YDR381W	YPL169C	YDR388W	YDR388W	YDR388W	YFL039C
YDR388W	YGL060W	YDR388W	YJR083C	YDR388W	YLR144C	YDR388W	YML058W
YDR388W	YMR192W	YDR388W	YNL094W	YDR388W	YNL138W	YDR388W	YOR181W
YDR388W	YPL249C	YDR388W	YPR171W	YDR390C	YKR002W	YDR390C	YPR180W
YDR392W	YER148W	YDR394W	YDR394W	YDR404C	YJL140W	YDR416W	YGR129W
YDR416W	YJR050W	YDR416W	YLL036C	YDR416W	YLR117C	YDR416W	YMR213W
YDR416W	YPL151C	YDR416W	YPR101W	YDR448W	YER148W	YDR468C	YMR197C
YDR468C	YOL018C	YDR472W	YKR068C	YDR473C	YPR178W	YDR477W	YDR477W
YDR477W	YNL257C	YDR480W	YGR040W	YDR480W	YHR084W	YDR484W	YJL029C
YDR507C	YHR107C	YDR507C	YJR076C	YDR507C	YKR048C	YDR507C	YLR314C
YEL005C	YEL013W	YEL009C	YEL009C	YEL013W	YHR195W	YEL013W	YPR185W
YEL015W	YEL015W	YEL015W	YJR022W	YEL023C	YML109W	YEL032W	YLR274W
YEL036C	YJR075W	YEL036C	YPL050C	YEL037C	YGL048C	YEL037C	YHR027C
YEL037C	YKL145W	YER008C	YPR165W	YER018C	YIL144W	YER018C	YMR117C
YER018C	YOL069W	YER020W	YOR371C	YER029C	YLR147C	YER031C	YNL263C
YER033C	YMR109W	YER059W	YPL031C	YER070W	YML058W	YER095W	YML032C
YER107C	YMR047C	YER110C	YLR293C	YER110C	YML007W	YER111C	YHR030C
YER111C	YLR182W	YER111C	YPR119W	YER112W	YER146W	YER112W	YGL173C
YER112W	YJL124C	YER112W	YJR022W	YER112W	YLR438CA	YER112W	YNL147W
YER112W	YOL149W	YER114C	YER124C	YER115C	YML109W	YER118C	YJL128C
YER118C	YKL086W	YER118C	YKR027W	YER118C	YOR181W	YER124C	YML109W
YER125W	YMR275C	YER133W	YFR003C	YER133W	YLR263W	YER133W	YOR329C
YER146W	YJL124C	YER146W	YJR022W	YER146W	YLR438CA	YER146W	YNL147W
YER148W	YER148W	YER148W	YGL241W	YER148W	YGR274C	YER148W	YOR194C
YER148W	YPL082C	YER157W	YGL223C	YER157W	YGR120C	YER157W	YPR105C
YER161C	YHR166C	YER165W	YGL049C	YER167W	YGR229C	YER172C	YIL061C
YER179W	YER179W	YFL005W	YNL272C	YFL008W	YFL008W	YFL008W	YFR031C
YFL008W	YIL026C	YFL008W	YJL074C	YFL009W	YJL194W	YFL009W	YOL133W
YFL011W	YPL240C	YFL016C	YJR045C	YFL024C	YJL081C	YFL024C	YOR244W
YFL037W	YOR265W	YFL038C	YNL263C	YFL039C	YFL039C	YFL039C	YLL050C
YFL039C	YLR319C	YFL039C	YNL138W	YFL039C	YNL271C	YFL039C	YOR122C
YFL039C	YOR181W	YFL039C	YOR244W	YFL039C	YPL242C	YFL059W	YFL059W
YFL059W	YMR095C	YFR002W	YML103C	YFR009W	YGL195W	YFR024CA	YGL060W
YFR024CA	YGL144C	YFR024CA	YGL181W	YFR024CA	YGR268C	YFR024CA	YHL027W
YFR024CA	YJR083C	YFR024CA	YKL214C	YFR024CA	YLR144C	YFR024CA	YMR192W
YFR024CA	YNL094W	YFR024CA	YNL152W	YFR024CA	YOR042W	YFR024CA	YOR181W
YFR024CA	YPL249C	YFR024CA	YPR091C	YFR024CA	YPR171W	YFR028C	YJL076W
YFR034C	YFR034C	YFR034C	YOL001W	YFR037C	YFR037C	YFR037C	YIL126W
YFR051C	YNL258C	YGL003C	YKL101W	YGL003C	YPR119W	YGL016W	YKL058W

YGL016W	YLR335W	YGL016W	YOR098C	YGL016W	YOR194C	YGL048C	YPL248C
YGL049C	YOL139C	YGL058W	YGR184C	YGL061C	YGR113W	YGL061C	YKR037C
YGL075C	YMR117C	YGL075C	YPL255W	YGL092W	YLR347C	YGL094C	YIR006C
YGL096W	YJR022W	YGL116W	YJL013C	YGL116W	YJL030W	YGL116W	YKL101W
YGL122C	YKR095W	YGL133W	YOR304W	YGL144C	YHR016C	YGL145W	YNL258C
YGL153W	YGL153W	YGL153W	YHR016C	YGL153W	YLR191W	YGL154C	YGL254W
YGL161C	YGR172C	YGL173C	YJR022W	YGL174W	YIR005W	YGL178W	YLR452C
YGL180W	YPR049C	YGL207W	YML069W	YGL212W	YOR106W	YGL215W	YPL031C
YGL223C	YGR120C	YGL238W	YLR293C	YGL238W	YNL189W	YGR002C	YNL107W
YGR009C	YOR327C	YGR009C	YPL232W	YGR009C	YPR032W	YGR040W	YHR084W
YGR040W	YPL049C	YGR047C	YGR246C	YGR047C	YNL039W	YGR060W	YLR100W
YGR082W	YMR203W	YGR082W	YNL070W	YGR082W	YNL131W	YGR104C	YHR041C
YGR113W	YPL209C	YGR120C	YNL041C	YGR120C	YPR105C	YGR129W	YLL036C
YGR129W	YLR117C	YGR129W	YMR213W	YGR136W	YOR181W	YGR158C	YJR022W
YGR172C	YNL263C	YGR185C	YGR229C	YGR188C	YOR026W	YGR218W	YLR293C
YGR218W	YML007W	YGR229C	YHR030C	YGR233C	YOL001W	YGR233C	YPL031C
YGR267C	YGR267C	YGR274C	YML114C	YGR274C	YMR005W	YHL002W	YNR006W
YHL003C	YKL008C	YHL007C	YLR229C	YHL018W	YHL018W	YHL031C	YLR026C
YHR005C	YLR362W	YHR014W	YHR185C	YHR016C	YJR083C	YHR016C	YLR144C
YHR016C	YMR192W	YHR016C	YNL094W	YHR016C	YOR042W	YHR016C	YOR181W
YHR016C	YPL249C	YHR016C	YPR171W	YHR023W	YPR188C	YHR030C	YLR182W
YHR030C	YOR231W	YHR030C	YPL089C	YHR030C	YPL140C	YHR030C	YPL240C
YHR034C	YJR022W	YHR035W	YJR022W	YHR061C	YHR061C	YHR061C	YHR107C
YHR061C	YKL082C	YHR061C	YLR229C	YHR061C	YML109W	YHR061C	YMR055C
YHR061C	YMR238W	YHR061C	YNL298W	YHR061C	YPL161C	YHR084W	YPL049C
YHR089C	YNL124W	YHR090C	YHR099W	YHR090C	YOR244W	YHR107C	YJR076C
YHR114W	YOR181W	YHR129C	YPL174C	YHR143WA	YIL021W	YHR158C	YHR158C
YHR170W	YMR080C	YHR171W	YHR171W	YHR171W	YNR007C	YHR183W	YPL240C
YHR185C	YIL007C	YIL004C	YIL109C	YIL004C	YPR181C	YIL022W	YJR045C
YIL022W	YNR017W	YIL034C	YKL007W	YIL035C	YNL088W	YIL046W	YNL103W
YIL050W	YPL031C	YIL063C	YLR293C	YIL095W	YIR006C	YIL115C	YLR347C
YIL129C	YNL161W	YIL144W	YMR117C	YIL144W	YOL069W	YIL156W	YMR109W
YIL159W	YMR032W	YIL159W	YMR109W	YIL159W	YOR122C	YIL173W	YJR022W
YIR006C	YNL084C	YIR012W	YLR075W	YIR018W	YIR018W	YIR038C	YIR038C
YJL005W	YNL138W	YJL013C	YOR026W	YJL020C	YMR109W	YJL020C	YOR181W
YJL026W	YJL026W	YJL034W	YOR254C	YJL036W	YLR423C	YJL048C	YKL130C
YJL054W	YOR297C	YJL081C	YOR244W	YJL090C	YKL108W	YJL095W	YMR109W
YJL115W	YMR127C	YJL115W	YOR213C	YJL115W	YPL153C	YJL124C	YLR438CA
YJL124C	YNL147W	YJL125C	YNL062C	YJL128C	YLR362W	YJL137C	YLR258W
YJL140W	YOR151C	YJL154C	YOR069W	YJL157C	YOR212W	YJL176C	YOR290C
YJL187C	YMR001C	YJR022W	YLR438CA	YJR022W	YMR268C	YJR022W	YNL050C
YJR022W	YNL118C	YJR022W	YNL147W	YJR022W	YNR050C	YJR022W	YNR053C
YJR022W	YOR076C	YJR022W	YOR319W	YJR022W	YPR178W	YJR032W	YPL240C
YJR045C	YOR232W	YJR050W	YJR050W	YJR050W	YLL036C	YJR050W	YLR117C
YJR050W	YMR213W	YJR053W	YML064C	YJR063W	YPR010C	YJR066W	YNL006W
YJR068W	YMR078C	YJR068W	YOR144C	YJR076C	YML109W	YJR090C	YPL256C
YJR093C	YKR002W	YJR093C	YNL317W	YJR093C	YPR107C	YJR094C	YMR139W
YJR135C	YPR046W	YKL006CA	YLR026C	YKL042W	YKL042W	YKL052C	YKR083C
YKL068W	YLR347C	YKL068W	YPL169C	YKL074C	YLR116W	YKL082C	YML109W

YKL117W	YPL240C	YKL129C	YLR337C	YKL129C	YOR181W	YKL130C	YKL130C
YKL196C	YLR026C	YKL196C	YMR197C	YKL203C	YNL006W	YKR002W	YLR277C
YKR002W	YNL317W	YKR002W	YPR107C	YKR068C	YML077W	YKR068C	YOR115C
YLL016W	YLR310C	YLL024C	YMR091C	YLL024C	YPL240C	YLL026W	YLL026W
YLL036C	YLL036C	YLL036C	YLR117C	YLL036C	YMR213W	YLL039C	YNL103W
YLR006C	YNR031C	YLR007W	YOL034W	YLR014C	YLR014C	YLR025W	YLR025W
YLR026C	YLR268W	YLR026C	YMR197C	YLR093C	YOR106W	YLR113W	YNL167C
YLR115W	YNL317W	YLR116W	YPL105C	YLR117C	YMR213W	YLR117C	YPL151C
YLR117C	YPR101W	YLR147C	YOR308C	YLR175W	YNL124W	YLR191W	YNL214W
YLR200W	YML094W	YLR207W	YMR297W	YLR207W	YOL013C	YLR216C	YMR186W
YLR216C	YPL240C	YLR226W	YPR161C	YLR229C	YNL271C	YLR229C	YNL298W
YLR229C	YOR127W	YLR229C	YPL115C	YLR229C	YPL161C	YLR229C	YPL242C
YLR234W	YMR190C	YLR245C	YLR245C	YLR256W	YLR256W	YLR256W	YPL240C
YLR259C	YOR020C	YLR263W	YLR263W	YLR277C	YNL317W	YLR288C	YOR368W
YLR293C	YLR347C	YLR293C	YMR308C	YLR293C	YNL189W	YLR293C	YOR160W
YLR310C	YNL098C	YLR310C	YPL240C	YLR313C	YLR362W	YLR335W	YLR347C
YLR337C	YMR032W	YLR337C	YMR109W	YLR337C	YOR181W	YLR347C	YMR047C
YLR347C	YNL189W	YLR347C	YOR098C	YLR360W	YPL120W	YLR362W	YLR362W
YLR362W	YPL240C	YLR371W	YPR165W	YLR381W	YPR046W	YLR396C	YOR106W
YLR433C	YOR324C	YLR438CA	YNL147W	YLR442C	YLR442C	YLR442C	YNL216W
YLR450W	YMR022W	YML057W	YOR324C	YML064C	YMR055C	YML109W	YML109W
YML109W	YNL271C	YML109W	YNL298W	YML115C	YPL050C	YMR038C	YMR038C
YMR043W	YMR043W	YMR078C	YNL290W	YMR078C	YOL094C	YMR080C	YNL112W
YMR091C	YPL240C	YMR109W	YNL271C	YMR109W	YOR181W	YMR109W	YOR389W
YMR117C	YMR117C	YMR117C	YOL069W	YMR125W	YPL178W	YMR167W	YNL082W
YMR167W	YOL090W	YMR167W	YPL164C	YMR186W	YOR027W	YMR186W	YOR057W
YMR190C	YNL088W	YMR197C	YOL018C	YMR197C	YOR036W	YMR197C	YOR106W
YMR198W	YPR141C	YMR203W	YNL131W	YMR213W	YPL151C	YMR224C	YMR224C
YMR240C	YOR319W	YMR255W	YOR046C	YMR309C	YPR041W	YNL070W	YNL131W
YNL086W	YOR069W	YNL088W	YNL088W	YNL090W	YPL161C	YNL102W	YPR135W
YNL103W	YNL103W	YNL113W	YPR110C	YNL118C	YOL149W	YNL138W	YNL138W
YNL151C	YNR003C	YNL151C	YPR190C	YNL189W	YOR098C	YNL189W	YPL178W
YNL232W	YOL021C	YNL250W	YNL250W	YNL271C	YOR122C	YNL271C	YPR165W
YNL289W	YPL031C	YNL290W	YOR144C	YNL333W	YNL333W	YNR003C	YPR190C
YNR017W	YPL063W	YOL001W	YPL031C	YOL068C	YOR279C	YOL090W	YOR033C
YOL094C	YOR144C	YOL135C	YOR174W	YOL139C	YOR276W	YOR027W	YPL240C
YOR036W	YPL240C	YOR098C	YOR160W	YOR116C	YOR224C	YOR127W	YPR165W
YOR181W	YPR154W	YOR224C	YOR341W	YOR244W	YPR023C	YOR270C	YPR036W
YPL106C	YPL240C	YPL153C	YPL153C	YPL161C	YPR165W	YPL240C	YPL240C
YPL240C	YPR201W	YPL253C	YPR141C				

Supporting Online Material Table S2. The PRS set

Interactions		Interactions		Interactions	
Protein A	**Protein B**	**Protein A**	**Protein B**	**Protein A**	**Protein B**
LSM6	LSM5	CDC53	MET30	RAD23	RPT6
RNA15	RNA14	DOC1	CDC16	SEC9	SSO1
SPC25	SPC24	GLE1	GFD1	SKP1	GRR1
CDD1	CDD1	GOS1	SED5	SLI15	IPL1
ACT1	ACT1	MAS6	TIM50	SPT15	TOA2
ACT1	SRV2	MCM3	CDC46	STE5	KSS1
AHA1	HSP82	MUD2	MSL5	TAF25	TAF19
CEG1	CET1	NIP1	PRT1	TAF25	TAF40
CWC2	PRP19	NTC20	CEF1	TLG1	VTI1
UBC9	SMT3	OST1	OST3	PCF11	RNA15
BUB1	BUB3	OST1	SWP1	ACT1	LAS17
NHP2	NAF1	PAB1	TIF4632	SBA1	HSP82
RVS161	RVS167	POL30	MSH6	CPR7	HSP82
RVS167	LAS17	RPG1	NIP1	GIC2	CDC42
SIT4	TAP42	RSC6	RSC8	ISY1	PRP19
TRS31	BET3	RVS161	FUS2	NTC20	PRP19
RFC5	RFC2	RVS167	GYL1	NUP57	NSP1
POL30	POL32	RVS167	GYP5	OST4	OST3
PRE1	PRE6	SKP1	CTF13	PAF1	CTR9
PRE7	PRE5	SPC25	TID3	PRP19	CEF1
SPT15	BRF1	STE20	CDC42	PRP19	PRP19
ABP1	APP1	TIF4631	CDC33	PRP9	PRP21
HHF1	HHT1	TIM17	MAS6	SIR2	SIR3
LSM5	LSM1	TIM44	MAS6	SSA1	YDJ1
PAB1	TIF4631	TIM44	SSC1	STI1	HSP82
SED5	SEC22	XRS2	MRE11	TOM20	TOM40
TRS23	BET3	YRB2	GSP1		
CDC53	CDC4	APC11	CDC16		
PPH22	TAP42	CDC28	CDC6		
PRP11	PRP21	CDC28	SIC1		
SKP1	CDC4	CDC4	CDC6		
TIF35	PRT1	CDC4	HRT1		
TIF35	TIF34	CDC53	GRR1		
CDC53	CDC34	CMD1	XCM1		
CDC53	HRT1	DAD1	DAM1		
CDC53	SKP1	DUO1	DAM1		
LSM4	LSM8	FUS3	DIG1		
MEC3	RAD17	KAP123	GSP1		
RPG1	PRT1	KSS1	STE12		
TID3	SPC24	MRS5	MRS11		
TIF34	PRT1	MSH6	MSH2		
TRS20	BET3	NIC96	NUP57		
ABP1	RVS167	NOP1	NOP58		
ABP1	SRV2	PCF11	RNA14		
BET3	BET5	PRE1	RPT6		

Supporting Online Material Table S3. The RRS set

Interactions		Interactions		Interactions	
Protein A	**Protein B**	**Protein A**	**Protein B**	**Protein A**	**Protein B**
YAL049C	EGD2	WSS1	YLR225C	SFB3	ADE17
HOM3	YGR271CA	YHR162W	DNA43	SSP1	YOR394CA
YBL044W	YBR053C	YHR180W	YJR083C	YIL105C	TOA2
ECM32	NOP13	YIL006W	ATP18	SIP4	CHS5
YLL014W	YOR223W	PRI1	YMR157C	YBL101WC	YOR041C
ERP2	RNH70	YJL032W	YLL017W	RPL21A	LAS21
PEX22	FUS1	YJL048C	CFT2	HPC2	YMR157C
YBL057C	SCS2	TAH11	YOL027C	YBR235W	YCR025C
YBL071CB	YNL022C	CYC1	YOL125W	RNQ1	YLL020C
HHF1	YML089C	ATP7	PEP5	YDL114WA	YKU70
IML3	YPL107W	YKL084W	YLR324W	YDL189W	YML058CA
GRS1	YKR046C	OAC1	YMR126C	FYV1	YOL124C
YBR161W	RCK2	UIP5	YMR029C	AFR1	YPR063C
KTR3	MSS18	YKR045C	YLR050C	YDR250C	YOR200W
TDP1	YJR003C	YLR326W	MET7	SAC7	NPL3
YBR235W	ADY3	SWP1	PDH1	ERD1	RSA3
YCL046W	YLR007W	ESBP6	GIS2	KRE22	YLR225C
PRD1	YHL039W	PUT4	MSS18	KRE31	YNL226W
PER1	SAS5	PDX3	CBS2	HSP12	YML058CA
YDL023C	YME1	AMN1	YOL160W	CDC14	SYF2
COX9	YHR162W	PDB1	RHO1	CDC14	YLL047W
YDL121C	HIS2	PRP5	YER138WA	PNC1	YOR214C
YDL183C	SPC1	ISW1	YHR022CA	YHR125W	YLR365W
YDR034WB	JNM1	ISW1	MSB4	MET30	DIA2
YDR100W	YDR540C	MAL33	YEL068C	MMF1	YNR003WA
YDR179C	ESC4	YCL042W	UGP1	YJL119C	YNL200C
ESC2	POR1	KRR1	ADE2		
SNM1	YLR434C	CHA1	CCT6		
YDR492W	RPD3	CSM1	KIN1		
YDR504C	ERG1	CDC7	PUT2		
STL1	YMR210W	YDL118W	TAP42		
GPA2	YOR389W	YDR128W	RNA14		
THO1	YOR356W	AHA1	CDH1		
GLO3	ECM12	PHM6	YGL160W		
HSP12	YOR394CA	GLC3	YCK3		
YFR026C	MRPL33	YAT2	YML037C		
ECO1	YLR161W	YER156C	EST1		
YGL176C	SUC2	SNO3	(MLP1)		
ZRT1	BOP2	SCW11	YKL056C		
BUD9	YPT6	SCW11	APC9		
YGR051C	ECM40	YGL042C	YJR096W		
YGR096W	YLL017W	SUT1	PGM1		
YGR165W	BUB3	MIG2	RRN7		
RNH70	YML122C	PPA1	GRE2		
ERP5	YNL140C	STE12	BAT1		

Supporting Online Material Table S4. The CCSB-YI1 set

Interactions		Interactions		Interactions		Interactions	
Protein A	Protein B	Protein A	Protein B	Protein A	Protein B	Protein A	Protein B
YLR291C	YNL229C	YPL031C	YNR012W	YLR297W	YDL100C	YGR121C	YIR038C
YLR291C	YCR086W	YER018C	YKL025C	YDL072C	YML029W	YPL022W	YLR135W
YLR291C	YPR062W	YOR304CA	YNL314W	YGL221C	YGL221C	YDR115W	YKL142W
YJL085W	YBR057C	YER063W	YDL084W	YER188W	YPL049C	YIL065C	YJL112W
YLR227C	YDR208W	YOR304CA	YDL239C	YAL021C	YJL112W	YDL076C	YLR098C
YER106W	YCR086W	YOR181W	YDR388W	YPL201C	YER062C	YDL084W	YDL084W
YLR010C	YDR082W	YJR046W	YDR520C	YPL070W	YLR321C	YKL052C	YKR083C
YDR013W	YPR135W	YLR393W	YDR100W	YGL156W	YOL083W	YMR047C	YGR218W
YLR291C	YGR267C	YHR123W	YPL094C	YOR283W	YOR229W	YIL160C	YHR160C
YLR291C	YOR111W	YJR047C	YHR068W	YHR034C	YCL028W	YDR328C	YLR267W
YLR291C	YLR377C	YEL034W	YHR068W	YML051W	YNR010W	YLR006C	YDL235C
YLR291C	YHR112C	YDR510W	YDL013W	YML051W	YMR223W	YJL124C	YLR438CA
YLR291C	YJR057W	YDR518W	YHR113W	YDL239C	YPL049C	YGR120C	YGR120C
YLR291C	YCL028W	YPL129W	YHR113W	YJR058C	YBL037W	YIL007C	YHR185C
YDR439W	YCR086W	YOL111C	YOR007C	YPL100W	YDR100W	YDR004W	YDR076W
YFR008W	YMR029C	YEL051W	YDR423C	YHR121W	YDR480W	YHR025W	YHR025W
YLR291C	YJL199C	YLR215C	YHR115C	YFL038C	YOR370C	YPL049C	YHR084W
YDR373W	YGL153W	YLR215C	YNL116W	YKL071W	YNR012W	YPL174C	YMR294W
YLR291C	YNR012W	YNR007C	YHR171W	YNR046W	YLR321C	YNL189W	YFR047C
YGL068W	YDR361C	YOR160W	YLR293C	YJL011C	YHR167W	YJL006C	YML112W
YMR077C	YJR102C	YHL039W	YMR111C	YOR109W	YDR100W	YDL084W	YDR510W
YGR024C	YHR112C	YPL125W	YLR293C	YOR054C	YKL088W	YGL058W	YLR024C
YNL204C	YDR100W	YDL239C	YPL070W	YOR117W	YJL184W	YBR109C	YGL106W
YJL137C	YJL137C	YPL020C	YGL053W	YMR314W	YBL023C	YDR142C	YIL160C
YKR010C	YCR086W	YMR061W	YBR103W	YKL189W	YPL049C	YJL124C	YER146W
YPR046W	YJR135C	YPL125W	YKR059W	YBR234C	YDR063W	YPR143W	YHR066W
YLR291C	YGL153W	YPL125W	YJL138C	YGR180C	YOR229W	YDR205W	YNR039C
YLR291C	YLR386W	YPL125W	YPR160W	YJL137C	YLR258W	YKL117W	YPL240C
YLR291C	YLL057C	YDR498C	YJL019W	YNL099C	YNL032W	YNL102W	YBL035C
YMR001C	YJL187C	YKR034W	YNL021W	YLR345W	YLR321C	YGL181W	YFR024CA
YDR300C	YDR300C	YMR096W	YMR095C	YJR136C	YKL033W	YNL334C	YFL059W
YHR022C	YDR361C	YGR262C	YBR103W	YLR345W	YGR158C	YLL042C	YHR171W
YCR060W	YHR034C	YMR146C	YDR429C	YJL058C	YER052C	YGL026C	YDR510W
YKR068C	YOR115C	YJL173C	YAR007C	YKL075C	YNL091W	YFL045C	YDR510W
YMR004W	YMR004W	YHL004W	YBR103W	YBR201W	YML029W	YKL211C	YDR510W
YBR166C	YBR166C	YFR024CA	YKL068W	YIL162W	YDL100C	YHR193C	YDR510W
YPL135W	YBR057C	YHR105W	YNL044W	YGL086W	YLR423C	YNL086W	YGR120C
YLR257W	YLR345W	YLR208W	YMR017W	YNL107W	YKL103C	YLL022C	YEL056W
YBR244W	YCR086W	YNL333W	YMR095C	YBR200W	YJL157C	YFR034C	YFR034C
YOL129W	YAR027W	YPL204W	YHR185C	YBL057C	YMR276W	YDR357C	YGL079W
YLR424W	YKR022C	YGR195W	YDR416W	YGR099W	YDR353W	YNL189W	YDR480W
YER023W	YER023W	YHR072WA	YNL124W	YKL192C	YOR124C	YGR075C	YBR152W
YNL024C	YDR386W	YBL101C	YNL225C	YOL111C	YDL100C	YNL155W	YBL058W
YDR284C	YDR284C	YNL063W	YKL142W	YJL189W	YMR139W	YOR162C	YOR162C
YMR312W	YHR187W	YGR119C	YLR423C	YER017C	YDL100C	YPL031C	YLR258W
YKL218C	YKL218C	YPL077C	YDR489W	YPL077C	YDR448W	YMR267W	YGR239C
YBR176W	YBR176W	YCL046W	YGL115W	YDR304C	YDL100C	YHR113W	YOL082W
YER081W	YER081W	YPL077C	YGR120C	YBR182C	YLR423C	YNL155W	YDL126C
YPR110C	YNL113W	YPL077C	YLR423C	YHR057C	YDL100C	YBR101C	YAL005C

YNL311C	YCR086W	YJL048C	YLR423C	YGR029W	YLR424W	YOR026W	YJL013C
YOL034W	YNL229C	YDR453C	YML028W	YMR314W	YPR135W	YLR432W	YLR432W
YAR027W	YAR027W	YLR089C	YLR423C	YBR276C	YER081W	YGR195W	YOL021C
YPL218W	YDR100W	YMR298W	YHL003C	YKL214C	YDL084W	YLR244C	YBR030W
YKR068C	YCR086W	YGL181W	YIL122W	YAL021C	YMR124W	YDL132W	YOL133W
YAL032C	YLR345W	YGL181W	YNL124W	YOL059W	YMR139W	YNL189W	YLR377C
YBR072W	YBR072W	YIL152W	YLR423C	YDR314C	YML011C	YKL003WA	YDR100W
YLL057C	YLL057C	YCR088W	YOR284W	YHR193C	YLR146C	YMR267W	YGL153W
YHR112C	YHR112C	YGR119C	YGL172W	YDL015C	YIR038C	YMR079W	YDR100W
YAL032C	YNL229C	YGR240C	YMR205C	YJR118C	YIR038C	YLR268W	YIR033W
YCL066W	YPL049C	YOR226C	YLR423C	YHR128W	YDL100C	YPR143W	YDR312W
YGL124C	YNL286W	YIL045W	YOR178C	YMR218C	YEL048C	YDR434W	YIR033W
YJL189W	YOR229W	YBL078C	YOL083W	YNL147W	YLR438CA	YLR291C	YBR252W
YDR480W	YPL049C	YGL145W	YNL258C	YML077W	YOR115C	YGL225W	YIR033W
YGL124C	YBR131W	YBR261C	YMR021C	YDR051C	YDR051C	YDR036C	YGL153W
YPL095C	YDR100W	YBR261C	YBR080C	YKL189W	YLR423C	YNL113W	YGL090W
YER087CA	YAR027W	YBR261C	YPL049C	YLR291C	YML099C	YOL126C	YOR347C
YLR177W	YDR099W	YBR261C	YML042W	YEL042W	YIR038C	YER087CA	YIR033W
YOR265W	YJR091C	YBR261C	YLL001W	YJL025W	YER125W	YPL135W	YDR100W
YDL006W	YDR162C	YBR261C	YLR098C	YHR113W	YKL103C	YGL225W	YAR027W
YPL020C	YMR071C	YBR261C	YJL218W	YLR268W	YIR038C	YDL236W	YDL236W
YMR300C	YMR300C	YBR261C	YNL044W	YPL122C	YDR448W	YDL101C	YPL269W
YDL239C	YLR098C	YBR261C	YIL074C	YDL157C	YCL056C	YMR071C	YDR479C
YPL020C	YDR479C	YKR048C	YDL090C	YPL280W	YPL280W	YJL097W	YDR479C
YMR289W	YOL083W	YDR100W	YDR479C	YOR136W	YKL103C	YCR086W	YER144C
YPR174C	YJL019W	YMR257C	YER125W	YER022W	YKL117W	YJL090C	YLR098C
YEL051W	YOR174W	YBR279W	YOR123C	YOR117W	YGR211W	YDR473C	YBL023C
YPL049C	YPL049C	YNR007C	YBL078C	YCR086W	YOR264W	YKR048C	YKR048C
YDL144C	YDL144C	YDR486C	YLR181C	YER134C	YHR171W	YJL011C	YGL096W
YNL086W	YOR174W	YMR024W	YDR479C	YDL190C	YFL044C	YLL014W	YDR479C
YGL208W	YDR477W	YDR001C	YLR270W	YIL051C	YGR144W	YER015W	YLR098C
YGL155W	YKL019W	YIL085C	YJL019W	YER015W	YER070W	YGL065C	YDR479C
YNR051C	YER151C	YGR177C	YNL044W	YLR244C	YNR029C	YMR314W	YNL229C
YOR026W	YGR188C	YBR188C	YLR117C	YDL006W	YBR222C	YDR122W	YBL023C
YNL001W	YKR084C	YKL019W	YOL135C	YLR011W	YLR011W	YOR101W	YML028W
YGL238W	YNL189W	YHR121W	YPL049C	YPL031C	YGR233C	YPR062W	YPR062W
YGR075C	YML051W	YER009W	YER009W	YDR296W	YLR386W	YDL239C	YNR012W
YLR291C	YGL252C	YKL168C	YDR099W	YLR389C	YNL229C	YJL097W	YAR027W
YLR291C	YJR010W	YKL019W	YDL090C	YML062C	YHR167W	YGL104C	YAR027W
YLR291C	YBL023C	YNL152W	YMR032W	YJL068C	YJL068C	YNL315C	YMR071C
YLR291C	YIL074C	YLR330W	YOR299W	YEL020C	YEL020C	YJL117W	YAR027W
YLR291C	YKL025C	YBL047C	YGR241C	YPR149W	YMR316CB	YCR068W	YIR033W
YLR291C	YJL112W	YGL071W	YGR211W	YNL286W	YMR288W	YOL126C	YIR033W
YLR291C	YBR080C	YJR056C	YJR056C	YNL219C	YML029W	YNL219C	YIR033W
YLR291C	YLR321C	YER010C	YER010C	YBR107C	YHR113W	YML055W	YIR033W
YOR192CA	YOR192CA	YHR111W	YHR111W	YJL121C	YJL121C	YOL034W	YPR105C
YIL144W	YOR174W	YPL077C	YHR161C	YKR043C	YKR043C	YBR241C	YIR033W
YIL105WA	YPL049C	YPL077C	YGR241C	YIL109C	YKL103C	YJL117W	YDR479C
YJR011C	YGR134W	YHR211W	YPL094C	YIL109C	YPR181C	YCR060W	YCL028W
YLR120WA	YPL208W	YGL181W	YGR241C	YFL044C	YBL058W	YDR059C	YPR093C
YGR268C	YER125W	YGL181W	YHR161C	YDR328C	YIL046W	YMR087W	YMR087W
YGR268C	YPL049C	YLR328W	YGR010W	YDR411C	YBR273C	YBR029C	YIR033W
YLR291C	YJL218W	YLR328W	YLR328W	YNL049C	YPR181C	YPL053C	YIR033W

YLR291C	YNL044W	YBR111C	YPL070W	YGL122C	YGL122C	YNL263C	YIR033W
YMR001C	YJL019W	YJR050W	YDR416W	YKR034W	YKR034W	YJR023C	YMR316CB
YHR167W	YLR423C	YDR397C	YER159C	YDR502C	YDR502C	YDR397C	YDR397C
YNR012W	YDR020C	YEL054C	YDR465C	YJL173C	YNL312W	YNL104C	YNL104C
YCL028W	YCL028W	YDR418W	YDR465C	YGR086C	YER047C	YMR322C	YPL280W
YDL239C	YOR380W	YAL044WA	YNL249C	YNL288W	YHL018W	YMR322C	YMR322C
YEL053C	YPR051W	YAL044WA	YDR098C	YMR092C	YFL039C	YOL133W	YGL060W
YDL239C	YLR423C	YDR411C	YAR027W	YML051W	YCL028W	YHL018W	YMR111C
YJL061W	YLR423C	YLR279W	YAR027W	YML051W	YDR146C	YMR322C	YOR391C
YNR011C	YNL041C	YPR191W	YGR120C	YGR195W	YDR448W	YBR006W	YBR006W
YLR315W	YDR383C	YHL004W	YGR120C	YNL093W	YOR370C	YNL040W	YNL040W
YIR017C	YLR423C	YFR024CA	YGR268C	YGR130C	YGR233C	YAL044WA	YNL218W
YGL208W	YGL115W	YHL004W	YLR423C	YBR195C	YLR017W	YLR291C	YKR034W
YNL086W	YKL061W	YHL004W	YOR284W	YHR096C	YIR038C	YLR132C	YKR034W
YDR240C	YLR423C	YJR023C	YLR404W	YGR074W	YKL183W	YAL046C	YKR034W
YDR473C	YLR423C	YNL078W	YMR139W	YGR038W	YIR038C	YDL239C	YKR034W
YPL018W	YDR132C	YDL220C	YDR082W	YPR113W	YAR027W	YBR188C	YKR034W
YLR442C	YGL175C	YLR268W	YPL094C	YBR243C	YIR038C	YBR111C	YLR245C
YLR175W	YNL124W	YPR107C	YJR093C	YIL124W	YIR038C	YGR195W	YKR034W
YLR015W	YDR469W	YDR364C	YLL036C	YBR126WA	YIR038C	YFL017WA	YKR034W
YER146W	YLR438CA	YKR068C	YDR472W	YML110C	YMR071C	YDR531W	YDR531W
YHR076W	YMR079W	YOR210W	YDR527W	YML051W	YBL093C	YDR063W	YKR034W
YNL094W	YAL049C	YMR028W	YDL188C	YML051W	YDL106C	YOL145C	YKR034W
YNL094W	YNL025C	YDR138W	YKL171W	YNR030W	YIR038C	YBR019C	YBR019C
YNL094W	YDR388W	YLR082C	YGL250W	YGL104C	YIR038C	YGR149W	YDR479C
YCR083W	YCR086W	YNL222W	YHR113W	YML035C	YBR284W	YGL240W	YKR048C
YOR007C	YCL028W	YNL075W	YBR233W	YIL109C	YOL130W	YJL134W	YDR479C
YNL138W	YFL039C	YLR291C	YHR113W	YJL025W	YMR111C	YNL316C	YOL082W
YGL181W	YDR388W	YLR291C	YER086W	YJL025W	YBL014C	YBR261C	YPR113W
YKL191W	YIL103W	YDR374C	YNR052C	YGR027C	YPL004C	YFL038C	YNL041C
YDL057W	YJL058C	YJR011C	YLR368W	YGL122C	YDL084W	YNL153C	YGL115W
YPL151C	YAL032C	YJR118C	YPL094C	YCL066W	YHR084W	YBR242W	YBR242W
YHR167W	YNL041C	YKL142W	YPL004C	YIL109C	YMR124W	YMR298W	YPL094C
YIL152W	YCR086W	YLR291C	YDR256C	YIL153W	YNL021W	YDL212W	YPL094C
YPL077C	YDR388W	YLR291C	YBR233W	YLR291C	YOR192CA	YDR027C	YFL029C
YGL181W	YMR182C	YCL033C	YOL082W	YDR361C	YER086W	YHL031C	YPL094C
YNR034W	YOR178C	YDR510W	YGL250W	YLR262C	YOR370C	YJR046W	YJL112W
YIL152W	YJL112W	YOL111C	YLR206W	YDR480W	YHR084W	YOL003C	YDR479C
YLR021W	YPL144W	YMR294WA	YBR233W	YCL033C	YKL103C	YDR411C	YJL019W
YML110C	YDR100W	YMR067C	YDL126C	YDR361C	YMR021C	YEL032W	YHR033W
YGR061C	YLR386W	YOR158W	YGR120C	YBL037W	YKL103C	YOR223W	YHL003C
YIL074C	YER081W	YGR268C	YGR268C	YGR177C	YNL263C	YNR075W	YDR479C
YDR142C	YGL153W	YGR024C	YGR024C	YML110C	YNL263C	YJR070C	YER090W
YFR027W	YJL019W	YPL149W	YGL115W	YPR181C	YHR098C	YPR174C	YER026C
YPR113W	YDR479C	YLR291C	YLR291C	YPL031C	YER059W	YJL104W	YMR071C
YGL187C	YML042W	YLR291C	YOR232W	YJR046W	YMR111C	YBR162WA	YPL094C
YNL094W	YBR260C	YLR031W	YDR532C	YPR113W	YML029W	YAL036C	YDR448W
YAL032C	YLR423C	YDR138W	YLR423C	YNL094W	YFR024CA	YDR431W	YPL094C
YAL032C	YDR416W	YLR291C	YGL175C	YLL036C	YPR152C	YGR261C	YNL199C
YJR102C	YPL002C	YJR003C	YLR423C	YOL061W	YER099C	YJL135W	YCR106W
YBR107C	YDR489W	YLR227C	YOR284W	YPL070W	YHL018W	YJL006C	YCR106W
YER182W	YKL142W	YKL142W	YKL142W	YGR250C	YPL178W	YGR140W	YCR106W
YGR261C	YOR284W	YHL004W	YDR416W	YKL154W	YDR292C	YJL077WB	YCR106W

YBR077C	YGR201C	YNL288W	YOR284W	YLR173W	YLR072W	YGR081C	YCR106W
YGR082W	YGR120C	YBR261C	YOR095C	YNL135C	YER052C	YGL247W	YCR106W
YOR124C	YGR268C	YLR291C	YOR095C	YDL195W	YLR208W	YPR046W	YCR106W
YNL107W	YIL119C	YOL054W	YKR034W	YIR036C	YIR036C	YBR134W	YCR106W
YIL084C	YLR423C	YOR095C	YOR095C	YNL277W	YNL277W	TORF47	YCR106W
YBL026W	YLR438CA	YOR159C	YPR182W	YMR079W	YCR007C	YPL034W	YCR106W
YMR052W	YFR008W	YNL288W	YLR245C	YLR455W	YLR223C	YMR001C	YOR192CA
YOR160W	YOR185C	YNL288W	YOR095C	YPR159CA	YIR033W	YMR141C	YCR106W
YBR252W	YBR252W	YER128W	YPR173C	YJR068W	YNL290W	YEL072W	YCR106W
YPR174C	YDR100W	YBR194W	YPR152C	YJR102C	YPL065W	YPL267W	YCR106W
YPL125W	YOR185C	YJR003C	YPR173C	YDR173C	YMR043W	YMR060C	YCR106W
YPL268W	YLR386W	YLR031W	YMR124W	YHR211W	YDR476C	YDR222W	YCR106W
YGL036W	YBR057C	YNL311C	YIL074C	YMR314W	YJR074W	YPL243W	YCR106W
YPL020C	YDR100W	YLR026C	YDR189W	YDR171W	YOL083W	Q0085	YCR106W
YIR032C	YIR032C	YOR094W	YBL060W	YLR215C	YER025W	TORF1	YCR106W
YNL329C	YDL166C	YPR082C	YBR055C	YOR159C	YLR438CA	YHR130C	YCR106W
YLR177W	YER177W	YIL079C	YBR233W	YDR142C	YCL056C	YLR424W	YKR034W
YAL034WA	YJR112W	YER126C	YPL004C	YGL095C	YDR323C	YDR174W	YDR174W
YKL159C	YBR247C	YGR263C	YMR070W	YLR291C	YER144C	YBL033C	YBL033C
YMR308C	YOR185C	YLR291C	YHL018W	YML051W	YKL171W	YGR047C	YKR034W
YCR086W	YCR086W	YLR291C	YDR032C	YPL070W	YJL218W	YOL123W	YCL028W
YLR377C	YLR377C	YIL095W	YER144C	YPL070W	YNL044W	YMR314W	YOR380W
YML100W	YBR126C	YPL031C	YPL049C	YKL181W	YHL011C	YKR066C	YCR007C
YNR012W	YNR012W	YDR212W	YOR284W	YML051W	YDL005C	YDL120W	YCR007C
YOR229W	YOR229W	YDL207W	YDR192C	YML051W	YHL012W	YCR021C	YDR479C
YBR126C	YBR126C	YDR036C	YLR397C	YNL189W	YJR010W	YAL032C	YJL112W
YJR021C	YLR386W	YDR100W	YPL094C	YNL189W	YPL049C	YGR261C	YDR520C
YDR100W	YAR027W	YDR107C	YMR070W	YNL189W	YHR025W	YNL263C	YDR479C
YNR046W	YDR140W	YPL135W	YOL082W	YJR003C	YDR448W	YBR122C	YGR211W
YBR261C	YBR072W	YOR160W	YER086W	YDR132C	YDR132C	YGR177C	YGL053W
YAL046C	YDR098C	YOR361C	YDR429C	YHR180W	YDL100C	YLR291C	YGL115W
YPL125W	YDR361C	YGL238W	YLR293C	YMR047C	YER081W	YOR160W	YPL088W
YMR071C	YAR027W	YJL097W	YPL094C	YJL025W	YLR423C	YGR203W	YKL171W
YDL239C	YGL153W	YBR261C	YHR074W	YMR016C	YHR185C	YJR076C	YLL019C
YPL124W	YPL124W	YBR261C	YHR111W	YML101C	YDL100C	YEL042W	YDR479C
YNL086W	YGL153W	YBR261C	YGR088W	YPL157W	YNR004W	YCR051W	YER184C
YJR013W	YAR027W	YBR261C	YBR186W	YER150W	YDL100C	YBL091CA	YDR479C
YDR100W	YDR100W	YDR296W	YER125W	YNL288W	YCL028W	YDR411C	YDR479C
YGL238W	YOR185C	YLR167W	YER125W	YDR328C	YMR258C	YHL031C	YDR479C
YDL190C	YBR170C	YIL109C	YKL068W	YBR126C	YMR261C	YIL153W	YNL229C
YMR294W	YHR129C	YGR123C	YKL117W	YDL184C	YKR048C	YDR296W	YPL049C
YNL056W	YNL032W	YDR086C	YPR071W	YLR096W	YBL023C	YBR182C	YER125W
YLR440C	YNL258C	YDR477W	YGL115W	YLL001W	YLL001W	YGL252C	YGL252C
YER128W	YLR181C	YDL090C	YMR139W	YGR099W	YKL033W	YNL021W	YNL021W
YLR026C	YNL044W	YDR214W	YMR186W	YGR099W	YML099C	YOR269W	YOR269W
YOL034W	YLR098C	YMR213W	YLR423C	YGR099W	YJL110C	YHR137W	YHR137W
YLR254C	YOR269W	YOR304CA	YNL041C	YGR099W	YKL068W	YDR242W	YDR242W
YGR177C	YDR100W	YNL288W	YLR423C	YDL239C	YDR520C	YJL183W	YDR479C
YNL315C	YDR100W	YAL036C	YLR423C	YPR049C	YLR098C	YDR488C	YHR129C
YJL104W	YDR100W	YLR262C	YNL041C	YNL044W	YNL044W	YDL164C	YNL044W
YMR024W	YDR100W	YOR308C	YNR032CA	YGR122W	YML099C	YNL315C	YER118C
YDR142C	YDL022W	YAL032C	YDR532C	YML051W	YKL135C	YER101C	YMR071C
YBR254C	YKR068C	YBL025W	YMR270C	YAL027W	YPL022W	YBR260C	YER144C

YER101C	YDR100W	YPR071W	YPR071W	YGL213C	YML108W	YDR284C	YPR071W
YDR173C	YMR042W	YLR291C	YOR380W	YOR301W	YLR404W	YNR027W	YEL029C
YIL039W	YIR038C	YLR376C	YIL132C	YHR211W	YIR038C	YNL286W	YOR284W
YGL044C	YMR061W	YGR261C	YOR380W	YOR321W	YIR038C	YCR060W	YKL117W
YMR021C	YOR111W	YER056CA	YGL153W	YHR026W	YIR038C	YDR036C	YKL142W
YOL059W	YKL142W	YAL020C	YBL071WA	YOR117W	YLR423C	YMR079W	YPR113W
YDR357C	YLR423C	YGR086C	YKL142W	YMR314W	YDR448W	YCR024C	YNL243W
YHR193C	YPL037C	YMR316W	YER125W	YDR159W	YLR423C	YGL187C	YDL066W
YNL249C	YNL249C	YNL204C	YJL151C	YKL159C	YKL019W	YPR113W	YAR033W
YDR045C	YIL122W	TORF21	YKR048C	YJL090C	YML099C	YHR072WA	YDL208W
YOL034W	YOR284W	YNL147W	YER146W	YCR063W	YOL135C	YKR097W	YKR097W
YOL034W	YLR423C	YOL059W	YKR048C	YJL011C	YKL015W	YFL017WA	YHR113W
YJR101W	YLR423C	YLR089C	YPR049C	YPR049C	YGR233C	YMR170C	YMR170C
YLL049W	YLR423C	YBR212W	YPL184C	YNL189W	YFL039C	YBR153W	YBR153W
YML041C	YLR423C	YGL048C	YGL004C	YOL018C	YIR038C	YAL012W	YAL012W
YML071C	YGL223C	YJR053W	YMR055C	YMR121C	YMR139W	YNL098C	YPL088W
YML071C	YNL041C	YKL168C	YER177W	YGL225W	YPR071W	YML079W	YML079W
YLR424W	YLR423C	YJL155C	YLR345W	YBL037W	YFR043C	YDR047W	YDR047W
YMR077C	YPL002C	YGR177C	YML011C	YJL058C	YLR423C	YDR399W	YDR399W
YMR077C	YPL065W	YKL211C	YER090W	YIL105C	YLR423C	YDL164C	YCR007C
YIL144W	YGR120C	YHR072WA	YPL208W	YPL020C	YAR027W	YCR020CA	YIL119C
YIL144W	YDR532C	YOR322C	YER125W	YOL089C	YBR150C	YKR094C	YDR330W
YOR158W	YLR423C	YHR131C	YER125W	YEL053C	YOR032C	YGR203W	YLR397C
YIL144W	YLR423C	YEL056W	YPL001W	YML064C	YOR284W	YMR079W	YGL053W
YLR291C	YPL069C	YGR063C	YML095C	YDR171W	YDR448W	YBR087W	YDR229W
YLR291C	YFL010C	YLR291C	YIR035C	YGR028W	YDL100C	YDL190C	YBR273C
YLR291C	YGR120C	YLR119W	YMR032W	YJL183W	YIR038C	YBR107C	YGL071W
YPL149W	YMR159C	YCR004C	YDR032C	YAL046C	YER174C	YDR361C	YJR056C
YLR291C	YLR423C	YBR052C	YDR032C	YKR048C	YOR032C	YGR268C	YDR330W
YLR291C	YDR428C	YNL334C	YNL333W	YKR048C	YMR139W	YPR037C	YPL094C
YLR291C	YOL143C	YFL060C	YNL333W	YML038C	YIR038C	YML125C	YDR479C
YLR291C	YOR284W	YFL060C	YFL059W	YJL097W	YIR038C	YLR350W	YDR479C
YOR284W	YOR284W	YBR261C	YHL018W	YJL011C	YDR448W	YDR476C	YDR479C
YLR082C	YLR082C	YBR261C	YDR032C	YLL014W	YIR038C	YLR227C	YDL070W
YJL030W	YBR080C	YBR261C	YFL059W	YJR073C	YIR038C	YML055W	YDR479C
YLR409C	YJL069C	YOL054W	YHL018W	YIL065C	YDL100C	YGR284C	YDR479C
YBR080C	YBR080C	YML053C	YJR009C	YPR075C	YDL100C	YNL315C	YAR027W
YER184C	YER184C	YLR291C	YLL001W	YDR526C	YDL100C	YMR227C	YDL070W
YHR129C	YHR129C	YDL113C	YJL036W	YPL070W	YBR080C	YNL029C	YJL019W
YOR276W	YOL139C	YDL164C	YDR100W	YPL070W	YHR129C	YIL046W	YBR080C
YML035C	YML035C	YDR320CA	YDR016C	YPL070W	YML042W	YGL104C	YDR479C
YIL074C	YIL074C	YLR424W	YJL110C	YPL070W	YPL049C	YNL263C	YAR027W
YJL019W	YJL019W	YLR291C	YML042W	YPL070W	YER086W	YLR291C	YBL058W
YPR108W	YER021W	YLL017W	YGR241C	YPL070W	YNL229C	YGR180C	YOR230W
YDL108W	YGL134W	YIL122W	YHR161C	YPL070W	YPL088W	YLR291C	YNL333W
YMR021C	YMR021C	YML028W	YML028W	YPL070W	YCL028W	YML097C	YJL151C
YCR020CA	YKL025C	YIL122W	YIL122W	YPL070W	YMR095C	YLR424W	YMR316CB
YDR378C	YER146W	YMR077C	YLR417W	YPL070W	YHR068W	YER087CA	YDR479C
YGR040W	YPL049C	YDR256C	YDR256C	YNL044W	YDR244W	YBR241C	YDR479C
YNL315C	YNL044W	YBR221C	YKL117W	YCR073C	YLR006C	YOR288C	YJL019W
YGR177C	YMR071C	TORF19	YDR361C	YNL189W	YHR113W	YPL144W	YBL023C
YJL110C	YDR520C	YCR020C	YCR020C	YNL189W	YPL088W	YPR082C	YPL049C
YOR250C	YKL020C	YHR060W	YLR447C	YML042W	YDR244W	YOL111C	YCL028W

YPR085C	YKL033W	YIL095W	YHR161C	YML014W	YGR233C	YOL065C	YDR479C
YDR473C	YNL229C	YML043C	YNL199C	YDR328C	YFL009W	YJR003C	YPL049C
YLR132C	YGR267C	YDR520C	YOL116W	YBL091CA	YIR038C	YLR036C	YDR479C
YEL051W	YGR120C	YIL095W	YGR241C	YNL135C	YPR093C	YNL249C	YPL125W
YGR223C	YDR100W	YJL030W	YOL116W	YPR173C	YDR448W	YDL108W	YNL025C
YLR385C	YLR424W	YGR261C	YLR423C	YML125C	YIR038C	YNR030W	YIR033W
YHL006C	YLR376C	YLR291C	YNL314W	YPL031C	YGL134W	YIL046W	YJR130C
YPR159CA	YAR027W	YLR291C	YDL144C	YPL031C	YIL050W	YNR034W	YLR273C
YDR195W	YGL153W	YLR291C	YER125W	YER056CA	YML042W	YGL181W	YPL049C
YNL111C	YNL111C	YCR009C	YDR388W	YJL025W	YBR057C	YGL053W	YDR479C
YLR291C	YLR011W	YBR150C	YOR174W	YDR476C	YIR038C	YDL057W	YPL049C
YFR008W	YOR111W	YLR291C	YNL307C	YIR015W	YLR345W	YDL057W	YLR098C
YLR291C	YER023W	YLR291C	YGR144W	YHL004W	YDR448W	YDL120W	YMR071C
YJL075C	YJL058C	YDR520C	YDR520C	YHL004W	YJL112W	YPR174C	YMR001C
YLR291C	YDR051C	YBR261C	YKL151C	YDL190C	YBL058W	YJL185C	YCL056C
YLR291C	YBR166C	YBR261C	YOL143C	YOR288C	YML029W	YFL028C	YER043C
YLR291C	YHL009C	YNL189W	YOR380W	YIL033C	YPL203W	YIL065C	YCL056C
YLR291C	YMR004W	YDL189W	YIL122W	YPL129W	YBR289W	YDL120W	YDR100W
YLR291C	YDR480W	YMR111C	YMR111C	YCR086W	YER086W	YNL131W	YCL056C
YOR379C	YJL103C	YGL181W	YGR178C	YLR291C	YKL103C	YGR203W	YIL119C
YGR142W	YCL028W	YOL109W	YMR070W	YGR268C	YOR042W	YMR308C	YOR380W
YBR244W	YLR345W	YJR013W	YPL094C	YHL003C	YPL094C	YDR063W	YDR124W
YLR376C	YMR168C	YIL008W	YHR111W	YKL189W	YOR353C	YIL153W	YLR423C
YNL263C	YNL044W	YJL127WA	YMR070W	YOL133W	YDR330W	YIR037W	YLR345W
YOL012C	YJL019W	YGL144C	YMR070W	YGR247W	YKR034W	YPL176C	YPR071W
YJL189W	YKR048C	YBL047C	YCR030C	YJL025W	YOR380W	YFL039C	YGL015C
YER180C	YPL049C	YGR130C	YPL094C	YPR017C	YLR017W	YML025C	YFR002W
YGL124C	YKL025C	YPR153W	YOR324C	YKL189W	YHR102W	YDL031W	YPL004C
YNL198C	YDR100W	YLR291C	YLR438CA	YCR009C	YBR108W	YPL260W	YDL025C
YDR177W	YPR093C	YFR008W	YDR532C	YGR142W	YJR127C	YPL164C	YPL004C
YBL001C	YBL001C	YHR184W	YDR416W	YGR142W	YBL091C	YGR067C	YOL116W
YML110C	YHR111W	YMR059W	YLR423C	YMR218C	YKL103C	YDL164C	YGL053W
YDR488C	YDR424C	YOR129C	YNL225C	YOL149W	YNL118C	YNL315C	YGL053W
YNL334C	YMR096W	YMR276W	YFL010C	YJR068W	YJL019W	YDR284C	YDR479C
YFL060C	YMR096W	YHR167W	YDL005C	YLR291C	YOL083W	YOR377W	YDR479C
YFL060C	YMR095C	YBR123C	YLR423C	YLR291C	YEL012W	YJR003C	YJL112W
YIL095W	YLR206W	YGR113W	YLR423C	YCR027C	YOL083W	YPR159CA	YDR479C
YHR074W	YHR074W	YDR121W	YBR278W	YHL033C	YML029W	YKL189W	YJL112W
YDL117W	YMR032W	YDL053C	YGR178C	YNL181W	YGR149W	YPL149W	YLR098C
YHR068W	YHR068W	YBR194W	YMR070W	YLR350W	YAR027W	YLR268W	YDR479C
YLR132C	YLL036C	YIL153W	YDR259C	YDL189W	YPL049C	YMR079W	YJL151C
YHR121W	YGR178C	YBR094W	YOL149W	YML051W	YOL148C	YMR079W	YER118C
YBR260C	YMR032W	YGR142W	YLR424W	YKL132C	YPR022C	YKL032C	YER047C
YDR142C	YMR095C	YDR374C	YLR423C	YGL053W	YML029W	YDL166C	YER047C
YBR188C	YMR124W	YGL051W	YGL051W	YOR124C	YMR048W	YMR197C	YDL056W
YJL030W	YHR113W	YCR086W	YKR034W	YDR373W	YNL267W	YBL091CA	YPL094C
YKL074C	YBR233W	YOL003C	YPL094C	YOR258W	YLR243W	YER143W	YER143W
YJL104W	YOL082W	YMR135C	YCL039W	YGR205W	YMR315W	YAL054C	YDR216W
YPL031C	YOR380W	YNL288W	YBR233W	YDR510W	YDR330W	YGL106W	YGL106W
YPL031C	YIL122W	YNL288W	YBR080C	YDR446W	YDR510W	YPR174C	YIR033W
YIL128W	YHR122W	YKR014C	YMR258C	YNL229C	YNL229C	YPL020C	YCR007C
YKL040C	YCL028W	YKL154W	YDL100C	YOL034W	YDR510W	YDR044W	YDR044W
YML055W	YAR027W	YNL263C	YPR028W	YMR233W	YDR510W	YLR377C	YJL103C

YIL153W	YNL314W	YJR039W	YOR111W	YPL209C	YBR156C	YIL065C	YAL016W
YDR320CA	YKR083C	YLR108C	YDR100W	YGL153W	YGL153W	YMR308C	YGR267C
YKR034W	YNL229C	YGR261C	YDR448W	YHR128W	YNR012W	YGR203W	YNL314W
YDR121W	YJL065C	YLR424W	YGL090W	YNL088W	YDR510W	YDR353W	YGR209C
YDL133CA	YKR048C	YGL090W	YDR388W	YDR510W	YDR510W	YBR107C	YDR421W
YKR034W	YDR520C	YAR028W	YAR027W	YKL032C	YDR510W	YCR105W	YCR105W
YPR066W	YPL003W	YJL117W	YIR038C	YML023C	YDR510W	YCL059C	YOR229W
YLL010C	YOR043W	YAR028W	YAR028W	YBR249C	YDR510W	YLR291C	YMR095C
YIL153W	YLL001W	YLR424W	YDR448W	YFL039C	YDR510W	YMR308C	YER086W
YNL078W	YKR048C	YDR132C	YHL009C	YGL087C	YDR092W	YMR308C	YKR034W
YER018C	YBR057C	YDR480W	YDR480W	YDR361C	YPL208W	YNR014W	YGR178C
YHL004W	YBR057C	YNL219C	YIR038C	YGR179C	YLR315W	YJL083W	YPL004C
YGL094C	YKL025C	YDR284C	YIR038C	YML042W	YML042W	YER052C	YER052C
YOR230W	YOR229W	YJL058C	YDR448W	YBL078C	YNL223W	YDR441C	YML022W
YMR210W	YKL142W	YJL058C	YDR480W	YPR019W	YBL023C	YGR284C	YAR027W
YDR142C	YGR239C	YLL049W	YMR294W	YJR052W	YLR442C	YJR121W	YJL218W
YGL130W	YPL228W	YJL058C	YBR057C	YAL016W	YNL127W	YDR212W	YPL049C
YKL019W	YOR380W	YHR022C	YDR448W	YLR328W	YDR510W	YDL073W	YER118C
YJL030W	YIL122W	YML041C	YDR448W	YMR111C	YDR510W	YBL020W	YDR479C
YDR378C	YLR438CA	YJR044C	YAR027W	YKL043W	YDR510W	YNR034W	YDL070W
YPL173W	YLR423C	YIL105C	YIL105C	YBR223C	YDR510W	YLR114C	YGL237C
YOR167C	YOL149W	YLR386W	YLR386W	YDR171W	YDR510W	YPL266W	YNL243W
YKL074C	YLR423C	YOL126C	YDL100C	YJR076C	YDR510W	YJL090C	YLR386W
YGR129W	YDR416W	YPR082C	YJL187C	YFR047C	YFR047C	YPL020C	YOL107W
YJR022W	YLR438CA	YPR118W	YPR118W	YPL129W	YDR510W	YJL097W	YAR028W
YDR142C	YHR160C	YAL055W	YDL100C	YDR335W	YDR146C	YJR102C	YDR132C
YKL071W	YDR259C	YJR075W	YIR038C	YHR090C	YFL024C	YER087CA	YLR404W
YIL079C	YLR423C	YJR010CA	YIR038C	YNL273W	YMR048W	YEL042W	YAR027W
YDR085C	YLR423C	YCL066W	YDR480W	YNL042W	YDR510W	YKR066C	YPL004C
YIL092W	YLR423C	YNL149C	YDL100C	YML064C	YPL049C	YLR186W	YDL189W
YML043C	YLR423C	YFL039C	YFL039C	YGR040W	YDR480W	YPR113W	YLR072W
YBR188C	YDR416W	YBR241C	YIR038C	YGR040W	YHR084W	YPL100W	YJL100W
YJL183W	YHL003C	YNL111C	YIR038C	YJL110C	YNL021W	YKL071W	YPL157W
YLR032W	YBR186W	YFL017C	YFL017C	YMR219W	YDR510W	YJL090C	YLR072W
YMR308C	YLR293C	YNL056W	YNL099C	YLR291C	YKR026C	YML018C	YGL051W
YPL108W	YLR405W	YIR038C	YIR038C	YKR014C	YOR370C	YGR017W	YFL042C
YAL036C	YOR174W	YPR048W	YKR071C	YML023C	YER038C	YCR086W	YJL110C
YDL045C	YGR077C	YOR111W	YOR111W	YLL060C	YLL060C	YMR308C	YPL088W
YHR134W	YMR095C	YNL219C	YAR027W	YBR234C	YDL029W	YCR063W	YPR152C
YDR476C	YJL019W	YGL225W	YIR038C	YPL031C	YOL001W	YOL111C	YLR245C
YDR239C	YBR260C	YER087CA	YIR038C	YDL044C	YLR386W	YJL183W	YHR036W
YLR385C	YOR174W	YDR045C	YDR448W	YOR144C	YDR510W	YPL125W	YPL088W
YMR111C	YGL250W	YJL058C	YNL229C	YDR174W	YDR510W	YOR304CA	YFL039C
YBL078C	YHR171W	YJL058C	YJL058C	YGL060W	YDR388W	YCR068W	YNL111C
YOR028C	YGL250W	YLR108C	YLR108C	YNL078W	YDR510W	YNL135C	YPL049C
YPR174C	YGL053W	YPL053C	YIR038C	YMR159C	YMR159C	YLR267W	YDL132W
YLR442C	YGL250W	YPL135W	YDR448W	YDL208W	YDR510W	YJL145W	YLR266C
YNL334C	YMR095C	YGL004C	YGR232W	YML016C	YKR072C	YOR160W	YOR095C
YLR291C	YHR111W	YDL100C	YGL153W	YLR423C	YLR423C	YLR021W	YHR113W
YLR291C	YPL070W	YPR158W	YNL007C	YIL109C	YDL195W	YIL018W	YPL004C
YLR291C	YPL088W	YLR345W	YLR345W	YHR134W	YDR510W	YIL033C	YIL033C
YLR291C	YGR088W	YAL032C	YDR448W	YGR238C	YHR158C	YJR039W	YMR021C
YLR291C	YLR245C	YKL122C	YDL092W	YPL031C	YPL219W	YJL058C	YJL112W

YLR291C	YML106W	YPR159CA	YIR038C	YMR047C	YGL170C	YAL021C	YMR181C
YBR261C	YGL037C	YML055W	YIR038C	YOL123W	YGL122C	YPL173W	YBR103W
YBR261C	YBR233W	YGR142W	YDR448W	YBR264C	YOR370C	YLR333C	YPL004C
YBR261C	YER086W	YDR284C	YNL111C	YFL009W	YFL009W	YML051W	YMR004W
YBR261C	YDR256C	YKL008C	YIR038C	YIR001C	YGR250C	YML051W	YER130C
YBR261C	YLR245C	YBR042C	YAR027W	YLR432W	YML056C	YML055W	YPL094C
YBR261C	YMR095C	YJR044C	YOL129W	YML064C	YLR328W	YLR291C	YLR258W
YBR261C	YPL088W	YNR064C	YNR064C	YGL108C	YDL126C	YJR058C	YGL175C
YBR261C	YOR108W	YHR022C	YOR032C	YER112W	YLR438CA	YML051W	YDR383C
YBR261C	YHR113W	YCR068W	YIR038C	YNL171C	YCR106W	YML051W	YDR273W
YDL209C	YLL036C	YIL026C	YPR068C	YIR003W	YER071C	YML051W	YDR308C
YBR102C	YLR423C	YOL145C	YGL153W	YPL070W	YLR245C	YPL268W	YLR423C
YKL157W	YKL142W	YNL111C	YIR033W	YGR144W	YGR144W	YGR099W	YPL235W
YLR132C	YLR423C	YLR385C	YGL244W	YDR214W	YPL240C	YJL097W	YPR071W
YKL069W	YGR209C	YDL189W	YDR480W	YLR058C	YKR099W	YBR261C	YGR267C
YHR114W	YLR423C	YBR200W	YAL041W	YKL197C	YNL329C	YLR359W	YLR359W
YML062C	YLR423C	YJR057W	YJR057W	YLR175W	YDL208W	YBL069W	YDR100W
YLR350W	YER019W	YJL117W	YIR033W	YJL183W	YDR245W	YBL091CA	YML029W
YPL251W	YGR267C	YKL189W	YDR480W	YML035C	YJL070C	YPL070W	YML035C
YPL022W	YML095C	YLR291C	YPR105C	YDL190C	YMR276W	YDR411C	YML029W
YHR113W	YHR113W	YNR067C	YDL100C	YNL062C	YJL125C	YJL058C	YIR025W
YOR108W	YOR108W	YLR291C	YNL025C	YAL055W	YGR133W	YHR123W	YIR038C
YFL017WA	YOR159C	YBR029C	YIR038C	YBR087W	YJR068W	YLR291C	YMR032W
YBR233W	YBR233W	YOL126C	YIR038C	YDR473C	YPR178W	YJL025W	YOR284W
YML008C	YML008C	YNL263C	YIR038C	YMR227C	YLR399C	YKL098W	YDR416W
YLR219W	YPL004C	YLR291C	YFL039C	YOR117W	YIL007C	YOR353C	YLR423C
YMR314W	YNL199C	YGL115W	YJL112W	YNL251C	YPL190C	YBR261C	YLR438CA
YGL187C	YBR133C	YPL149W	YIL033C	YGL051W	YAR033W	YBR261C	YPL069C
YKL069W	YKL069W	YLR291C	YPL049C	YPR069C	YLR146C	YBR261C	YOR192CA
YOL034W	YPL070W	YGR142W	YMR021C	YJR007W	YER025W	YAL044WA	YER174C
YJR068W	YDR229W	YOL145C	YGR233C	YJL061W	YJL041W	YBR261C	YOR284W
YOL034W	YOL082W	YNL311C	YKL001C	YGL112C	YBR198C	YBR261C	YCL028W
YJR075W	YPL094C	YDR132C	YFL009W	YMR124W	YER149C	YBR261C	YCR007C
YNL219C	YPL094C	YGR142W	YCR073C	YIL144W	YOL069W	YLR439W	YLR423C
YDR284C	YPL094C	YDR132C	YJL218W	YLR399C	YDL070W	YJR003C	YDR480W
YLR291C	YOR042W	YPL267W	YDR099W	YDL064W	YDR510W	YLR291C	YCR020C
YMR033W	YDR256C	YML051W	YGR146C	YGL090W	YOR005C	YGL054C	YIR038C
YCL021WA	YPL094C	YML051W	YOR359W	YAL024C	YHR158C	YBL020W	YIR038C
YPR159CA	YPL094C	YML051W	YOR197W	YJL031C	YPR176C	YOL003C	YIR038C
YMR117C	YER018C	YNL094W	YOR043W	YLR335W	YDR510W	YER018C	YDR448W
YDL015C	YOR324C	YML051W	YOR355W	YNL021W	YDR510W	YBR205W	YIR038C
YPL135W	YDR229W	YML051W	YCR065W	YNL094W	YHR114W	YJL025W	YGR233C
YOR124C	YOR138C	YML051W	YLR206W	YDL105W	YOL034W	YPR113W	YIR038C
YMR028W	YDL134C	YML051W	YDR123C	YOL133W	YGR003W	YMR314W	YHL009C
YGL225W	YPL094C	YGR240C	YGR240C	YGR098C	YDR113C	YMR104C	YML099C
YCR009C	YER125W	YPL070W	YPL070W	YNL189W	YDR510W	YNL217W	YIR038C
YKR068C	YLR328W	YPL070W	YKL151C	YOL018C	YGL095C	YML051W	YFL010C
YOR385W	YER125W	YPL070W	YGL037C	YOL034W	YER047C	YJR084W	YDR363WA
YJR102C	YLR417W	YPL070W	YHR111W	YDR510W	YER047C	YML051W	YOL067C
YGL037C	YGL037C	YPL070W	YDR256C	YPL031C	YNL025C	YGR038W	YML029W
YOL143C	YOL143C	YEL042W	YPL094C	YFL044C	YDL126C	YML029W	YML029W
YNL104C	YOR108W	YMR047C	YDR229W	YFR024CA	YPR171W	YMR024W	YGR125W
YDL125C	YHL018W	YAL021C	YNR052C	YBR088C	YDR510W	YLR291C	YDR520C

YGL122C	YBR233W	YDR473C	YBR233W	YBL026W	YGR158C	YPR017C	YPL049C
YNL078W	YOL070C	YDR473C	YPL004C	YOR353C	YHR102W	YGL141W	YKR064W
YIL053W	YPL201C	YJL097W	YML029W	YPL070W	YPR193C	YLR385C	YKL103C
YPL201C	YHR113W	YLL014W	YML029W	YNL189W	YLR245C	YDR510W	YOR032C
YIL109C	YLR245C	YGR099W	YMR047C	YER157W	YGR120C	YGR027C	YGR086C
YNL124W	YDL208W	YLL045C	YML029W	YPL259C	YKL135C	YGR268C	YLR206W
YMR096W	YMR096W	YDR100W	YML029W	YNL189W	YGR144W	YPL070W	YFL059W
YPL094C	YPL094C	YNL126W	YLR212C	YDL055C	YDR510W	YOL145C	YKL103C
YMR096W	YFL059W	YMR308C	YHR113W	YDR167W	YML114C	YCR083W	YDR448W
YMR096W	YNL333W	YPL088W	YPL088W	YER092W	YLR423C	YKL212W	YML029W
YLR245C	YLR245C	YFL047W	YKL171W	YGR262C	YER174C	YJL134W	YML029W
YDR502C	YLR180W	YMR111C	YDL013W	YHR106W	YDR353W	YDR116C	YBR233W
YLR157C	YKL117W	YML106W	YML106W	YLR438CA	YLR438CA	YPR113W	YJL019W
YGL122C	YLR206W	YLR177W	YGL122C	YKR026C	YKR026C	YER086W	YER086W
YNL153C	YHR113W	YIL092W	YGL122C	YAR033W	YAR033W	YNL189W	YOR095C
YFR024CA	YOR042W	YGL156W	YKL103C	YDL190C	YDL126C	YNL189W	YDR256C
YIR034C	YOR138C	YIL079C	YGL122C	YLR181C	YPR173C	YBR261C	YNL239W
YNL124W	YNL124W	YDR171W	YDR171W	YDR328C	YLR368W	YJL183W	YPL094C
YIL069C	YPL004C	YML082W	YIL046W	YNL288W	YNR052C	YNL189W	YBR080C
YLR392C	YER125W	YDR488C	YPL174C	YHR107C	YJR076C	YIL153W	YLR258W
YGR286C	YMR070W	YGR088W	YNR052C	YMR275C	YER125W	YLR132C	YNL286W
YKL063C	YPL094C	YNL189W	YGL037C	YPR176C	YOR370C	YML051W	YOR370C
YJR024C	YJR024C	YPR049C	YKL103C	YLR293C	YDR335W	YNL189W	YHR112C
YOL133W	YJL047C	YER024W	YAR035W	YAL036C	YDR152W	YBR261C	YHR112C
YER056CA	YDR244W	YPR193C	YPR193C	YGR057C	YKL015W	YBR261C	YDR100W
YGR086C	YPL004C	YOR007C	YOR007C	YLR452C	YHR158C	YBR261C	YJL199C
YLR180W	YLR180W	YDL239C	YKL103C	YKL103C	YKL103C	YBR261C	YJL151C
YIR035C	YIR035C	YHR140W	YIR038C	YLR275W	YPR182W	YML051W	YPL047W
YHL018W	YHL018W	YNL189W	YGR267C	YNL113W	YHL018W	YML051W	YKL015W
YNL333W	YNL333W	YNL044W	YGL153W	YFL037W	YOR265W	YNL189W	YOR229W
YNL333W	YFL059W	YOL018C	YDL100C	YNL102W	YPR135W		
YDR032C	YDR032C	YDR513W	YDL100C	YLR350W	YDR510W		
YHR105W	YDR100W	YNL189W	YCL028W	YOR194C	YKL058W		

Supporting Online Material Table S5. The Y2H-union set

Interactions		Interactions		Interactions		Interactions	
Protein A	Protein B	Protein A	Protein B	Protein A	Protein B	Protein A	Protein B
YAL005C	YBR101C	YDL207W	YDR192C	YFR008W	YMR052W	YJL187C	YPR082C
YAL012W	YAL012W	YDL208W	YDR510W	YFR008W	YOL135C	YJL189W	YKR048C
YAL016W	YIL065C	YDL208W	YHR072WA	YFR008W	YOR111W	YJL189W	YMR139W
YAL016W	YNL127W	YDL208W	YLR175W	YFR008W	YPR046W	YJL189W	YOR229W
YAL020C	YBL071WA	YDL208W	YNL124W	YFR015C	YFR015C	YJL199C	YJL199C
YAL021C	YJL112W	YDL209C	YLL036C	YFR015C	YJL137C	YJL199C	YLR291C
YAL021C	YMR124W	YDL210W	YGL230C	YFR015C	YLR258W	YJL199C	YML064C
YAL021C	YMR181C	YDL212W	YDR508C	YFR017C	YPR184W	YJL199C	YNL189W
YAL021C	YNR052C	YDL212W	YPL094C	YFR024CA	YGL181W	YJL200C	YOL133W
YAL024C	YHR158C	YDL215C	YLR432W	YFR024CA	YGR268C	YJL218W	YJL218W
YAL027W	YPL022W	YDL215C	YPR048W	YFR024CA	YKL068W	YJL218W	YJR121W
YAL028W	YDL239C	YDL216C	YMR025W	YFR024CA	YNL094W	YJL218W	YLR291C
YAL032C	YDR416W	YDL217C	YHR114W	YFR024CA	YOR042W	YJL218W	YML064C
YAL032C	YDR448W	YDL218W	YGL044C	YFR024CA	YPR171W	YJL218W	YNL189W
YAL032C	YDR532C	YDL220C	YDR082W	YFR027W	YJL019W	YJL218W	YPL070W
YAL032C	YJL112W	YDL224C	YER059W	YFR033C	YNL236W	YJR003C	YLR423C
YAL032C	YLR345W	YDL226C	YER118C	YFR034C	YFR034C	YJR003C	YPL049C
YAL032C	YLR423C	YDL226C	YGL198W	YFR036W	YJR091C	YJR003C	YPR173C
YAL032C	YNL229C	YDL226C	YGR172C	YFR037C	YML127W	YJR009C	YML053C
YAL032C	YPL151C	YDL226C	YJL151C	YFR037C	YMR091C	YJR010W	YJR010W
YAL034WA	YGL172W	YDL226C	YKR088C	YFR042W	YPR159W	YJR010W	YLR291C
YAL034WA	YGR120C	YDL226C	YOL129W	YFR043C	YPR029C	YJR010W	YNL189W
YAL034WA	YJR112W	YDL226C	YOR327C	YFR047C	YFR047C	YJR011C	YLR368W
YAL034WA	YKL103C	YDL226C	YPR113W	YFR047C	YLL046C	YJR011C	YNR069C
YAL036C	YDR152W	YDL226C	YPR183W	YFR047C	YNL189W	YJR013W	YPL094C
YAL036C	YDR448W	YDL235C	YLR006C	YFR049W	YOR047C	YJR021C	YLR386W
YAL036C	YLR423C	YDL236W	YDL236W	YFR052W	YJR133W	YJR021C	YNL189W
YAL036C	YOR174W	YDL236W	YNL189W	YGL004C	YGL048C	YJR022W	YLR438CA
YAL040C	YJL013C	YDL237W	YPR148C	YGL004C	YGR232W	YJR023C	YLR404W
YAL041W	YBR200W	YDL239C	YDR148C	YGL013C	YGL013C	YJR023C	YMR316CB
YAL044WA	YDR098C	YDL239C	YDR176W	YGL015C	YLR319C	YJR024C	YJR024C
YAL044WA	YER174C	YDL239C	YDR273W	YGL019W	YGR068C	YJR034W	YNL236W
YAL044WA	YNL218W	YDL239C	YDR520C	YGL024W	YOL130W	YJR039W	YMR021C
YAL044WA	YNL249C	YDL239C	YGL153W	YGL025C	YOL130W	YJR039W	YOR111W
YAL046C	YDR098C	YDL239C	YGR268C	YGL030W	YHR204W	YJR044C	YOL129W
YAL046C	YER174C	YDL239C	YHR184W	YGL037C	YGL037C	YJR046W	YMR111C
YAL046C	YKR034W	YDL239C	YKL103C	YGL037C	YNL189W	YJR052W	YLR442C
YAL049C	YNL094W	YDL239C	YKR034W	YGL037C	YPL070W	YJR053W	YMR055C
YAL054C	YDR216W	YDL239C	YLR072W	YGL040C	YGL040C	YJR055W	YPL193W
YAL054C	YLR049C	YDL239C	YLR098C	YGL040C	YML064C	YJR056C	YJR056C
YAL054C	YNL189W	YDL239C	YLR423C	YGL040C	YNL189W	YJR056C	YNL189W
YAL055W	YDL100C	YDL239C	YML042W	YGL044C	YMR061W	YJR057W	YJR057W
YAL055W	YGR133W	YDL239C	YNR012W	YGL044C	YMR270C	YJR057W	YLR291C
YAL060W	YER081W	YDL239C	YOL091W	YGL051W	YGL051W	YJR068W	YNL290W
YAL062W	YLR267W	YDL239C	YOR304CA	YGL051W	YML018C	YJR072C	YLR150W
YAR003W	YBR175W	YDL239C	YOR324C	YGL053W	YGR177C	YJR072C	YLR243W
YAR003W	YDR140W	YDL239C	YOR380W	YGL053W	YML029W	YJR072C	YOR262W
YAR007C	YJL173C	YDL239C	YPL049C	YGL053W	YMR079W	YJR074W	YLR293C
YAR014C	YER133W	YDL239C	YPL070W	YGL053W	YNL315C	YJR074W	YMR314W

YAR018C	YAR018C	YDL239C	YPL124W	YGL053W	YOR059C	YJR074W	YOR185C
YAR027W	YAR027W	YDL239C	YPL255W	YGL053W	YPL020C	YJR075W	YPL094C
YAR027W	YAR028W	YDL246C	YDL246C	YGL053W	YPR174C	YJR076C	YLL019C
YAR027W	YBR042C	YDL246C	YJR159W	YGL054C	YIR038C	YJR083C	YLR295C
YAR027W	YDR100W	YDR001C	YLR270W	YGL058W	YLR024C	YJR086W	YOR212W
YAR027W	YDR411C	YDR002W	YKR048C	YGL060W	YOL133W	YJR091C	YKL002W
YAR027W	YEL042W	YDR004W	YDR076W	YGL061C	YGR113W	YJR091C	YKL076C
YAR027W	YER087CA	YDR005C	YER081W	YGL061C	YKR037C	YJR091C	YKL113C
YAR027W	YGL104C	YDR008C	YJR091C	YGL071W	YGR211W	YJR091C	YKR037C
YAR027W	YGL225W	YDR013W	YDR489W	YGL071W	YIR018W	YJR091C	YLR059C
YAR027W	YGR284C	YDR013W	YPR135W	YGL079W	YGR113W	YJR091C	YLR156W
YAR027W	YJL097W	YDR016C	YDR320CA	YGL086W	YLR423C	YJR091C	YLR392C
YAR027W	YJL117W	YDR016C	YGL061C	YGL090W	YLR424W	YJR091C	YLR420W
YAR027W	YJR013W	YDR016C	YGR113W	YGL090W	YNL113W	YJR091C	YML015C
YAR027W	YJR044C	YDR016C	YKR037C	YGL090W	YOR005C	YJR091C	YMR067C
YAR027W	YLR279W	YDR017C	YDR099W	YGL092W	YKL057C	YJR091C	YNR048W
YAR027W	YLR350W	YDR020C	YDR020C	YGL094C	YKL025C	YJR091C	YOR014W
YAR027W	YML055W	YDR020C	YNR012W	YGL095C	YOL018C	YJR091C	YOR265W
YAR027W	YMR071C	YDR022C	YLR423C	YGL096W	YJL011C	YJR091C	YOR317W
YAR027W	YNL219C	YDR026C	YDR110W	YGL104C	YIR038C	YJR091C	YPL159C
YAR027W	YNL263C	YDR027C	YFL029C	YGL106W	YGL106W	YJR093C	YNL092W
YAR027W	YNL315C	YDR032C	YDR032C	YGL112C	YMR236W	YJR093C	YPR107C
YAR027W	YOL129W	YDR032C	YLR291C	YGL112C	YMR255W	YJR094C	YMR139W
YAR027W	YPL020C	YDR034C	YER043C	YGL112C	YOR220W	YJR097W	YNL092W
YAR027W	YPR113W	YDR034C	YGR113W	YGL115W	YGL208W	YJR101W	YLR423C
YAR027W	YPR159CA	YDR036C	YGL153W	YGL115W	YJL112W	YJR102C	YLR417W
YAR028W	YAR028W	YDR036C	YKL142W	YGL115W	YLR291C	YJR102C	YML101C
YAR028W	YJL097W	YDR036C	YLR397C	YGL115W	YNL153C	YJR102C	YMR077C
YAR031W	YBR217W	YDR044W	YDR044W	YGL115W	YPL149W	YJR102C	YPL002C
YAR031W	YCR030C	YDR044W	YDR077W	YGL116W	YJL030W	YJR102C	YPL065W
YAR033W	YAR033W	YDR045C	YDR448W	YGL122C	YGL122C	YJR103W	YJR103W
YAR033W	YGL051W	YDR045C	YIL122W	YGL122C	YIL079C	YJR118C	YPL094C
YAR033W	YPR113W	YDR047W	YDR047W	YGL122C	YIL092W	YJR125C	YOR111W
YAR035W	YER024W	YDR051C	YDR051C	YGL122C	YKR026C	YJR133W	YNL189W
YAR066W	YDR074W	YDR051C	YLR291C	YGL122C	YLR177W	YJR134C	YMR047C
YBL001C	YBL001C	YDR052C	YLR423C	YGL122C	YLR206W	YJR135C	YPR046W
YBL006C	YDR489W	YDR054C	YNL236W	YGL122C	YMR255W	YJR136C	YKL033W
YBL007C	YHR016C	YDR059C	YPR093C	YGL122C	YNL016W	YJR141W	YLR447C
YBL010C	YKR022C	YDR063W	YDR124W	YGL122C	YOL123W	YJR159W	YNL189W
YBL014C	YJL025W	YDR063W	YKR034W	YGL124C	YKL025C	YKL001C	YNL311C
YBL016W	YDR480W	YDR070C	YFL017C	YGL124C	YNL286W	YKL002W	YLR423C
YBL016W	YPL049C	YDR073W	YML068W	YGL126W	YPL161C	YKL002W	YMR117C
YBL020W	YDR479C	YDR074W	YER019CA	YGL127C	YLR423C	YKL002W	YOR047C
YBL020W	YIR038C	YDR076W	YER095W	YGL127C	YOL135C	YKL008C	YMR298W
YBL021C	YGL237C	YDR078C	YHL006C	YGL127C	YOR047C	YKL012W	YNL236W
YBL021C	YOR358W	YDR078C	YIL152W	YGL127C	YOR128C	YKL015W	YML051W
YBL023C	YDR122W	YDR078C	YJL092W	YGL127C	YOR174W	YKL017C	YOL108C
YBL023C	YDR473C	YDR082W	YLR010C	YGL127C	YPR168W	YKL019W	YKL159C
YBL023C	YLR096W	YDR084C	YGL127C	YGL130W	YPL228W	YKL019W	YOL135C
YBL023C	YLR291C	YDR084C	YGL161C	YGL134W	YPL031C	YKL019W	YOR380W
YBL023C	YMR314W	YDR084C	YGL198W	YGL141W	YKR064W	YKL020C	YOR250C
YBL023C	YPL144W	YDR085C	YLR423C	YGL144C	YMR070W	YKL023W	YKR092C
YBL023C	YPR019W	YDR086C	YPR071W	YGL145W	YNL258C	YKL025C	YLR291C

YBL025W	YMR270C	YDR091C	YLR192C	YGL145W	YPR105C	YKL028W	YKR062W
YBL026W	YCR077C	YDR092W	YGL087C	YGL150C	YOR355W	YKL033W	YPR085C
YBL026W	YGR158C	YDR098C	YGL071W	YGL153W	YGL153W	YKL035W	YKL035W
YBL026W	YLR438CA	YDR098C	YGL220W	YGL153W	YIR034C	YKL035W	YML064C
YBL033C	YBL033C	YDR099W	YKL168C	YGL153W	YLR291C	YKL038W	YOR047C
YBL033C	YNL105W	YDR099W	YLR177W	YGL153W	YMR267W	YKL044W	YLR288C
YBL033C	YPR172W	YDR099W	YNL042W	YGL153W	YNL044W	YKL050C	YLR423C
YBL035C	YNL102W	YDR099W	YPL267W	YGL153W	YNL086W	YKL052C	YKR083C
YBL037W	YFR043C	YDR100W	YDR100W	YGL153W	YOL105C	YKL052C	YMR077C
YBL037W	YJR058C	YDR100W	YDR479C	YGL153W	YOL145C	YKL058W	YOR194C
YBL037W	YKL103C	YDR100W	YER101C	YGL153W	YOR180C	YKL061W	YNL086W
YBL039C	YJR103W	YDR100W	YGR177C	YGL153W	YPR105C	YKL061W	YNL122C
YBL042C	YER021W	YDR100W	YGR223C	YGL154C	YGL254W	YKL063C	YPL094C
YBL043W	YBL101WA	YDR100W	YHR105W	YGL154C	YOR128C	YKL067W	YKL067W
YBL043W	YDR099W	YDR100W	YJL104W	YGL155W	YKL019W	YKL067W	YLR347C
YBL045C	YPR191W	YDR100W	YKL003WA	YGL156W	YKL103C	YKL067W	YML064C
YBL046W	YNL201C	YDR100W	YLR108C	YGL156W	YOL082W	YKL067W	YNL189W
YBL047C	YCR030C	YDR100W	YLR393W	YGL156W	YOL083W	YKL068W	YMR047C
YBL047C	YGR241C	YDR100W	YML029W	YGL158W	YLR113W	YKL069W	YKL069W
YBL051C	YIL151C	YDR100W	YML110C	YGL161C	YGL198W	YKL071W	YNR012W
YBL051C	YKR096W	YDR100W	YMR024W	YGL166W	YJL154C	YKL071W	YPL157W
YBL056W	YDR071C	YDR100W	YMR079W	YGL166W	YKR011C	YKL074C	YLR423C
YBL057C	YMR276W	YDR100W	YNL189W	YGL166W	YLL028W	YKL075C	YNL091W
YBL058W	YDL190C	YDR100W	YNL198C	YGL166W	YML006C	YKL088W	YOR054C
YBL058W	YFL044C	YDR100W	YNL204C	YGL166W	YNL189W	YKL090W	YPL128C
YBL058W	YLR291C	YDR100W	YNL315C	YGL166W	YOR210W	YKL103C	YKL103C
YBL058W	YNL155W	YDR100W	YOR109W	YGL166W	YOR220W	YKL103C	YLR291C
YBL060W	YOR094W	YDR100W	YPL020C	YGL170C	YMR047C	YKL103C	YLR385C
YBL068W	YOL061W	YDR100W	YPL094C	YGL172W	YGR119C	YKL103C	YML064C
YBL069W	YDR100W	YDR100W	YPL095C	YGL172W	YNL041C	YKL103C	YMR218C
YBL077W	YBL077W	YDR100W	YPL100W	YGL172W	YNL086W	YKL103C	YNL107W
YBL078C	YHR171W	YDR100W	YPL135W	YGL174W	YIR005W	YKL103C	YNL189W
YBL078C	YNL223W	YDR100W	YPL218W	YGL175C	YGL175C	YKL103C	YOL082W
YBL078C	YNR007C	YDR100W	YPR174C	YGL175C	YJR058C	YKL103C	YOL145C
YBL078C	YOL083W	YDR105C	YER081W	YGL175C	YLR291C	YKL103C	YOR136W
YBL081W	YDL167C	YDR106W	YHR129C	YGL175C	YLR442C	YKL103C	YPR049C
YBL091C	YGR142W	YDR107C	YMR070W	YGL175C	YNL189W	YKL107W	YLR288C
YBL091CA	YDR479C	YDR108W	YGR234W	YGL180W	YPR185W	YKL117W	YLR157C
YBL091CA	YIR038C	YDR113C	YGR098C	YGL181W	YGR178C	YKL117W	YPL240C
YBL091CA	YML029W	YDR115W	YKL142W	YGL181W	YGR241C	YKL130C	YKL130C
YBL091CA	YPL094C	YDR121W	YJL065C	YGL181W	YHR161C	YKL130C	YMR314W
YBL093C	YML051W	YDR122W	YOL082W	YGL181W	YHR177W	YKL130C	YNL023C
YBL101C	YNL225C	YDR123C	YML051W	YGL181W	YIL122W	YKL130C	YNL189W
YBL101WA	YFL002WA	YDR123C	YOL108C	YGL181W	YMR182C	YKL130C	YPR020W
YBL101WA	YJL162C	YDR128W	YLR208W	YGL181W	YNL124W	YKL132C	YPR022C
YBL101WA	YNL229C	YDR132C	YDR132C	YGL181W	YPL013C	YKL135C	YML051W
YBL102W	YGR068C	YDR132C	YFL009W	YGL181W	YPL049C	YKL135C	YOL108C
YBL102W	YLR453C	YDR132C	YHL009C	YGL187C	YGL213C	YKL135C	YPL259C
YBL102W	YOR036W	YDR132C	YHR170W	YGL187C	YML042W	YKL135C	YPR029C
YBL105C	YML109W	YDR132C	YJL218W	YGL189C	YHR114W	YKL142W	YKL142W
YBR006W	YBR006W	YDR132C	YJR102C	YGL189C	YLL027W	YKL142W	YKL157W
YBR006W	YDR382W	YDR132C	YPL018W	YGL189C	YLR435W	YKL142W	YMR165C
YBR006W	YKL023W	YDR138W	YKL171W	YGL190C	YLR373C	YKL142W	YMR210W

YBR019C	YBR019C	YDR138W	YLR423C	YGL190C	YML109W	YKL142W	YMR243C
YBR029C	YIR033W	YDR140W	YIL151C	YGL198W	YPL095C	YKL142W	YNL063W
YBR029C	YIR038C	YDR140W	YNR046W	YGL201C	YIL150C	YKL142W	YNL210W
YBR030W	YLR244C	YDR142C	YGL153W	YGL213C	YML108W	YKL142W	YOL059W
YBR034C	YGR165W	YDR142C	YGR239C	YGL214W	YLR435W	YKL142W	YPL004C
YBR034C	YIL061C	YDR142C	YHR160C	YGL220W	YLR052W	YKL143W	YMR047C
YBR038W	YPR106W	YDR142C	YIL160C	YGL221C	YGL221C	YKL143W	YNL178W
YBR040W	YCL040W	YDR142C	YMR095C	YGL221C	YML064C	YKL151C	YPL070W
YBR041W	YDL153C	YDR145W	YLR390W	YGL221C	YNL189W	YKL171W	YML051W
YBR042C	YER081W	YDR146C	YDR335W	YGL223C	YML071C	YKL183W	YNL104C
YBR052C	YDR032C	YDR146C	YML051W	YGL225W	YHR114W	YKL186C	YPL138C
YBR055C	YLR446W	YDR148C	YDR510W	YGL225W	YIR033W	YKL189W	YLR423C
YBR055C	YPR082C	YDR148C	YFR049W	YGL225W	YIR038C	YKL189W	YOR353C
YBR056W	YFR007W	YDR148C	YKL010C	YGL225W	YPL094C	YKL189W	YPL049C
YBR057C	YCL055W	YDR148C	YNL092W	YGL225W	YPR071W	YKL192C	YOR124C
YBR057C	YDR206W	YDR152W	YGR173W	YGL229C	YJL013C	YKL197C	YNL329C
YBR057C	YER018C	YDR159W	YLR423C	YGL229C	YJL030W	YKL204W	YNL154C
YBR057C	YGL036W	YDR167W	YLR432W	YGL229C	YJL178C	YKL212W	YML029W
YBR057C	YGL192W	YDR167W	YML015C	YGL229C	YJL211C	YKL218C	YKL218C
YBR057C	YHL004W	YDR167W	YML114C	YGL229C	YMR181C	YKR014C	YMR258C
YBR057C	YJL025W	YDR171W	YDR171W	YGL229C	YOR062C	YKR014C	YOR370C
YBR057C	YJL058C	YDR171W	YDR448W	YGL229C	YPR040W	YKR022C	YLR424W
YBR057C	YJL085W	YDR171W	YDR510W	YGL230C	YKL110C	YKR022C	YNL258C
YBR057C	YPL135W	YDR171W	YOL083W	YGL230C	YOR161C	YKR026C	YKR026C
YBR059C	YBR059C	YDR173C	YMR042W	YGL233W	YLR166C	YKR026C	YLR291C
YBR059C	YER144C	YDR173C	YMR043W	YGL237C	YGR146C	YKR026C	YLR432W
YBR059C	YGL213C	YDR174W	YDR174W	YGL237C	YLR114C	YKR026C	YMR267W
YBR059C	YML014W	YDR174W	YDR510W	YGL237C	YLR423C	YKR026C	YMR269W
YBR072W	YBR072W	YDR174W	YIL013C	YGL237C	YOR047C	YKR034W	YKR034W
YBR072W	YBR261C	YDR174W	YKR092C	YGL237C	YOR358W	YKR034W	YLR132C
YBR072W	YDL239C	YDR174W	YML015C	YGL238W	YLR293C	YKR034W	YLR291C
YBR072W	YML064C	YDR174W	YNL189W	YGL238W	YNL189W	YKR034W	YLR424W
YBR072W	YNL189W	YDR174W	YPR104C	YGL238W	YNL236W	YKR034W	YMR308C
YBR077C	YGR201C	YDR176W	YDR448W	YGL238W	YOR185C	YKR034W	YNL021W
YBR077C	YKR007W	YDR176W	YLR423C	YGL240W	YKR048C	YKR034W	YNL229C
YBR077C	YMR004W	YDR177W	YPR093C	YGL242C	YKR099W	YKR034W	YOL054W
YBR080C	YBR080C	YDR179C	YKR060W	YGL244W	YLR385C	YKR034W	YOL145C
YBR080C	YBR261C	YDR179C	YMR025W	YGL250W	YLR082C	YKR037C	YLR423C
YBR080C	YIL046W	YDR189W	YLR026C	YGL250W	YLR442C	YKR043C	YKR043C
YBR080C	YJL030W	YDR190C	YPL235W	YGL250W	YMR068W	YKR048C	YKR048C
YBR080C	YLR291C	YDR192C	YER081W	YGL250W	YMR111C	YKR048C	YMR139W
YBR080C	YNL189W	YDR194C	YER081W	YGL250W	YOR028C	YKR048C	YNL078W
YBR080C	YNL288W	YDR195W	YGL153W	YGL252C	YGL252C	YKR048C	YOL059W
YBR080C	YPL070W	YDR200C	YMR052W	YGL252C	YLR291C	YKR048C	YOR032C
YBR087W	YDR229W	YDR200C	YNL127W	YGL254W	YGR047C	YKR055W	YNL127W
YBR087W	YJR068W	YDR201W	YIL144W	YGL254W	YHR215W	YKR059W	YPL125W
YBR088C	YDR510W	YDR201W	YKR037C	YGL254W	YOR039W	YKR066C	YPL004C
YBR094W	YLR264W	YDR201W	YKR083C	YGR003W	YOL133W	YKR068C	YLR328W
YBR094W	YOL149W	YDR201W	YNL189W	YGR004W	YPR028W	YKR068C	YOR115C
YBR102C	YLR423C	YDR203W	YJR091C	YGR010W	YGR010W	YKR071C	YPR048W
YBR103W	YGR262C	YDR205W	YNR039C	YGR010W	YLR328W	YKR072C	YML016C
YBR103W	YHL004W	YDR206W	YER027C	YGR010W	YLR438W	YKR083C	YLR423C
YBR103W	YIL112W	YDR206W	YJL030W	YGR010W	YNL189W	YKR084C	YNL001W

YBR103W	YJR141W	YDR206W	YOL149W	YGR013W	YKL012W	YKR097W	YKR097W
YBR103W	YMR061W	YDR206W	YOR047C	YGR014W	YIL144W	YKR099W	YLR058C
YBR103W	YPL173W	YDR207C	YOL082W	YGR014W	YJL013C	YKR104W	YOL143C
YBR107C	YDR421W	YDR207C	YOR355W	YGR014W	YJL030W	YLL001W	YLL001W
YBR107C	YDR489W	YDR208W	YLR227C	YGR014W	YPL211W	YLL001W	YLR291C
YBR107C	YGL071W	YDR212W	YLR030W	YGR017W	YLR072W	YLL010C	YOR043W
YBR107C	YHR113W	YDR212W	YOR284W	YGR017W	YLR403W	YLL014W	YML029W
YBR108W	YCR009C	YDR212W	YPL049C	YGR020C	YHR060W	YLL032C	YML119W
YBR108W	YDR388W	YDR214W	YJL030W	YGR024C	YGR024C	YLL036C	YLR132C
YBR108W	YGR136W	YDR214W	YMR186W	YGR024C	YHR112C	YLL036C	YPR152C
YBR109C	YGL106W	YDR214W	YOL052C	YGR024C	YIL082W	YLL045C	YML029W
YBR111C	YLR245C	YDR214W	YPL240C	YGR024C	YKL090W	YLL049W	YLR423C
YBR111C	YPL070W	YDR215C	YKR024C	YGR024C	YLR291C	YLL049W	YMR294W
YBR122C	YGR211W	YDR215C	YPL175W	YGR024C	YNL189W	YLL049W	YNR069C
YBR123C	YLR423C	YDR218C	YJR076C	YGR024C	YPL110C	YLL057C	YLL057C
YBR125C	YDR071C	YDR225W	YKR048C	YGR027C	YGR086C	YLL057C	YLR291C
YBR126C	YBR126C	YDR229W	YJR068W	YGR027C	YPL004C	YLL060C	YLL060C
YBR126C	YML100W	YDR229W	YMR047C	YGR029W	YLR424W	YLL062C	YOL143C
YBR126C	YMR261C	YDR229W	YNL041C	YGR038W	YIR038C	YLR011W	YLR011W
YBR126WA	YIR038C	YDR229W	YPL135W	YGR038W	YML029W	YLR011W	YLR291C
YBR130C	YBR130C	YDR233C	YOR285W	YGR040W	YHR084W	YLR014C	YLR014C
YBR131W	YGL124C	YDR236C	YDR398W	YGR040W	YPL049C	YLR017W	YPR017C
YBR133C	YDL154W	YDR240C	YLR423C	YGR041W	YGR041W	YLR019W	YOR043W
YBR133C	YGL187C	YDR242W	YDR242W	YGR046W	YNL236W	YLR021W	YPL144W
YBR134W	YCR106W	YDR244W	YER056CA	YGR047C	YKR034W	YLR025W	YLR025W
YBR134W	YOR128C	YDR244W	YML042W	YGR048W	YPL222W	YLR025W	YMR154C
YBR135W	YBR160W	YDR244W	YNL044W	YGR049W	YGR278W	YLR025W	YOR275C
YBR135W	YBR252W	YDR245W	YJL183W	YGR057C	YIL109C	YLR025W	YPR173C
YBR135W	YDL155W	YDR252W	YGR134W	YGR057C	YKL015W	YLR026C	YNL044W
YBR135W	YER102W	YDR255C	YKL144C	YGR058W	YGR058W	YLR031W	YMR124W
YBR135W	YGR108W	YDR256C	YDR256C	YGR058W	YGR136W	YLR049C	YPL161C
YBR135W	YPR119W	YDR256C	YGL153W	YGR058W	YLR113W	YLR070C	YLR070C
YBR137W	YBR137W	YDR256C	YLR291C	YGR058W	YNL047C	YLR072W	YLR173W
YBR137W	YML064C	YDR256C	YMR033W	YGR058W	YOR097C	YLR072W	YPR113W
YBR137W	YMR047C	YDR256C	YNL189W	YGR058W	YOR264W	YLR082C	YLR082C
YBR137W	YNL189W	YDR256C	YPL070W	YGR061C	YLR386W	YLR089C	YLR423C
YBR141C	YDR372C	YDR259C	YDR311W	YGR063C	YML095C	YLR089C	YPR049C
YBR141C	YGL091C	YDR259C	YGL181W	YGR067C	YOL116W	YLR098C	YOL034W
YBR150C	YOL089C	YDR259C	YGR066C	YGR071C	YJL058C	YLR098C	YPL149W
YBR150C	YOR174W	YDR259C	YIL153W	YGR074W	YKL183W	YLR098C	YPR049C
YBR152W	YGR075C	YDR259C	YKL071W	YGR075C	YML051W	YLR102C	YMR092C
YBR153W	YBR153W	YDR259C	YLR423C	YGR082W	YGR120C	YLR108C	YLR108C
YBR154C	YFL023W	YDR259C	YLR447C	YGR083C	YLR291C	YLR119W	YMR032W
YBR155W	YER081W	YDR259C	YNL092W	YGR086C	YKL142W	YLR120WA	YPL208W
YBR156C	YPL209C	YDR261WA	YDR261WA	YGR086C	YPL004C	YLR125W	YLR288C
YBR162WA	YPL094C	YDR261WA	YDR261WB	YGR088W	YLR291C	YLR125W	YMR030W
YBR166C	YBR166C	YDR264C	YHR135C	YGR088W	YNR052C	YLR132C	YLR423C
YBR166C	YLR291C	YDR264C	YNL154C	YGR092W	YIL106W	YLR132C	YNL286W
YBR170C	YDL126C	YDR264C	YOR101W	YGR097W	YGR097W	YLR135W	YPL022W
YBR170C	YDL190C	YDR267C	YHR122W	YGR099W	YJL110C	YLR146C	YPR069C
YBR170C	YGR048W	YDR271C	YOR128C	YGR099W	YKL033W	YLR170C	YPR029C
YBR176W	YBR176W	YDR273W	YFR052W	YGR099W	YKL068W	YLR175W	YNL124W
YBR176W	YLR347C	YDR273W	YML051W	YGR099W	YML099C	YLR180W	YLR180W

YBR176W	YML064C	YDR277C	YLR447C	YGR099W	YMR047C	YLR181C	YPR173C
YBR176W	YNL189W	YDR279W	YLR154C	YGR099W	YPL235W	YLR182W	YOL131W
YBR176W	YPL070W	YDR284C	YDR284C	YGR101W	YHL021C	YLR200W	YML094W
YBR182C	YER125W	YDR284C	YDR479C	YGR110W	YHR114W	YLR200W	YMR052W
YBR182C	YLR423C	YDR284C	YIR038C	YGR113W	YIL144W	YLR206W	YML051W
YBR186W	YBR261C	YDR284C	YNL111C	YGR113W	YKR037C	YLR206W	YOL111C
YBR186W	YLR032W	YDR284C	YPL094C	YGR113W	YLR423C	YLR208W	YMR017W
YBR187W	YNR032W	YDR284C	YPR071W	YGR113W	YLR424W	YLR209C	YNL189W
YBR188C	YDR416W	YDR292C	YKL154W	YGR117C	YNL236W	YLR211C	YLR446W
YBR188C	YKR034W	YDR292C	YMR163C	YGR119C	YJL041W	YLR212C	YNL126W
YBR188C	YLR117C	YDR296W	YER125W	YGR119C	YKL061W	YLR215C	YLR386W
YBR188C	YMR124W	YDR296W	YLR386W	YGR119C	YLR423C	YLR215C	YNL116W
YBR190W	YLR117C	YDR296W	YPL049C	YGR119C	YMR236W	YLR219W	YPL004C
YBR193C	YER022W	YDR299W	YER127W	YGR120C	YGR120C	YLR222C	YNR041C
YBR193C	YGL127C	YDR300C	YDR300C	YGR120C	YHL004W	YLR223C	YLR455W
YBR193C	YGR104C	YDR308C	YGL127C	YGR120C	YIL144W	YLR223C	YOR247W
YBR193C	YLR295C	YDR308C	YML051W	YGR120C	YLR291C	YLR227C	YOR284W
YBR194W	YMR070W	YDR308C	YOL135C	YGR120C	YLR423C	YLR238W	YPR110C
YBR194W	YPR152C	YDR308C	YOR174W	YGR120C	YMR025W	YLR243W	YOR258W
YBR195C	YLR017W	YDR311W	YGR120C	YGR120C	YNL086W	YLR244C	YNR029C
YBR195C	YPR018W	YDR311W	YKL028W	YGR120C	YNR025C	YLR245C	YLR245C
YBR196C	YGL229C	YDR311W	YKL103C	YGR120C	YOR158W	YLR245C	YLR291C
YBR198C	YGL112C	YDR311W	YLR288C	YGR120C	YOR353C	YLR245C	YNL189W
YBR200W	YJL157C	YDR311W	YLR423C	YGR120C	YPL077C	YLR245C	YNL288W
YBR201W	YML029W	YDR311W	YMR294W	YGR120C	YPR105C	YLR245C	YOL111C
YBR205W	YIR038C	YDR311W	YOL082W	YGR120C	YPR185W	YLR245C	YPL070W
YBR205W	YPR107C	YDR312W	YPR143W	YGR120C	YPR191W	YLR254C	YOR269W
YBR212W	YDL167C	YDR313C	YPL133C	YGR121C	YIR038C	YLR257W	YLR345W
YBR212W	YPL184C	YDR314C	YML011C	YGR122W	YLR025W	YLR258W	YLR258W
YBR216C	YML007W	YDR315C	YJR117W	YGR122W	YML099C	YLR258W	YLR291C
YBR217W	YHR171W	YDR315C	YLR264W	YGR123C	YKL117W	YLR258W	YPL031C
YBR217W	YLR423C	YDR315C	YLR323C	YGR125W	YMR024W	YLR262C	YNL041C
YBR217W	YMR159C	YDR315C	YOR078W	YGR130C	YGR233C	YLR262C	YOR370C
YBR217W	YPL149W	YDR318W	YNL189W	YGR130C	YPL094C	YLR264W	YOL149W
YBR221C	YKL117W	YDR320CA	YKR083C	YGR134W	YJR011C	YLR268W	YPL094C
YBR221C	YLR345W	YDR321W	YDR321W	YGR136W	YNL189W	YLR273C	YNR034W
YBR222C	YDL006W	YDR323C	YGL095C	YGR136W	YOR181W	YLR275W	YPR182W
YBR223C	YDR510W	YDR326C	YER007CA	YGR142W	YJR127C	YLR284C	YOR180C
YBR228W	YLR135W	YDR326C	YIL105C	YGR142W	YLR424W	YLR288C	YMR159C
YBR233W	YBR233W	YDR328C	YFL009W	YGR142W	YMR021C	YLR288C	YOR368W
YBR233W	YBR261C	YDR328C	YIL046W	YGR144W	YGR144W	YLR291C	YLR291C
YBR233W	YDR116C	YDR328C	YLR267W	YGR144W	YIL051C	YLR291C	YLR321C
YBR233W	YDR473C	YDR328C	YLR352W	YGR144W	YLR291C	YLR291C	YLR377C
YBR233W	YGL122C	YDR328C	YLR368W	YGR144W	YNL189W	YLR291C	YLR386W
YBR233W	YIL079C	YDR328C	YLR429W	YGR146C	YML051W	YLR291C	YLR423C
YBR233W	YKL074C	YDR328C	YML088W	YGR149W	YNL181W	YLR291C	YLR438CA
YBR233W	YLR291C	YDR328C	YMR258C	YGR158C	YLR345W	YLR291C	YML042W
YBR233W	YMR294WA	YDR330W	YDR510W	YGR161CC	YKL057C	YLR291C	YML099C
YBR233W	YNL075W	YDR330W	YGR268C	YGR163W	YKR007W	YLR291C	YML106W
YBR233W	YNL288W	YDR330W	YKR094C	YGR172C	YNL263C	YLR291C	YMR004W
YBR234C	YDL029W	YDR330W	YOL133W	YGR172C	YPL095C	YLR291C	YMR032W
YBR234C	YDR063W	YDR335W	YLR293C	YGR177C	YML011C	YLR291C	YMR095C
YBR237W	YDR073W	YDR348C	YMR295C	YGR177C	YMR071C	YLR291C	YNL025C

YBR239C	YPL133C	YDR353W	YGR099W	YGR177C	YNL044W	YLR291C	YNL044W
YBR241C	YDR479C	YDR353W	YGR209C	YGR177C	YNL263C	YLR291C	YNL229C
YBR241C	YIR033W	YDR353W	YHR106W	YGR178C	YGR218W	YLR291C	YNL307C
YBR241C	YIR038C	YDR357C	YGL079W	YGR178C	YHR121W	YLR291C	YNL314W
YBR242W	YBR242W	YDR357C	YLR423C	YGR178C	YNR014W	YLR291C	YNL333W
YBR243C	YIR038C	YDR357C	YPR182W	YGR179C	YLR315W	YLR291C	YNR012W
YBR244W	YCR086W	YDR361C	YER086W	YGR180C	YOR229W	YLR291C	YOL083W
YBR244W	YLR117C	YDR361C	YGL068W	YGR180C	YOR230W	YLR291C	YOL130W
YBR244W	YLR345W	YDR361C	YHR022C	YGR185C	YPL013C	YLR291C	YOL143C
YBR246W	YDR520C	YDR361C	YJR056C	YGR188C	YOR026W	YLR291C	YOR042W
YBR247C	YKL159C	YDR361C	YMR021C	YGR192C	YNL189W	YLR291C	YOR095C
YBR249C	YDR510W	YDR361C	YPL125W	YGR195W	YKR034W	YLR291C	YOR111W
YBR252W	YBR252W	YDR361C	YPL208W	YGR195W	YOL021C	YLR291C	YOR192CA
YBR252W	YLR291C	YDR363WA	YJR084W	YGR203W	YIL119C	YLR291C	YOR232W
YBR252W	YNL189W	YDR364C	YLL036C	YGR203W	YKL171W	YLR291C	YOR284W
YBR253W	YMR112C	YDR366C	YER071C	YGR203W	YLR397C	YLR291C	YOR380W
YBR254C	YDR472W	YDR373W	YGL153W	YGR203W	YNL314W	YLR291C	YPL049C
YBR254C	YKR068C	YDR373W	YNL267W	YGR205W	YMR315W	YLR291C	YPL069C
YBR255W	YIL106W	YDR374C	YLR423C	YGR209C	YKL069W	YLR291C	YPL070W
YBR260C	YDR239C	YDR374C	YNR052C	YGR211W	YOR117W	YLR291C	YPL088W
YBR260C	YER144C	YDR376W	YIR024C	YGR213C	YHR134W	YLR291C	YPL124W
YBR260C	YGR196C	YDR378C	YER146W	YGR218W	YKL143W	YLR291C	YPR062W
YBR260C	YMR032W	YDR378C	YLR438CA	YGR218W	YML007W	YLR291C	YPR105C
YBR260C	YNL094W	YDR383C	YLR315W	YGR218W	YMR047C	YLR293C	YMR308C
YBR261C	YCL028W	YDR383C	YML051W	YGR218W	YMR124W	YLR293C	YOR160W
YBR261C	YCR007C	YDR383C	YNL189W	YGR218W	YOL149W	YLR293C	YPL125W
YBR261C	YDR032C	YDR386W	YNL024C	YGR223C	YOR089C	YLR294C	YOR348C
YBR261C	YDR100W	YDR386W	YPR119W	YGR229C	YKR099W	YLR295C	YOL050C
YBR261C	YDR256C	YDR388W	YGL060W	YGR233C	YJL025W	YLR303W	YNL189W
YBR261C	YER086W	YDR388W	YGL090W	YGR233C	YML014W	YLR305C	YOR047C
YBR261C	YFL059W	YDR388W	YGL181W	YGR233C	YOL145C	YLR305C	YOR355W
YBR261C	YGL037C	YDR388W	YNL094W	YGR233C	YPL031C	YLR312C	YOL088C
YBR261C	YGR088W	YDR388W	YOR181W	YGR233C	YPR049C	YLR315W	YPR105C
YBR261C	YGR267C	YDR388W	YPL077C	YGR238C	YHR158C	YLR321C	YLR345W
YBR261C	YHL018W	YDR389W	YJR091C	YGR239C	YMR267W	YLR321C	YNR046W
YBR261C	YHR074W	YDR394W	YGR232W	YGR240C	YGR240C	YLR321C	YPL070W
YBR261C	YHR111W	YDR394W	YOR117W	YGR240C	YMR205C	YLR324W	YLR324W
YBR261C	YHR112C	YDR397C	YDR397C	YGR241C	YIL095W	YLR324W	YMR153W
YBR261C	YHR113W	YDR397C	YER159C	YGR241C	YLL017W	YLR324W	YPR028W
YBR261C	YIL074C	YDR398W	YMR093W	YGR241C	YNL020C	YLR328W	YLR328W
YBR261C	YJL151C	YDR399W	YDR399W	YGR241C	YPL077C	YLR328W	YLR438W
YBR261C	YJL199C	YDR408C	YGL127C	YGR247W	YKR034W	YLR328W	YML064C
YBR261C	YJL218W	YDR408C	YOR174W	YGR247W	YOR327C	YLR328W	YNL189W
YBR261C	YKL151C	YDR411C	YDR479C	YGR250C	YIR001C	YLR330W	YOR299W
YBR261C	YLL001W	YDR411C	YJL019W	YGR250C	YPL178W	YLR333C	YPL004C
YBR261C	YLR098C	YDR411C	YML029W	YGR253C	YPR185W	YLR345W	YLR345W
YBR261C	YLR245C	YDR412W	YPR119W	YGR261C	YLR423C	YLR347C	YLR377C
YBR261C	YLR438CA	YDR416W	YGR129W	YGR261C	YNL199C	YLR347C	YPL124W
YBR261C	YML042W	YDR416W	YGR195W	YGR261C	YOR284W	YLR359W	YLR359W
YBR261C	YMR021C	YDR416W	YHL004W	YGR261C	YOR380W	YLR376C	YMR168C
YBR261C	YMR095C	YDR416W	YHR184W	YGR263C	YMR070W	YLR377C	YLR377C
YBR261C	YNL044W	YDR416W	YJR050W	YGR267C	YGR267C	YLR377C	YML064C
YBR261C	YNL239W	YDR416W	YKL098W	YGR267C	YLR132C	YLR377C	YNL189W

YBR261C	YOL143C	YDR418W	YDR465C	YGR267C	YLR291C	YLR385C	YLR424W
YBR261C	YOR095C	YDR422C	YHR114W	YGR267C	YMR308C	YLR385C	YOR174W
YBR261C	YOR108W	YDR423C	YEL051W	YGR267C	YNL189W	YLR386W	YLR386W
YBR261C	YOR192CA	YDR423C	YMR047C	YGR267C	YPL251W	YLR386W	YML092C
YBR261C	YOR284W	YDR424C	YDR488C	YGR268C	YGR268C	YLR386W	YNL041C
YBR261C	YPL049C	YDR425W	YGL161C	YGR268C	YHR016C	YLR386W	YPL268W
YBR261C	YPL069C	YDR425W	YGL198W	YGR268C	YLR206W	YLR389C	YNL229C
YBR261C	YPL088W	YDR425W	YJL036W	YGR268C	YOR042W	YLR399C	YMR227C
YBR261C	YPR113W	YDR425W	YJR110W	YGR268C	YOR124C	YLR403W	YOR025W
YBR264C	YOR370C	YDR428C	YLR291C	YGR268C	YOR138C	YLR404W	YOR301W
YBR270C	YDR259C	YDR429C	YFL017C	YGR268C	YPL049C	YLR405W	YPL108W
YBR270C	YER093C	YDR429C	YMR146C	YGR286C	YMR070W	YLR417W	YMR077C
YBR270C	YIL105C	YDR429C	YOR361C	YGR294W	YHL018W	YLR417W	YPL002C
YBR270C	YKR026C	YDR429C	YPL105C	YHL002W	YNR005C	YLR423C	YLR423C
YBR270C	YLR423C	YDR431W	YPL094C	YHL002W	YNR006W	YLR423C	YLR424W
YBR270C	YMR236W	YDR434W	YIR033W	YHL003C	YJL183W	YLR423C	YLR439W
YBR270C	YNL047C	YDR441C	YML022W	YHL003C	YKL008C	YLR423C	YML041C
YBR270C	YPL124W	YDR446W	YDR510W	YHL003C	YMR298W	YLR423C	YML043C
YBR270C	YPL255W	YDR448W	YER018C	YHL003C	YOR223W	YLR423C	YML062C
YBR273C	YDL190C	YDR448W	YGR142W	YHL003C	YPL094C	YLR423C	YML064C
YBR273C	YDR411C	YDR448W	YGR195W	YHL004W	YJL112W	YLR423C	YMR059W
YBR274W	YLR258W	YDR448W	YGR252W	YHL004W	YLR423C	YLR423C	YMR124W
YBR274W	YMR255W	YDR448W	YGR261C	YHL004W	YOR284W	YLR423C	YMR213W
YBR276C	YER081W	YDR448W	YHL004W	YHL004W	YPL255W	YLR423C	YNL182C
YBR278W	YDR121W	YDR448W	YHR022C	YHL006C	YLR046C	YLR423C	YNL288W
YBR279W	YOR123C	YDR448W	YJL011C	YHL006C	YLR376C	YLR423C	YOL034W
YBR281C	YDL153C	YDR448W	YJL058C	YHL006C	YNL021W	YLR423C	YOR117W
YBR281C	YNL287W	YDR448W	YJR003C	YHL009C	YLR291C	YLR423C	YOR158W
YBR284W	YDL238C	YDR448W	YLR424W	YHL009C	YMR314W	YLR423C	YOR226C
YBR284W	YML035C	YDR448W	YML041C	YHL009C	YNL189W	YLR423C	YOR353C
YBR288C	YGR261C	YDR448W	YMR314W	YHL011C	YKL181W	YLR423C	YPL077C
YBR289W	YPL129W	YDR448W	YPL077C	YHL012W	YML051W	YLR423C	YPL159C
YCL010C	YDR176W	YDR448W	YPL122C	YHL018W	YHL018W	YLR423C	YPL173W
YCL019W	YDR261WA	YDR448W	YPL135W	YHL018W	YLR291C	YLR423C	YPL268W
YCL019W	YDR261WB	YDR448W	YPR173C	YHL018W	YMR111C	YLR424W	YMR316CB
YCL020W	YDR261WA	YDR453C	YIL039W	YHL018W	YNL113W	YLR424W	YOR158W
YCL020W	YDR510W	YDR453C	YML028W	YHL018W	YNL189W	YLR432W	YLR432W
YCL020W	YFL002WA	YDR453C	YNL189W	YHL018W	YNL288W	YLR432W	YML056C
YCL021WA	YPL094C	YDR455C	YLR295C	YHL018W	YOL054W	YLR433C	YNL047C
YCL024W	YKR048C	YDR460W	YPR025C	YHL018W	YPL070W	YLR438CA	YLR438CA
YCL028W	YCL028W	YDR465C	YEL054C	YHL019C	YKL135C	YLR438CA	YNL147W
YCL028W	YCR060W	YDR469W	YHR060W	YHL019C	YPR029C	YLR438CA	YOR159C
YCL028W	YGR142W	YDR469W	YLR015W	YHL025W	YLR438W	YLR440C	YNL258C
YCL028W	YHR034C	YDR469W	YLR432W	YHL027W	YJL056C	YLR447C	YOR028C
YCL028W	YKL040C	YDR472W	YKR068C	YHL031C	YPL094C	YLR447C	YOR047C
YCL028W	YLR291C	YDR473C	YLR423C	YHL033C	YML029W	YLR447C	YOR332W
YCL028W	YML051W	YDR473C	YNL229C	YHL039W	YMR111C	YLR453C	YNL216W
YCL028W	YNL189W	YDR473C	YPL004C	YHL042W	YOR127W	YLR465C	YML035C
YCL028W	YNL288W	YDR473C	YPR178W	YHL046C	YOR355W	YML007W	YMR047C
YCL028W	YOL111C	YDR476C	YDR479C	YHR005C	YOR212W	YML008C	YML008C
YCL028W	YOL123W	YDR476C	YHR211W	YHR009C	YOR359W	YML008C	YOR097C
YCL028W	YOR007C	YDR476C	YIR038C	YHR014W	YHR185C	YML015C	YML098W
YCL028W	YPL070W	YDR476C	YJL019W	YHR016C	YLR243W	YML015C	YMR077C

YCL029C	YER016W	YDR477W	YER027C	YHR016C	YMR255W	YML028W	YML028W
YCL032W	YDR032C	YDR477W	YGL115W	YHR022C	YOR032C	YML028W	YNL189W
YCL032W	YLR362W	YDR477W	YGL208W	YHR025W	YHR025W	YML028W	YOR101W
YCL032W	YLR423C	YDR479C	YEL042W	YHR025W	YML064C	YML029W	YML029W
YCL033C	YKL103C	YDR479C	YER087CA	YHR025W	YNL189W	YML029W	YNL219C
YCL033C	YOL082W	YDR479C	YGL053W	YHR026W	YIR038C	YML029W	YOR288C
YCL039W	YMR135C	YDR479C	YGL065C	YHR026W	YJR091C	YML029W	YPR113W
YCL040W	YCL040W	YDR479C	YGL104C	YHR030C	YPL140C	YML031W	YMR153W
YCL040W	YDR516C	YDR479C	YGR149W	YHR035W	YPR119W	YML035C	YML035C
YCL040W	YML099C	YDR479C	YGR284C	YHR036W	YJL183W	YML035C	YPL070W
YCL040W	YNL189W	YDR479C	YHL031C	YHR057C	YJR091C	YML037C	YNL092W
YCL046W	YGL115W	YDR479C	YJL097W	YHR060W	YLR447C	YML042W	YML042W
MEL1	YJL092W	YDR479C	YJL117W	YHR060W	YPL019C	YML042W	YNL189W
Q0085	YCR106W	YDR479C	YJL134W	YHR060W	YPR105C	YML042W	YPL070W
TORF1	YCR106W	YDR479C	YJL183W	YHR066W	YPR143W	YML043C	YNL199C
TORF19	YDR361C	YDR479C	YLL014W	YHR068W	YHR068W	YML051W	YMR004W
TORF21	YKR048C	YDR479C	YLR036C	YHR068W	YJR047C	YML051W	YMR223W
TORF47	YCR106W	YDR479C	YLR268W	YHR068W	YPL070W	YML051W	YNR010W
YCL054W	YNL154C	YDR479C	YLR324W	YHR072WA	YNL124W	YML051W	YOL067C
YCL055W	YGL036W	YDR479C	YLR350W	YHR072WA	YPL208W	YML051W	YOL148C
YCL055W	YGL192W	YDR479C	YML055W	YHR074W	YHR074W	YML051W	YOR197W
YCL056C	YDL157C	YDR479C	YML125C	YHR076W	YMR079W	YML051W	YOR355W
YCL056C	YDR142C	YDR479C	YMR024W	YHR084W	YPL049C	YML051W	YOR359W
YCL056C	YIL065C	YDR479C	YMR071C	YHR091C	YOL088C	YML051W	YOR370C
YCL056C	YJL185C	YDR479C	YNL263C	YHR096C	YIR038C	YML051W	YPL047W
YCL056C	YNL131W	YDR479C	YNR075W	YHR098C	YJR048W	YML055W	YPL094C
YCL056C	YOR037W	YDR479C	YOL003C	YHR098C	YPR181C	YML057W	YNL047C
YCL059C	YGL201C	YDR479C	YOL065C	YHR102W	YKL189W	YML064C	YNL044W
YCL059C	YOR229W	YDR479C	YOR377W	YHR102W	YOR353C	YML064C	YOR020C
YCL063W	YLR423C	YDR479C	YPL020C	YHR105W	YNL044W	YML064C	YOR284W
YCL066W	YDR480W	YDR479C	YPR113W	YHR107C	YJR076C	YML064C	YPL049C
YCL066W	YHR084W	YDR479C	YPR159CA	YHR111W	YHR111W	YML064C	YPL111W
YCL066W	YPL049C	YDR480W	YDR480W	YHR111W	YIL008W	YML071C	YNL041C
YCR004C	YDR032C	YDR480W	YGR040W	YHR111W	YLR291C	YML075C	YOR102W
YCR005C	YCR005C	YDR480W	YHR039C	YHR111W	YML110C	YML077W	YOR115C
YCR007C	YDL120W	YDR480W	YHR084W	YHR111W	YPL070W	YML079W	YML079W
YCR007C	YDL164C	YDR480W	YHR121W	YHR112C	YHR112C	YML095C	YPL022W
YCR007C	YKR066C	YDR480W	YJL058C	YHR112C	YLR291C	YML099C	YMR104C
YCR007C	YMR079W	YDR480W	YJR003C	YHR112C	YNL189W	YML106W	YML106W
YCR007C	YPL020C	YDR480W	YKL189W	YHR113W	YHR113W	YML110C	YMR071C
YCR009C	YDR388W	YDR480W	YLR291C	YHR113W	YJL030W	YML110C	YNL263C
YCR009C	YER125W	YDR480W	YNL189W	YHR113W	YKL103C	YML121W	YML121W
YCR009C	YMR232W	YDR480W	YPL049C	YHR113W	YLR021W	YML125C	YMR153W
YCR011C	YNL154C	YDR482C	YGL028C	YHR113W	YLR291C	YMR001C	YOR192CA
YCR020C	YCR020C	YDR482C	YOR276W	YHR113W	YML064C	YMR001C	YPR174C
YCR020C	YLR291C	YDR486C	YLR181C	YHR113W	YMR308C	YMR004W	YMR004W
YCR020CA	YEL053C	YDR487C	YNL189W	YHR113W	YNL153C	YMR021C	YMR021C
YCR020CA	YIL119C	YDR488C	YHR129C	YHR113W	YNL189W	YMR021C	YOR111W
YCR020CA	YKL025C	YDR488C	YPL174C	YHR113W	YNL222W	YMR025W	YNR052C
YCR021C	YDR479C	YDR489W	YFR043C	YHR113W	YOL082W	YMR032W	YNL152W
YCR022C	YDL017W	YDR489W	YJL072C	YHR113W	YPL129W	YMR039C	YMR316CB
YCR023C	YMR075CA	YDR489W	YML034W	YHR113W	YPL201C	YMR047C	YNL078W
YCR024C	YNL243W	YDR489W	YPL077C	YHR114W	YIL132C	YMR047C	YOL149W

YCR027C	YOL083W	YDR490C	YGR086C	YHR114W	YJL086C	YMR047C	YOR112W
YCR035C	YHR114W	YDR490C	YHR207C	YHR114W	YJL180C	YMR047C	YOR289W
YCR036W	YGL153W	YDR490C	YIR044C	YHR114W	YJL203W	YMR048W	YNL273W
YCR045C	YOR348C	YDR490C	YLR466W	YHR114W	YLR112W	YMR048W	YOR124C
YCR050C	YDL017W	YDR498C	YJL019W	YHR114W	YLR423C	YMR068W	YNL047C
YCR051W	YER184C	YDR502C	YDR502C	YHR114W	YNL092W	YMR070W	YOL109W
YCR052W	YFR037C	YDR502C	YLR180W	YHR114W	YNL094W	YMR071C	YNL315C
YCR052W	YOR232W	YDR502C	YPL125W	YHR114W	YOL018C	YMR071C	YPL020C
YCR057C	YGR154C	YDR503C	YKL130C	YHR114W	YOR059C	YMR077C	YPL002C
YCR059C	YDR400W	YDR504C	YJL070C	YHR115C	YLR215C	YMR077C	YPL065W
YCR059C	YJL160C	YDR505C	YGL122C	YHR115C	YOR215C	YMR079W	YPR113W
YCR060W	YHR034C	YDR510W	YDR510W	YHR121W	YPL049C	YMR087W	YMR087W
YCR060W	YKL117W	YDR510W	YER047C	YHR122W	YIL128W	YMR095C	YMR096W
YCR063W	YDR408C	YDR510W	YFL039C	YHR123W	YIR038C	YMR095C	YNL333W
YCR063W	YOL135C	YDR510W	YFL045C	YHR123W	YPL094C	YMR095C	YNL334C
YCR063W	YPR152C	YDR510W	YGL026C	YHR128W	YNR012W	YMR095C	YPL070W
YCR065W	YML051W	YDR510W	YGL250W	YHR128W	YPR185W	YMR096W	YMR096W
YCR066W	YGL058W	YDR510W	YHR134W	YHR129C	YHR129C	YMR096W	YMR322C
YCR066W	YOR128C	YDR510W	YHR193C	YHR129C	YJR008W	YMR096W	YNL333W
YCR067C	YOR128C	YDR510W	YJL092W	YHR129C	YMR294W	YMR096W	YNL334C
YCR068W	YIR033W	YDR510W	YJR076C	YHR129C	YPL070W	YMR102C	YNL218W
YCR068W	YIR038C	YDR510W	YKL032C	YHR129C	YPL174C	YMR111C	YMR111C
YCR068W	YNL111C	YDR510W	YKL043W	YHR130C	YJR091C	YMR117C	YOL034W
YCR073C	YGR142W	YDR510W	YKL211C	YHR134W	YMR095C	YMR121C	YMR139W
YCR073C	YLR006C	YDR510W	YLR263W	YHR137W	YHR137W	YMR125W	YPL178W
YCR076C	YNL189W	YDR510W	YLR295C	YHR140W	YIR038C	YMR129W	YMR153W
YCR077C	YDL139C	YDR510W	YLR328W	YHR156C	YJR010W	YMR133W	YPL114W
YCR077C	YDL175C	YDR510W	YLR335W	YHR158C	YJR122W	YMR139W	YNL078W
YCR077C	YJL124C	YDR510W	YLR350W	YHR158C	YLR452C	YMR139W	YOL059W
YCR082W	YER022W	YDR510W	YML023C	YHR158C	YMR181C	YMR146C	YPL105C
YCR082W	YOR023C	YDR510W	YMR111C	YHR158C	YOR047C	YMR153W	YMR153W
YCR083W	YCR086W	YDR510W	YMR219W	YHR160C	YIL160C	YMR159C	YMR159C
YCR083W	YDR448W	YDR510W	YMR233W	YHR161C	YIL095W	YMR159C	YPL149W
YCR086W	YCR086W	YDR510W	YNL021W	YHR161C	YIL122W	YMR170C	YMR170C
YCR086W	YDL089W	YDR510W	YNL042W	YHR161C	YPL077C	YMR180C	YNL154C
YCR086W	YDR061W	YDR510W	YNL078W	YHR166C	YLR451W	YMR181C	YPR105C
YCR086W	YDR439W	YDR510W	YNL088W	YHR166C	YPL124W	YMR193W	YPR086W
YCR086W	YER086W	YDR510W	YNL189W	YHR167W	YJL011C	YMR224C	YNL023C
YCR086W	YER106W	YDR510W	YOL034W	YHR167W	YLR423C	YMR226C	YNL189W
YCR086W	YER144C	YDR510W	YOR032C	YHR167W	YML062C	YMR228W	YOR348C
YCR086W	YGL175C	YDR510W	YOR144C	YHR167W	YNL041C	YMR233W	YOL006C
YCR086W	YGR155W	YDR510W	YPL129W	YHR169W	YKL075C	YMR236W	YOR128C
YCR086W	YIL152W	YDR518W	YHR113W	YHR171W	YLL042C	YMR239C	YNL189W
YCR086W	YJL110C	YDR520C	YDR520C	YHR171W	YNR007C	YMR267W	YNL154C
YCR086W	YKR010C	YDR520C	YGR261C	YHR184W	YHR184W	YMR280C	YOR047C
YCR086W	YKR034W	YDR520C	YJL110C	YHR185C	YIL007C	YMR288W	YNL286W
YCR086W	YKR068C	YDR520C	YJR046W	YHR185C	YMR016C	YMR289W	YOL083W
YCR086W	YLR291C	YDR520C	YKR034W	YHR185C	YPL204W	YMR294W	YOL069W
YCR086W	YNL311C	YDR520C	YLR291C	YHR187W	YMR312W	YMR294W	YPL174C
YCR086W	YOL020W	YDR520C	YOL116W	YHR193C	YLR146C	YMR294W	YPR083W
YCR086W	YOR264W	YDR527W	YOR210W	YHR193C	YPL037C	YMR298W	YPL094C
YCR086W	YOR281C	YDR529C	YHR114W	YHR197W	YLR423C	YMR300C	YMR300C
YCR087CA	YKR092C	YDR531W	YDR531W	YHR211W	YIR038C	YMR308C	YOR185C

YCR088W	YOR284W	YDR532C	YFR008W	YHR211W	YPL094C	YMR308C	YOR380W
YCR093W	YDR376W	YDR532C	YIL144W	YHR216W	YNL189W	YMR308C	YPL088W
YCR095C	YNL099C	YDR532C	YLR031W	YIL001W	YOL133W	YMR309C	YNL047C
YCR105W	YCR105W	YDR533C	YNL189W	YIL007C	YOR117W	YMR309C	YNL244C
YCR106W	YDR222W	YDR541C	YLR025W	YIL011W	YMR201C	YMR309C	YOR284W
YCR106W	YEL072W	YEL005C	YGL079W	YIL018W	YPL004C	YMR314W	YNL199C
YCR106W	YGL247W	YEL005C	YNL086W	YIL026C	YPR068C	YMR314W	YNL229C
YCR106W	YGR081C	YEL009C	YHR145C	YIL033C	YIL033C	YMR314W	YOR380W
YCR106W	YGR140W	YEL009C	YPL038W	YIL033C	YJL164C	YMR314W	YPR135W
YCR106W	YHR130C	YEL012W	YLR291C	YIL033C	YKL166C	YMR316CB	YPR149W
YCR106W	YJL006C	YEL013W	YJR091C	YIL033C	YPL149W	YMR317W	YOL108C
YCR106W	YJL077WB	YEL015W	YEL015W	YIL033C	YPL203W	YMR322C	YMR322C
YCR106W	YJL135W	YEL015W	YER105C	YIL039W	YIR038C	YMR322C	YNL333W
YCR106W	YMR060C	YEL015W	YLR264W	YIL045W	YOR178C	YMR322C	YOR391C
YCR106W	YMR141C	YEL015W	YNL118C	YIL046W	YJR130C	YMR322C	YPL280W
YCR106W	YNL171C	YEL015W	YOL149W	YIL046W	YML082W	YNL007C	YPR158W
YCR106W	YPL034W	YEL015W	YOR167C	YIL050W	YLR190W	YNL021W	YNL021W
YCR106W	YPL243W	YEL017W	YEL017W	YIL050W	YPL031C	YNL025C	YNL094W
YCR106W	YPL267W	YEL018W	YOR128C	YIL053W	YPL201C	YNL025C	YPL031C
YCR106W	YPR046W	YEL020C	YEL020C	YIL062C	YKL013C	YNL032W	YNL056W
YDL001W	YDL133W	YEL029C	YNR027W	YIL065C	YJL112W	YNL032W	YNL093W
YDL001W	YMR079W	YEL032W	YHR033W	YIL065C	YJR091C	YNL032W	YNL099C
YDL002C	YER092W	YEL034W	YHR068W	YIL065C	YLR321C	YNL037C	YOR136W
YDL002C	YGL150C	YEL041W	YJR049C	YIL069C	YPL004C	YNL040W	YNL040W
YDL002C	YLR052W	YEL042W	YIR038C	YIL074C	YIL074C	YNL041C	YNR011C
YDL005C	YHR167W	YEL042W	YPL094C	YIL074C	YLR291C	YNL041C	YOR304CA
YDL005C	YML051W	YEL043W	YOR164C	YIL074C	YNL311C	YNL042W	YOR014W
YDL006W	YDR162C	YEL048C	YGR040W	YIL075C	YLR421C	YNL044W	YNL044W
YDL011C	YEL023C	YEL048C	YMR218C	YIL079C	YLR423C	YNL044W	YNL189W
YDL012C	YDR151C	YEL051W	YGR120C	YIL084C	YLR423C	YNL044W	YNL263C
YDL012C	YFR047C	YEL051W	YOR174W	YIL085C	YJL019W	YNL044W	YNL315C
YDL012C	YHR032W	YEL053C	YOR032C	YIL092W	YLR423C	YNL044W	YPL070W
YDL012C	YHR140W	YEL053C	YPR051W	YIL095W	YLR206W	YNL047C	YPL059W
YDL012C	YIL172C	YEL056W	YLL022C	YIL103W	YKL191W	YNL049C	YPR181C
YDL012C	YJL065C	YEL056W	YPL001W	YIL104C	YNL124W	YNL056W	YNL099C
YDL012C	YOR355W	YEL060C	YML032CA	YIL105C	YIL105C	YNL078W	YOL070C
YDL013W	YDR510W	YEL062W	YOR138C	YIL105C	YKL130C	YNL086W	YOL069W
YDL013W	YER116C	YEL062W	YPL255W	YIL105C	YLR423C	YNL086W	YOL130W
YDL013W	YJR091C	YEL066W	YEL066W	YIL105C	YMR068W	YNL086W	YOR174W
YDL013W	YMR111C	YEL066W	YML064C	YIL105C	YNL047C	YNL086W	YPR185W
YDL015C	YIR038C	YEL066W	YNL189W	YIL105C	YPL059W	YNL091W	YNL164C
YDL015C	YOR324C	YER009W	YER009W	YIL105WA	YPL049C	YNL091W	YNL288W
YDL017W	YDL160C	YER010C	YER010C	YIL106W	YNL161W	YNL091W	YOR355W
YDL017W	YEL023C	YER015W	YER070W	YIL109C	YKL068W	YNL091W	YPL229W
YDL017W	YFR057W	YER015W	YLR098C	YIL109C	YKL103C	YNL092W	YOR329C
YDL017W	YGR099W	YER016W	YGL061C	YIL109C	YLR245C	YNL093W	YOR370C
YDL017W	YJL088W	YER018C	YKL025C	YIL109C	YMR124W	YNL094W	YOR043W
YDL017W	YKL039W	YER018C	YMR117C	YIL109C	YOL130W	YNL098C	YPL088W
YDL017W	YNR048W	YER019W	YLR350W	YIL109C	YPR181C	YNL102W	YPR135W
YDL017W	YOR006C	YER021W	YPR108W	YIL119C	YNL107W	YNL104C	YNL104C
YDL022W	YDR142C	YER022W	YHR058C	YIL122W	YIL122W	YNL104C	YOR108W
YDL025C	YPL260W	YER022W	YKL117W	YIL122W	YJL030W	YNL111C	YNL111C
YDL030W	YDR026C	YER022W	YML007W	YIL122W	YPL031C	YNL113W	YPR110C

YDL031W	YPL004C	YER022W	YNL288W	YIL124W	YIR038C	YNL118C	YOL149W
YDL044C	YLR386W	YER023W	YER023W	YIL132C	YLR321C	YNL124W	YNL124W
YDL045C	YGR077C	YER023W	YLR291C	YIL132C	YLR322W	YNL135C	YPL049C
YDL053C	YGR178C	YER023W	YPL169C	YIL132C	YLR376C	YNL135C	YPR093C
YDL055C	YDR510W	YER025W	YJR007W	YIL144W	YLR423C	YNL135C	YPR119W
YDL056W	YMR197C	YER025W	YLR215C	YIL144W	YOL069W	YNL154C	YOR355W
YDL057W	YJL058C	YER026C	YPR174C	YIL144W	YOR174W	YNL159C	YNL159C
YDL057W	YLR098C	YER027C	YGL115W	YIL144W	YPL174C	YNL189W	YNL331C
YDL057W	YPL049C	YER038C	YML023C	YIL144W	YPL260W	YNL189W	YOL058W
YDL063C	YDR381W	YER039C	YGL070C	YIL151C	YLR121C	YNL189W	YOL082W
YDL063C	YPL131W	YER043C	YFL028C	YIL152W	YJL112W	YNL189W	YOR020C
YDL064W	YDR510W	YER047C	YGR086C	YIL152W	YLR423C	YNL189W	YOR095C
YDL065C	YGR119C	YER047C	YKL032C	YIL153W	YLL001W	YNL189W	YOR155C
YDL065C	YGR218W	YER047C	YOL034W	YIL153W	YLR258W	YNL189W	YOR229W
YDL065C	YLR071C	YER052C	YER052C	YIL153W	YLR423C	YNL189W	YOR284W
YDL065C	YMR047C	YER052C	YJL058C	YIL153W	YNL021W	YNL189W	YOR380W
YDL065C	YMR163C	YER052C	YNL135C	YIL153W	YNL229C	YNL189W	YPL049C
YDL066W	YGL187C	YER056CA	YGL153W	YIL153W	YNL314W	YNL189W	YPL088W
YDL070W	YLR227C	YER056CA	YML042W	YIL163C	YPL161C	YNL189W	YPL111W
YDL070W	YLR399C	YER059W	YJL084C	YIR015W	YLR345W	YNL189W	YPL214C
YDL070W	YMR227C	YER059W	YLR190W	YIR016W	YNL161W	YNL189W	YPR062W
YDL070W	YNR034W	YER059W	YPL031C	YIR017C	YLR423C	YNL189W	YPR193C
YDL071C	YDR183W	YER062C	YPL201C	YIR025W	YJL058C	YNL199C	YPR048W
YDL071C	YEL068C	YER065C	YNL189W	YIR032C	YIR032C	YNL201C	YOR047C
YDL071C	YFL017C	YER071C	YIR003W	YIR033W	YJL117W	YNL201C	YOR355W
YDL071C	YGR269W	YER071C	YLR200W	YIR033W	YLR268W	YNL201C	YPR115W
YDL071C	YNL155W	YER079W	YNL154C	YIR033W	YML055W	YNL218W	YNL218W
YDL072C	YML029W	YER081W	YER081W	YIR033W	YNL111C	YNL219C	YPL094C
YDL073W	YER118C	YER081W	YIL074C	YIR033W	YNL219C	YNL225C	YOR129C
YDL076C	YLR098C	YER081W	YMR047C	YIR033W	YNL263C	YNL228W	YNL228W
YDL081C	YGR209C	YER081W	YNL054WB	YIR033W	YNR030W	YNL229C	YNL229C
YDL081C	YLR340W	YER081W	YOR318C	YIR033W	YOL126C	YNL229C	YOL034W
YDL081C	YPR086W	YER081W	YPL233W	YIR033W	YPL053C	YNL229C	YPL070W
YDL084W	YDL084W	YER081W	YPR126C	YIR033W	YPR159CA	YNL236W	YOR355W
YDL084W	YDR510W	YER081W	YPR136C	YIR033W	YPR174C	YNL243W	YPL266W
YDL084W	YER063W	YER086W	YER086W	YIR034C	YOR138C	YNL249C	YNL249C
YDL084W	YGL122C	YER086W	YLR291C	YIR035C	YIR035C	YNL249C	YPL125W
YDL084W	YKL214C	YER086W	YMR308C	YIR035C	YLR291C	YNL251C	YPL190C
YDL088C	YML031W	YER086W	YOR160W	YIR036C	YIR036C	YNL263C	YPR028W
YDL088C	YMR153W	YER086W	YPL070W	YIR037W	YLR216C	YNL277W	YNL277W
YDL089W	YDL089W	YER087CA	YIR033W	YIR037W	YLR345W	YNL279W	YOL108C
YDL089W	YDR233C	YER087CA	YIR038C	YIR038C	YIR038C	YNL286W	YOR284W
YDL089W	YLR324W	YER087CA	YLR404W	YIR038C	YJL097W	YNL288W	YNR052C
YDL089W	YML008C	YER090W	YJR070C	YIR038C	YJL117W	YNL288W	YOR095C
YDL089W	YMR316CB	YER090W	YKL211C	YIR038C	YJL183W	YNL288W	YOR284W
YDL089W	YPR028W	YER092W	YLR052W	YIR038C	YJR010CA	YNL290W	YOL094C
YDL090C	YKL019W	YER092W	YLR423C	YIR038C	YJR073C	YNL314W	YNL314W
YDL090C	YKR048C	YER095W	YER095W	YIR038C	YJR075W	YNL314W	YOR304CA
YDL090C	YMR139W	YER095W	YPL204W	YIR038C	YJR118C	YNL316C	YOL082W
YDL092W	YKL122C	YER096W	YHR114W	YIR038C	YKL008C	YNL331C	YNL331C
YDL097C	YEL009C	YER099C	YKL181W	YIR038C	YLL014W	YNL333W	YNL333W
YDL098C	YGR075C	YER099C	YOL061W	YIR038C	YLR268W	YNL333W	YNL334C
YDL100C	YDL121C	YER099C	YOL069W	YIR038C	YML038C	YNR004W	YPL157W

YDL100C	YDR304C	YER101C	YMR071C	YIR038C	YML055W	YNR010W	YOR174W
YDL100C	YDR513W	YER102W	YFL017C	YIR038C	YML125C	YNR012W	YNR012W
YDL100C	YDR526C	YER105C	YJL030W	YIR038C	YNL111C	YNR012W	YPL031C
YDL100C	YER017C	YER105C	YMR153W	YIR038C	YNL217W	YNR022C	YPR119W
YDL100C	YER150W	YER107C	YMR047C	YIR038C	YNL219C	YNR032CA	YOR308C
YDL100C	YGL153W	YER112W	YLR438CA	YIR038C	YNL263C	YNR032W	YPR040W
YDL100C	YGR028W	YER118C	YER118C	YIR038C	YNR030W	YNR034W	YOR178C
YDL100C	YGR189C	YER118C	YMR079W	YIR038C	YOL003C	YNR064C	YNR064C
YDL100C	YHL004W	YER118C	YNL315C	YIR038C	YOL018C	YNR068C	YNR069C
YDL100C	YHR057C	YER125W	YGR268C	YIR038C	YOL126C	YOL001W	YPL031C
YDL100C	YHR128W	YER125W	YHR131C	YIR038C	YOR321W	YOL003C	YPL094C
YDL100C	YHR180W	YER125W	YJL025W	YIR038C	YPL053C	YOL034W	YOL082W
YDL100C	YIL065C	YER125W	YLR167W	YIR038C	YPR113W	YOL034W	YOR284W
YDL100C	YIL162W	YER125W	YLR291C	YIR038C	YPR159CA	YOL034W	YPL070W
YDL100C	YJL153C	YER125W	YLR392C	YJL001W	YLR386W	YOL034W	YPR105C
YDL100C	YKL154W	YER125W	YMR257C	YJL006C	YML112W	YOL082W	YOR115C
YDL100C	YKR100C	YER125W	YMR275C	YJL011C	YKL015W	YOL082W	YOR353C
YDL100C	YLR297W	YER125W	YMR316W	YJL013C	YNL236W	YOL082W	YPL091W
YDL100C	YML101C	YER125W	YOR322C	YJL013C	YOR026W	YOL082W	YPL135W
YDL100C	YNL149C	YER125W	YOR385W	YJL019W	YJL019W	YOL106W	YPR182W
YDL100C	YNL199C	YER126C	YHR204W	YJL019W	YJR068W	YOL107W	YPL020C
YDL100C	YNR067C	YER126C	YPL004C	YJL019W	YMR001C	YOL111C	YOR007C
YDL100C	YOL018C	YER127W	YLR423C	YJL019W	YNL029C	YOL126C	YOR347C
YDL100C	YOL111C	YER128W	YLR181C	YJL019W	YOL012C	YOL135C	YOR174W
YDL100C	YOL126C	YER128W	YPR173C	YJL019W	YOR288C	YOL139C	YOR276W
YDL100C	YOR164C	YER130C	YML051W	YJL019W	YPR113W	YOL143C	YOL143C
YDL100C	YPR075C	YER131W	YLL027W	YJL019W	YPR174C	YOL149W	YOR167C
YDL101C	YPL269W	YER131W	YLR435W	YJL025W	YLR423C	YOL149W	YPL204W
YDL105W	YOL034W	YER133W	YNL233W	YJL025W	YMR111C	YOR007C	YOR007C
YDL106C	YML051W	YER134C	YHR171W	YJL025W	YOR284W	YOR020C	YOR020C
YDL108W	YGL134W	YER143W	YER143W	YJL025W	YOR380W	YOR034C	YOR171C
YDL108W	YNL025C	YER143W	YJR141W	YJL030W	YNL218W	YOR036W	YPL151C
YDL110C	YKL015W	YER144C	YIL095W	YJL030W	YNL236W	YOR039W	YOR061W
YDL110C	YOR078W	YER144C	YLR291C	YJL030W	YOL116W	YOR039W	YOR303W
YDL111C	YGR158C	YER144C	YMR032W	YJL031C	YPR176C	YOR047C	YOR302W
YDL113C	YJL036W	YER146W	YJL124C	YJL036W	YLR423C	YOR047C	YOR358W
YDL116W	YDR113C	YER146W	YLR438CA	YJL039C	YMR153W	YOR047C	YPR103W
YDL116W	YKR082W	YER146W	YNL147W	YJL041W	YJL061W	YOR069W	YOR132W
YDL117W	YMR032W	YER149C	YMR124W	YJL047C	YOL133W	YOR095C	YOR095C
YDL118W	YLR295C	YER151C	YNR051C	YJL048C	YKL130C	YOR095C	YOR160W
YDL120W	YDR100W	YER157W	YGR120C	YJL048C	YLR423C	YOR108W	YOR108W
YDL120W	YMR071C	YER174C	YGR262C	YJL057C	YMR129W	YOR111W	YOR111W
YDL125C	YHL018W	YER177W	YKL168C	YJL057C	YMR153W	YOR124C	YOR138C
YDL126C	YDL190C	YER177W	YLR177W	YJL058C	YJL058C	YOR128C	YOR128C
YDL126C	YFL044C	YER179W	YER179W	YJL058C	YJL075C	YOR128C	YPR088C
YDL126C	YGL108C	YER179W	YIL105C	YJL058C	YJL112W	YOR155C	YOR155C
YDL126C	YMR067C	YER180C	YGL026C	YJL058C	YLR295C	YOR155C	YPL070W
YDL126C	YNL155W	YER180C	YGL070C	YJL058C	YLR423C	YOR159C	YPR182W
YDL127W	YDR146C	YER180C	YPL049C	YJL058C	YML098W	YOR160W	YOR185C
YDL130W	YKL002W	YER182W	YKL142W	YJL058C	YNL229C	YOR160W	YPL088W
YDL130W	YLR287C	YER184C	YER184C	YJL061W	YLR423C	YOR162C	YOR162C
YDL130W	YLR340W	YER188W	YPL049C	YJL061W	YMR047C	YOR164C	YPR105C
YDL132W	YLR267W	YFL009W	YFL009W	YJL064W	YNR029C	YOR185C	YPL125W

YDL132W	YOL133W	YFL010C	YLR291C	YJL065C	YNR029C	YOR192CA	YOR192CA
YDL133CA	YKR048C	YFL010C	YML051W	YJL068C	YJL068C	YOR202W	YOR202W
YDL134C	YHR114W	YFL010C	YMR276W	YJL069C	YLR409C	YOR226C	YPL088W
YDL134C	YMR028W	YFL010C	YNL189W	YJL070C	YML035C	YOR229W	YOR229W
YDL134C	YPR040W	YFL010C	YPR054W	YJL083W	YPL004C	YOR229W	YOR230W
YDL135C	YLR229C	YFL017C	YFL017C	YJL084C	YOR348C	YOR229W	YOR283W
YDL139C	YGL153W	YFL017C	YOL059W	YJL090C	YLR072W	YOR269W	YOR269W
YDL144C	YDL144C	YFL017C	YOR362C	YJL090C	YLR098C	YOR275C	YPR173C
YDL144C	YDR088C	YFL017WA	YHR113W	YJL090C	YLR386W	YOR284W	YOR284W
YDL144C	YLR291C	YFL017WA	YKR034W	YJL090C	YML099C	YOR285W	YPR183W
YDL146W	YKL070W	YFL017WA	YOR159C	YJL092W	YOR355W	YOR324C	YPR153W
YDL147W	YJR091C	YFL018C	YHR114W	YJL097W	YML029W	YOR331C	YPR105C
YDL149W	YLR065C	YFL023W	YLR200W	YJL097W	YPL094C	YOR355W	YPR048W
YDL150W	YKR025W	YFL024C	YHR090C	YJL097W	YPR071W	YOR370C	YPR176C
YDL153C	YNL280C	YFL029C	YPR054W	YJL100W	YPL100W	YOR380W	YOR380W
YDL154W	YFL003C	YFL034CB	YIR016W	YJL103C	YLR377C	YOR380W	YPL031C
YDL154W	YGL025C	YFL034CB	YKL002W	YJL103C	YOR379C	YPL003W	YPR066W
YDL154W	YGL170C	YFL034CB	YOL036W	YJL104W	YMR071C	YPL004C	YPL164C
YDL154W	YIL144W	YFL037W	YOR265W	YJL104W	YOL082W	YPL031C	YPL049C
YDL154W	YMR224C	YFL038C	YNL041C	YJL110C	YLR424W	YPL031C	YPL219W
YDL155W	YPL124W	YFL038C	YOR370C	YJL110C	YNL021W	YPL049C	YPL049C
YDL160C	YEL015W	YFL039C	YFL039C	YJL112W	YJR003C	YPL049C	YPL070W
YDL160C	YGR178C	YFL039C	YGL015C	YJL112W	YJR046W	YPL049C	YPR017C
YDL160C	YOL149W	YFL039C	YLR291C	YJL112W	YKL189W	YPL049C	YPR082C
YDL161W	YOR111W	YFL039C	YMR092C	YJL112W	YLL001W	YPL070W	YPL070W
YDL164C	YDR100W	YFL039C	YNL138W	YJL112W	YLR291C	YPL070W	YPL088W
YDL164C	YGL053W	YFL039C	YNL189W	YJL121C	YJL121C	YPL070W	YPR193C
YDL164C	YNL044W	YFL039C	YOR304CA	YJL124C	YLR438CA	YPL088W	YPL088W
YDL165W	YGR014W	YFL042C	YGR017W	YJL124C	YOR375C	YPL088W	YPL125W
YDL165W	YKL002W	YFL047W	YKL171W	YJL125C	YNL062C	YPL094C	YPL094C
YDL166C	YER047C	YFL056C	YNL201C	YJL127WA	YMR070W	YPL094C	YPR037C
YDL166C	YNL329C	YFL059W	YFL059W	YJL134W	YML029W	YPL094C	YPR159CA
YDL168W	YER081W	YFL059W	YFL060C	YJL137C	YJL137C	YPL111W	YPL111W
YDL184C	YKR048C	YFL059W	YMR095C	YJL137C	YLR258W	YPL124W	YPL124W
YDL188C	YMR028W	YFL059W	YMR096W	YJL138C	YPL125W	YPL125W	YPR160W
YDL188C	YPR040W	YFL059W	YMR322C	YJL141C	YOL133W	YPL176C	YPR071W
YDL189W	YDR480W	YFL059W	YNL189W	YJL145W	YLR266C	YPL192C	YPL192C
YDL189W	YIL122W	YFL059W	YNL333W	YJL151C	YML097C	YPL214C	YPL214C
YDL189W	YLR186W	YFL059W	YNL334C	YJL151C	YMR079W	YPL280W	YPL280W
YDL189W	YPL049C	YFL059W	YPL070W	YJL151C	YNL204C	YPR048W	YPR070W
YDL190C	YFL044C	YFL060C	YMR095C	YJL155C	YLR345W	YPR062W	YPR062W
YDL190C	YMR276W	YFL060C	YMR096W	YJL173C	YNL312W	YPR071W	YPR071W
YDL195W	YIL109C	YFL060C	YNL333W	YJL183W	YPL094C	YPR105C	YPR191W
YDL195W	YLR208W	YFL061W	YNL189W	YJL184W	YOR117W	YPR118W	YPR118W
YDL203C	YGR058W	YFR002W	YGR120C	YJL184W	YPL174C	YPR158WA	YPR158WA
YDL203C	YOR372C	YFR002W	YML025C	YJL185C	YMR204C	YPR193C	YPR193C
YDL203C	YPL124W	YFR002W	YMR153W	YJL185C	YOR127W		
YDL204W	YER118C	YFR008W	YMR029C	YJL187C	YMR001C		